ALMA MATER STUDIORUM - UNIVERSITÀ DI BOLOGNA

SCUOLA DI INGEGNERIA E ARCHITETTURA

DIPARTIMENTO DI INGEGNERIA INDUSTRIALE

CORSO DI LAUREA MAGISTRALE IN INGEGNERIA MECCANICA

TESI DI LAUREA

in

MOTORI A COMBUSTIONE INTERNA E PROPULSORI IBRIDI M

Thermal management model for a Plug-In Hybrid Electric Vehicle

CANDIDATO
Lorenzo Morini

RELATORE:
Prof. Nicolò Cavina

CORRELATORI
Prof. Davide Moro
Prof. Enrico Corti
Ing. Michele Caggiano
Ing. David Hemkemeyer
Ing. Enrico Suzzani

Anno Accademico 2015/2016

Sessione III

Ai miei genitori

Contents

Abstract……...ii
List of figures…….....……..vii
List of tables…….....……x
Notations……xi

1.State of the art of thermal management for PHEV and BEV……...1
1.1 Cooling system general requirements.....2
1.2 Thermal management Layout for Hybrid Vehicle.....8
1.3 Control strategies……14
1.4 Predictive thermal management……..…18

2. Introduction to the thermal model……...25
2.1 Hydraulic modelling background……....25
2.2 Heat transfer theory……30

3. PHEV thermal management modelling…….....35
3.1 Scope of the model……...35
3.2 Description of the circuits and data available……...36
3.3 PHEV Thermal management model……....38
3.3.1 Hydraulic model……38
3.3.2 Thermal model map-based……45
3.3.3 Thermal model with thermal masses……..64

4. Results and validation……71

4.1 Hydraulic validation……71

4.2 Thermal model map-based validation……..75

4.3 Thermal model with thermal masses validation……..82

4.4 Validation summary ……....91

5. Conclusions and future developments……93

Appendix……....97

Bibliography…….....101

Acknowledgements……..103

Abstract

Vehicle electrification becomes more and more important in order to reduce fuel consumption and satisfy more restrictive emission legislations. Plug-in hybrid electric vehicles can use energy from the grid to recharge their high voltage battery. This is converted with much higher efficiency, and less CO_2 emissions, compared to the combustion engine and so they will have a significant role in the present transition from conventional to electric vehicles. The addition of new components, such as power electronics, electric machine and high voltage battery, increases the maximum torque available and the energy stored on-board, but increases the weight as well. In addition, although they have really high efficiency, they produce a significant amount of heat that has to be removed. To guarantee system efficiency and reliability, a completely new thermal management layout has to be designed. Thermal requirements of power electronics components are completely different from the ICE requirements, much lower temperature can be accepted and higher values can request power de-rating in order to preserve their integrity. High voltage battery is even more critic, since it can work correctly only in a specific temperature window and outside this, it has a rapid thermal degradation as well. The other thermal management main issue for PHEV and, especially, for BEV is cabin heating since the engine waste heat is not more available. The development of a vehicle thermal management model can surely help to better understand how design the entire system. The vehicle considered is a PHEV with a P1-P4 architecture and it has three separated cooling circuits for engine, electric machines and high voltage battery. The model developed in the present work allows to predict coolant flow rate, pressure and temperature for the three circuits. Firstly, the hydraulic part has been modelled, including pumps and pressure losses characteristic curves. Secondly, the model has been completed with the thermal description. The approach to the thermal model is simplified: for both heat sources and heat sinks the heat exchange with the coolant is calculated from a thermal/efficiency map. This limits its accuracy but guarantees low computational time. Globally, the model input are powertrain parameters (engine and e-motor rotational speed and torque) plus the control signals (for pumps, fans and HV compressor) and the output are coolant hydraulic and thermal behavior, coolant thermal heat flows, e-motor and battery temperature.

In chapter 1, a review on state of the art of PHEV and BEV thermal management has been studied. Many different layout can be developed and different circuit integrations are studied to reduce number of components and costs. In addition, control strategies can have a very significant role in reduce the cooling system impact on fuel consumption. Some innovative and predictive approaches are studied from literature. In chapter 2, basic equations that governs a thermal-hydraulic model are reported, such as pump characteristic, pressure drops calculation and heat transfer correlations. Chapter 3 describes how the model has been built in the software in a detailed way. A step-by-step procedure has been followed, starting from a hydraulic model and adding the thermal contribution only after the first part was validated. This kind of procedure is time-consuming but allows to simplify the calibration and validation of model parameters. In chapter 4, the main results obtained are compared to experimental data, made available for the present work, and the model validation is evaluated. Final chapter 5 reports the conclusions and possible future developments to complete and improve the present work.

Abstract in lingua italiana

L'elettrificazione dei veicoli diventerà sempre più preminente sia per ridurre i consumi sia per soddisfare le sempre più stringenti normative sulle emissioni. I veicoli elettrici plug-in possono utilizzare l'energia della rete per ricaricare la batteria (ad alto voltaggio). I rendimenti elettrici caratteristici dei grossi impianti di produzione di energia elettrica sono molto più elevati di quelli di un motore a combustione interna; ciò consente di ricaricare il veicolo riducendo le emissioni di CO_2 e dà a questo tipo di veicoli un ruolo importante nella attuale transizioni da veicoli convenzionali a veicoli elettrici. L'aggiunta di nuovi componenti, cioè motori elettrici, inverter e batteria ad alto voltaggio, permette di aumentare la massima coppia disponibile alle ruote e l'energia immagazzinata a bordo, ma aumenta anche il peso della vettura. Inoltre, questi componenti, pur avendo una efficienza molto elevata, producono una rilevante quantità di calore che deve essere opportunamente rimossa. Al fine di garantire efficienza e affidabilità dell'intero sistema veicolo, l'impianto di raffreddamento deve essere riprogettato. I limiti termici dei componenti di elettronica di potenza sono completamente differenti da quelli del motore a combustione, le temperature limite sono molto più basse e valori più elevati possono costringere a diminuirne la potenza, al fine di preservarne l'integrità. La batteria è ancora più critica, dato che funziona in modo ottimale solo all'interno di una specifica finestra di temperature e all'infuori di essa ha un rapido degrado termico. Un altro importante aspetto del thermal management per veicoli ibridi e, ancor di più, elettrici è il riscaldamento della cabina poiché il calore di scarto del motore termico non può più essere utilizzato. Lo sviluppo di un modello termico può certamente aiutare a progettare al meglio il completo sistema di gestione e controllo della temperatura, visti i molteplici aspetti da considerare. Il veicolo considerato nel presente lavoro di tesi ha un'architettura ibrida P1-P4 e comprende tre circuiti di raffreddamento tra loro separati. Il modello permette di conoscere portata, pressioni e temperature del refrigerante. In primo luogo, la parte idraulica è stata modellata, comprensiva di curva caratteristica della pompa e perdite di carico. In secondo luogo, è stata inclusa la descrizione termica. L'approccio al modello termico è semplificato, infatti sia le sorgenti termiche che i dissipatori basano il calcolo del calore scambiato su delle mappe. Questo tipo di approccio limita l'accuratezza del modello ma anche il tempo computazionale. L'obiettivo principale del presente lavoro era quello di costruire un ambiente in cui successivamente

sviluppare strategie di controllo di gestione termica e ciò giustifica un approccio alla modellazione di questo tipo. Gli input del modello sono principalmente parametri legati al powertrain (coppia e velocità di rotazione del motore termico ed elettrico) più i segnali di controllo (per pompe elettriche, ventilatori e compressore) mentre gli output sono la descrizione idraulica e termica del refrigerante nei tre diversi circuiti, più le temperature di batteria e motori elettrici.

Nel capitolo 1 è riportata una descrizione dello stato dell'arte attuale riguardo al thermal management in veicoli ibridi plug-in ed elettrici. I layout dei circuiti di raffreddamento sono diversi e varie integrazioni sono studiate per ridurre ingombri e costi. È evidenziata anche l'importanza delle strategie di controllo, riportando alcuni studi di strategie predittive e ottime. Il capitolo 2 comprende una introduzione al modello e sono richiamate le equazioni di base lato idraulico e lato termico. Nel capitolo 3 è descritto nel dettaglio lo sviluppo del modello: è stata seguita una procedura step-by-step che da un lato richiede tempo ma dall'altro semplifica la fase di validazione, rendendo non interdipendenti tra di loro i parametri idraulici e termici. Nel capitolo 4 sono riportati i principali risultati ottenuti, confrontandoli con dati sperimentali a disposizione. Viene valutata la validità e la robustezza del modello sviluppato nei diversi test precedentemente realizzati. Infine, nel capitolo 5 sono descritte le principali conclusioni e sottolineati possibili migliorie e sviluppi futuri.

List of figures

Chapter 1

Figure 1a: Sankey diagram for gasoline internal combustion engines……3

Figure 1b: Engine cooling system……..…….3

Figure 2: battery electric power available as function of the average temperature……..5

Figure 3: Chevrolet Volt HV Battery Heating and Cooling System……6

Figure 4: parallel hybrid possible architectures……..8

Figure 5: general schematic of a plug-in hybrid cooling system…….....10

Figure 6: Range reduction of a BEV as function of cabin heating power……..11

Figure 7: indirect heat pump system with HV battery as heat source……12

Figure 8: integrated cooling circuit for BEV with PCM storage……...14

Figure 9: ADAS-ECU communication system…….…20

Figure 10: Comparison of battery temperature for a predictive and non-predictive strategies in a RDE cycle……..22

Chapter 2

Figure 11: Moody's diagram for friction factor calculation……..26

Figure 12: pump and plant characteristic curves……...28

Figure 13: pump losses distribution as function of the specific speed…….....29

Chapter 3

Figure 14: centrifugal pump component……...38

Figure 14a: electric pump characteristic curve…….40

Figure 15: ideal fixed displacement hydraulic pump……40

Figure 16: hydraulic orifice component……41

Figure 17: inverter pressure drops, datasheet and experimental values…….44

Figure 18: hydraulic model for front axle circuit……..45

Figure 19: thermal hydraulic capacity……..48

Figure 20: AMESim radiator block (cooling library)……...50

Figure 21: radiator heat exchanged map, function of coolant flow rate and air velocity……...51

Figure 22: power losses electric motor estimation……52

Figure 23: engine left radiator, model and experimental data……...53

Figure 24: condenser block (cooling library)……54

Figure 25: simplified map-based chiller model……55

Figure 26: map-based power losses calculation for inverter and electric motor……...…...57

Figure 27a: thermal heat flows for electric motor…….58

Figure 27b: thermal heat flows for inverter front axle……...58

Figure 28: engine power losses…….60

Figure 29: comparison of engine heat rejected to coolant and engine rotational speed…….....61

Figure 30: two ways thermostat for the engine coolant circuit……..62

Figure 31: battery power losses estimation and comparison with experimental results……63

Figure 32: thermal-hydraulic pipe with heat-exchange……65

Figure 33: electric motor thermal masses for temperature prediction……...67

Figure 34: battery cooling circuit with thermal mass……68

Chapter 4

Figure 35a: volumetric flow rate validation for medium temperature circuit……72

Figure 35b: pressure validation for medium temperature circuit……..73

Figure 36a: engine flow rate validation for high temperature circuit……74

Figure 36b: engine pressure validation for high temperature circuit……74

Figure 37: engine coolant temperature, model values and measurements……76

Figure 38: electric motor power losses and heat experimental coolant heat exchange……..77

Figure 39a: velocity and IPU1 current for handling electric cycle……78

Figure 39b: e-motor and radiator coolant temperature……..78

Figure 40: ISG losses and experimental coolant heat exchange……79

Figure 41a: velocity and ISG current for handling_corsa……80

Figure 41b: ISG and radiator outlet coolant temperature……..80

Figure 42a: battery and chiller heat flows……81

Figure 42b: battery coolant temperature for validation……82

Figure 43a: EM power losses and coolant heat exchange calibration in hand_electric test…...83

Figure 43b: electric motor and inverter temperature calibration, handling electric……...84

Figure 44a: electric motor power losses and coolant heat flow validation……85

Figure 44b: e-motor and DCDC outlet coolant temperature validation……86

Figure 44c: e-motor and inverter temperature validation……..86

Figure 45a: ISG power losses and coolant heat flow validation……88

Figure 45b: ISG and IPU outlet coolant temperature validation……...88

Figure 45c: ISG and inverter temperature validation……89

Figure 46: battery and coolant temperature calibration……90

Figure 47: battery and coolant temperature for validation……91

List of tables

Table 1 estimation of the distributive pressure drops……43

Table 2 estimation of the concentrated pressure drops……..43

Table 3: summary of external model input……...64

Table 4: complete input list for simulations……..71

Table 5: summary hydraulic circuit errors……75

Table 6: electric motor parameters for two thermal masses model……...83

Table 7: battery parameters setting for thermal mass model…….87

Table 8: validation final summary……91

Table 9: thermal management model circuits list …….92

Notations

PHEV - Plug-In Hybrid Electric Vehicle

BEV – Battery Electric Vehicle

ICE – Internal Combustion Engine

HV – High Voltage

PEEM – Power Electronics and Electric Machine

ESS – Energy Storage System

BMS – Battery Management System

AER – All Electric Range

HVAC – Heating Ventilating and Air Conditioning

PTC – Positive Temperature Coefficient

PCM – Phase Changing Material

HCU – Hybrid Control Unit

ISG – Integrated Starter Generator

1.State of the art of thermal management for PHEV and BEV

Vehicle electrification brings new challenges to guarantee powertrain reliability, one of them is to design a completely new thermal management architecture. Thermal management for an electric-hybrid vehicle is more complex compared to a conventional one, since more heat sources have to be taken into account. The additional e-components, such as electric motors, high voltage battery and power electronics, generate heat and need a proper thermal management system to maintain the temperature in the optimal range both for efficiency as well as for safety. Electric machines and power electronics have very high efficiencies compared to internal combustion engines, however they produce a considerable amount of heat that it has to be removed by a coolant. Like for the ICE, the external air could cool down the components, but in general its thermal power is not sufficient and so a liquid cooling circuit better fits the hybrid powertrain requirements. A more complex cooling system requires a higher energy consumption and has a stronger impact on the total energy (fuel + electrical) consumption. Like for energy management, thermal management becomes more critical in PHEV and especially in BEV, where the energy stored on-board is limited. To reduce its impact on the energy balance, both hardware and software solutions can be applied and combined, some of them are described in this chapter.

As an introduction, a brief description of the typical cooling/heating circuits of internal combustion engines, electric motors, batteries, and vehicle cabins are reported. After that, the complete layout is considered, underling the possible integrations of the different circuits.

One of the biggest constraints for hybrid and electric vehicles is cabin climatization, especially because the engine waste heat is not more available. In the present review of vehicle thermal management, new solutions are considered. The use of heat pumps and/or of phase changing material allows a significant reduction of the thermal management impact on fuel consumption. A description of control strategies is reported as well. First, standard strategies are considered and the importance of more on-demand sensors is underlined. Then, some examples of optimal and predictive approaches allow to demonstrate that a significant amount of energy can be saved.

1.1Cooling system general requirements

Coolant properties

The coolant is a mix of deionized water and ethylene glycol, usually a 50/50 mix is used. The ethylene glycol is necessary to decrease the freezing point: with the mentioned mix the freezing point of the coolant is -36 °C. It also has an important role in avoiding the corrosion of pipes. Thanks to these properties, this mixture is used in most cooling circuits in the automotive field. The use of deionized water in hybrid cars is a necessity not only to prevent corrosion issues but also to ensure high voltage isolation.

It is interesting to notice that the addition of ethylene glycol to pure water modifies in a significant way other important properties of the coolant. Comparing it to pure water, the coolant has higher dynamic viscosity and therefore the pressure losses in the pipes are higher as well. In addition, the density is higher but the specific heat capacity is lower. At room temperature, the density is 1.077 times the density of pure water and the specific heat capacity is 0.815. This means that in order to have the same heat transfer with the same inlet and outlet temperatures, the volumetric flow rate has to be increased (approximately by 15%) [1].

Considering a hybrid electric vehicle, for each component, different thermal limits are imposed. The three main heat sources require different temperature to ensure reliability and avoid aging effects.

Internal Combustion Engine

The traditional internal combustion engine, that remains the main torque source in PHEV, need a proper cooling system to remove the amount of heat produced. Usually, it is considered that for a gasoline engine, the primary chemical energy of the fuel is divided in three equal part: mechanical work, enthalpy remained in exhaust gases and energy absorbed by the cooling system. An example is shown in the Sankey diagram in *figure 1a*.

It is known that for the internal combustion engine, the coolant should stay around 90°C and not overreach approximately 110°C (it depends on the pressure of the circuit). This limit is due to the boiling point of the coolant, that for the mixture considered is 107.2°C at atmospheric pressure and it increases following the pressure [1].

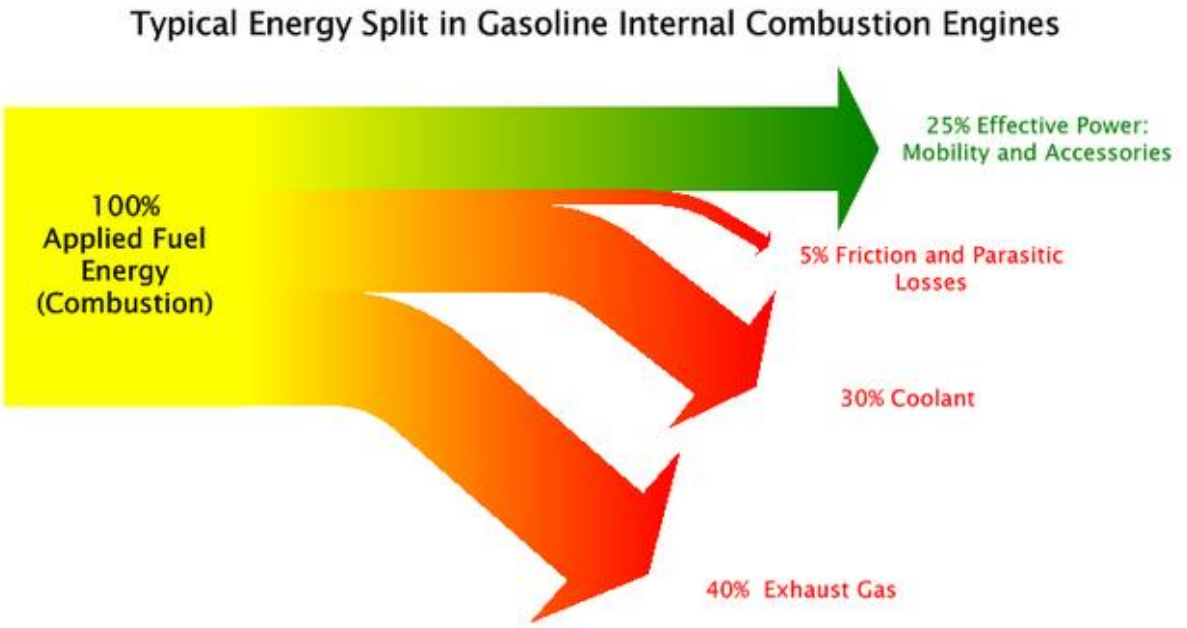

Figure 1a: Sankey diagram for gasoline internal combustion engines

The cooling system includes the water pump, generally moved by a belt, the radiator and its fan, the heater core, the degas bottle. The pump could be also an electric pump, better solution for a more efficient control.

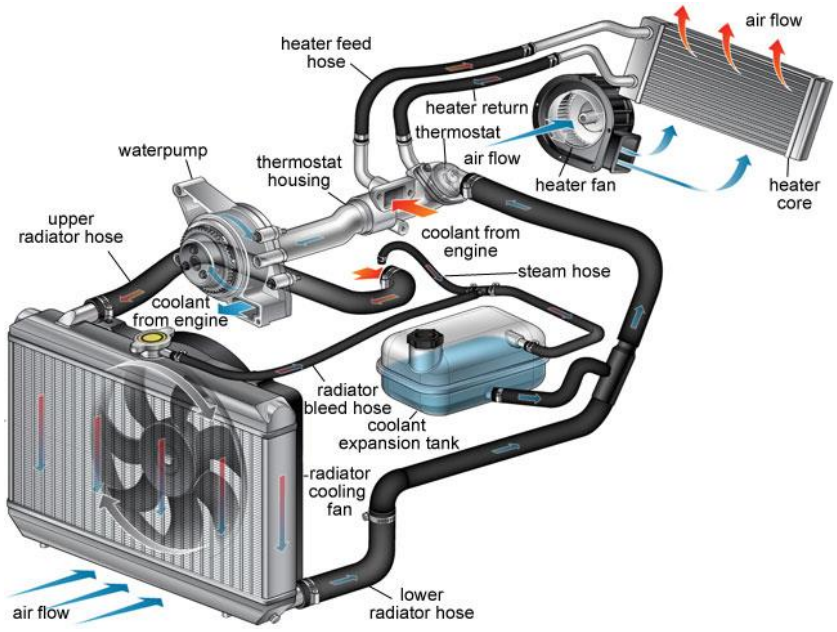

Figure 1b: Engine cooling system

The thermostat is included as well. The valve is closed until the coolant reaches roughly 90°C and then it opens and the coolant can flow through the radiator. This guarantees a rapid warm up in order to decrease all the negative effects of a cold engine and cold oil. The cold start is critic for the fuel consumption because low coolant temperature means higher viscosity and bad lubrification, so higher friction. In addition, the three-way catalytic converter has to be heated up as fast as possible to avoid emissions. To do so, the spark advance is delayed (CAT-heating) and the fuel consumption increases. Once the engine is warmed-up, the use of its waste heat to heat up the cabin is very convenient in terms of efficiency, it is possible to heat the cabin without consuming additional energy. A general scheme of a conventional engine cooling circuit is shown in *figure 1b*.

Engine thermal management does not only have to guarantee the correct temperature but plays an important role in CO_2 equivalent consumption. As mentioned, to reduce fuel consumption control strategies need to evolve and new sensors and actuators are necessary. This means that from conventional water pump, mechanical and full electrical components should be used. On-demand components permit an active control of the circuits, in order to use as less energy as possible in each operating condition.

Electric motor and inverter

Electric motors have a very high efficiency, generally around 90%. Thanks to this and to the high-power density, they find a perfect application in vehicle traction. They are fit for the downsizing concept also because they can produce maximum torque at low rotational speed.

The motors used are AC, synchronous or asynchronous. Therefore, an inverter, that converts direct current (DC) from the battery to alternating current (AC), is necessary. In addition, in a plug-in hybrid or an electric car other power electronic devices are included. The DC/DC converter is necessary to convert the high voltage of the battery (360 – 400 V) to the lower one (12 V). The plug – in charger rectifies 120-240 volt household alternating current (AC) from the grid into the direct current (DC) necessary to charge the high voltage battery.

In the cooling circuit for the electric motor, the temperature limits are lower than for the conventional engine system. The material properties of the motor impose the temperature limit, as will be better explained in the following chapter, and the coolant should not overreach

50/60°C. The same is valid for the inverter and for the DC/DC converter. Higher temperatures can request power de-rating in order to preserve the integrity of the machines.

The power losses are divided in cooper and iron losses. The first are due to Joule losses, the second are due to eddy current and hysteresis effect. Compared to the conventional engine losses, they are quite low because the power is generally lower and the efficiency is much higher. The pumps are electric and are connected to the low voltage circuit. They allow a more efficient control of temperature and energy usage, compared to the driven belt pump of a conventional engine. As mentioned, the coolant temperature is lower and the electric machine does not need a fast warm up. The lower the temperature, the better it is for the machine. So, a thermostat is not used in this cooling circuit. In addition, the power losses are not enough to heat up the cabin and a heater core is not included as well.

Battery

The high voltage battery is the most critical component. Its range of temperature is really specific and a special thermal management is necessary (Battery Thermal Management, BTM). Generally, Li-ion or Li-polymer batteries are used, thanks to high power and energy density. These kinds of batteries must work on a specific window of temperature, between 5°C and 40/45°C (*figure 2*). [2].

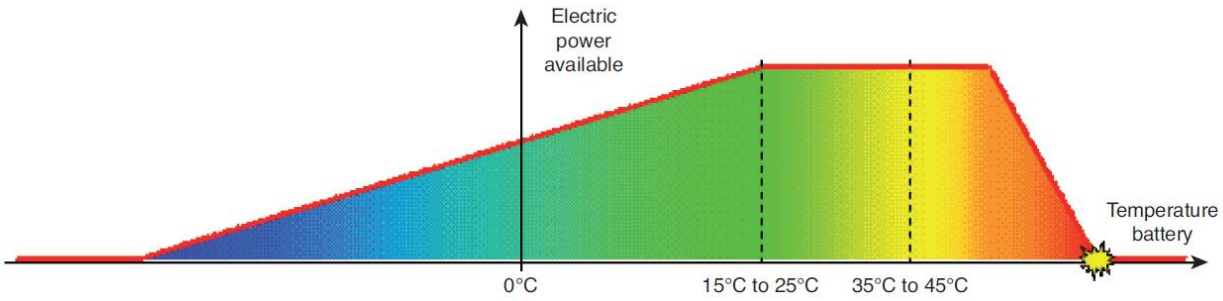

Figure 2: battery electric power available as function of the average temperature

In order to guarantee the power output, it is necessary not only to cool down it but also to heat up during cold conditions. Temperature cycles have a strong impact on battery life and aging effects. In order not to compromise battery life, its temperature should always remain in the optimal range.

For both PHEV and BEV, the battery cooling circuit is integrated with the air conditioning. The refrigerant (R134a or R1234yf) cools down the battery coolant in a heat exchanger, the chiller. In fact, the coolant must remain at no more than 30°C to be able to cool down the battery from its maximum temperature of 40°C. Therefore, the radiator could not be sufficient in a summer scenario with air temperature around these values and the integration with air conditioning become necessary.

In *figure 3*, the Chevrolet Bolt HV Battery cooling system is reported. The battery cooling system has its 12-volt coolant pump, heat exchanger (chiller) and a 3-way coolant flow control valve to route coolant through the radiator, the chiller, or the bypass. [3]

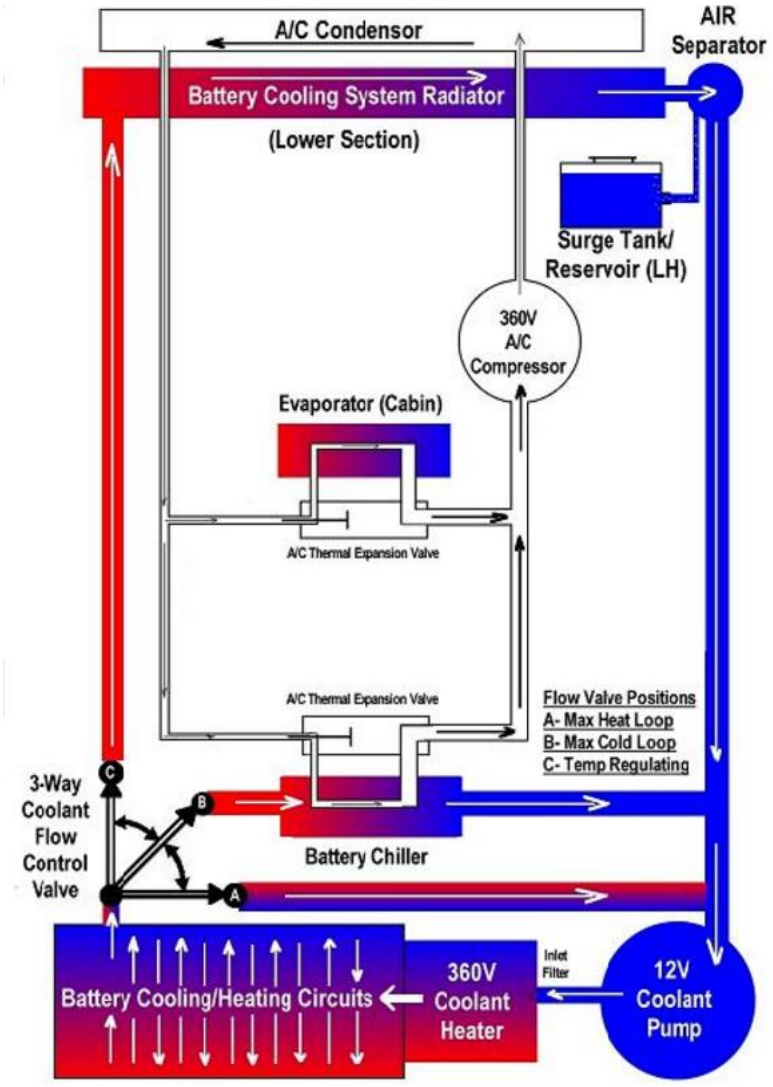

Figure 3: Chevrolet Volt HV Battery Heating and Cooling System [2]

The thermal management control unit monitors ambient conditions, coolant inlet and outlet temperatures, cells temperature, as well as refrigerant temperatures and pressures to establish battery heating or cooling requirements. Then, it turns the coolant pump on or off, positions the coolant flow control valve, and depending on whether cooling or heating is required, it requests either the electric A/C compressor to operate or to turn on the battery electric heater.
It is interesting to notice that for PHEV and BEV the thermal management is not reduce to the driving cycle but it is active also during recharging cycles. The plug-in charger and the other electronic components should be cooled down in case of high power charging rates. More related to electric vehicle, it is also possible begin to heat the cabin when the car is still connected to the plug with a predictive strategy, this allows to save the energy of the battery and increase the all-electric range (AER).

When battery heating is required the 3-way coolant flow control valve will be in position "A" (*figure* 3) and allows fast heating of the Li-ion cells in cold weather.
Whenever the Li-ion battery cells are too hot, the flow control valve will typically be commanded to position "B" and by operating the electric air-conditioning compressor, the battery coolant goes to the chiller and is strongly cooled down by the refrigerant. During stable operating conditions, the flow control valve will typically be commanded to position "C" circulating the flow of the battery coolant out to the battery cooling radiator and back to the pump. This allows to reach a thermal balance and maintain battery temperature at this optimum value (from 25°C to 30°C).

Cabin climatization

The cabin climatization of a PHEV or a BEV is completely different compared to a conventional vehicle. In the latter, as mentioned above, the engine gives its waste heat during a winter scenario, and on the other hand, an air conditioning system (at 12 V) uses a refrigerant to cool down the cabin in summer. The engine moves the compressor, a clutch allows to switch on or off the machine.

In electric vehicles, the waste heat (power losses) by the e-motors is not enough to heat the cabin because the efficiency is really high. Therefore, positive temperature coefficient (PTC) cabin heaters are used. PTC elements are ceramic stones that increase their electrical resistance

with the temperature. They have an extremely low electrical resistance at low temperature, this means a high current flow is converted into heat. When the temperature rises, less heat is released.

They are used also to warm up the battery 'coolant' when the battery is below the threshold (liquid PTC heaters). In some cases, they are also used in conventional vehicle to allow a faster heating of the cabin. The heaters affect the energy available and the AER in a significant way.

The winter scenario is critic for electric vehicle both for battery heating and for cabin heating. To improve performance, other solutions are applied, such as heat pump systems (explained in the following paragraph). For what concerns the air conditioning, the system is the same as conventional cars but the compressor has its own electric motor that receives current and voltage from the HV battery. As shown in *figure* 3, the air conditioning does not only have to cool down the cabin but also the high voltage battery. Therefore, the power of the compressor must be higher than in a conventional system.

1.2 Thermal management Layout for Hybrid Vehicle

As it has been explained, each heat source needs a different coolant temperature. The possibilities to design a complete thermal management layout of the vehicle are various, and some of them are described in this paragraph. The layout is strictly connected to the hybrid architecture, that is the position of the electric motors in the powertrain. The hybrid powertrain considered has a parallel architecture, both the ICE and the electric motors can directly power the wheels.

Parallel Hybrid topology

The driveline topology is the starting point for thermal management layout. Depending upon the electric motor position, the hybrid topology takes different names, as shown in *figure* 4:

- P0, the electric motor is the integrated starter generator mechanically connected to the engine.
- P1, in which the motor/generator is located on the engine shaft, before the clutch, so their rotational speed are the same.

- P2, in which the electric motor is downstream the clutch and so pure electric driving is possible.
- P3, where the motor is after the secondary shaft of the gearbox.
- P4, where the motor is on the axle directly.

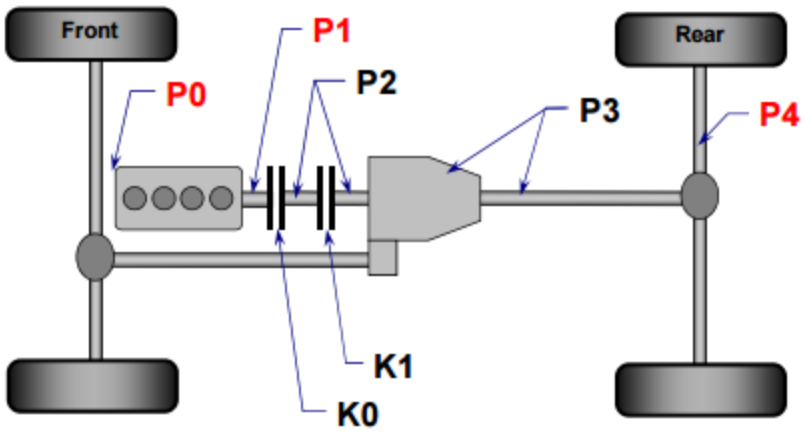

Figure *4: parallel hybrid possible architectures*

The battery position plays a key role in the entire thermal management layout as well. Packaging problems must be considered in details in order to design cooling circuits avoiding too complex layout and limiting their lengths.

For high voltage battery, an additional problem is due to electric high voltage connections. They need special isolations for obvious safety reasons.

In the P0 and P1 configuration, the cooling of the electric motor and of the inverter become more critic because they are heated not only by its power losses but also by the ICE.

Example of cooling systems layout

An example of a complete system is shown in *figure 5*. The circuits are divided in:

- High temperature circuit, including ICE and high temperature radiator (and engine oil)
- Medium temperature circuit (or Low temperature 1), including electric drives and power electronics and also lubricant for transmission

- Low temperature circuit (or low temperature 2), including HVAC system and battery cooling

At least three circulation pumps are necessary. In addition, the air conditioning compressor has to be powered. The entire system becomes more expensive and more energy consuming compared to the cooling system of a conventional vehicle. Although the temperature requirements are quite different from the three circuits, attempts to integrate some circuits are made in [4]. The idea is that if the peaks of thermal loads are misaligned, an integration of ICE cooling and electric drive cooling could be made. This allows to save greatly on costs, using less pumps and less radiators. An important attempt to reduce energy consumption for cooling and cabin confort is due to the Optemus project (Optimized Energy Management and Use). The aim of the project is to develop new integrated thermal management solutions and demonstrate a minimum of 32% of energy consumption reduction for component cooling and 60% for passenger comfort, as well as an additional 15% being available for traction, leading to an increase of the driving range in extreme weather conditions of at least 38% in a hot environment and 70% in a cold environment. [5]

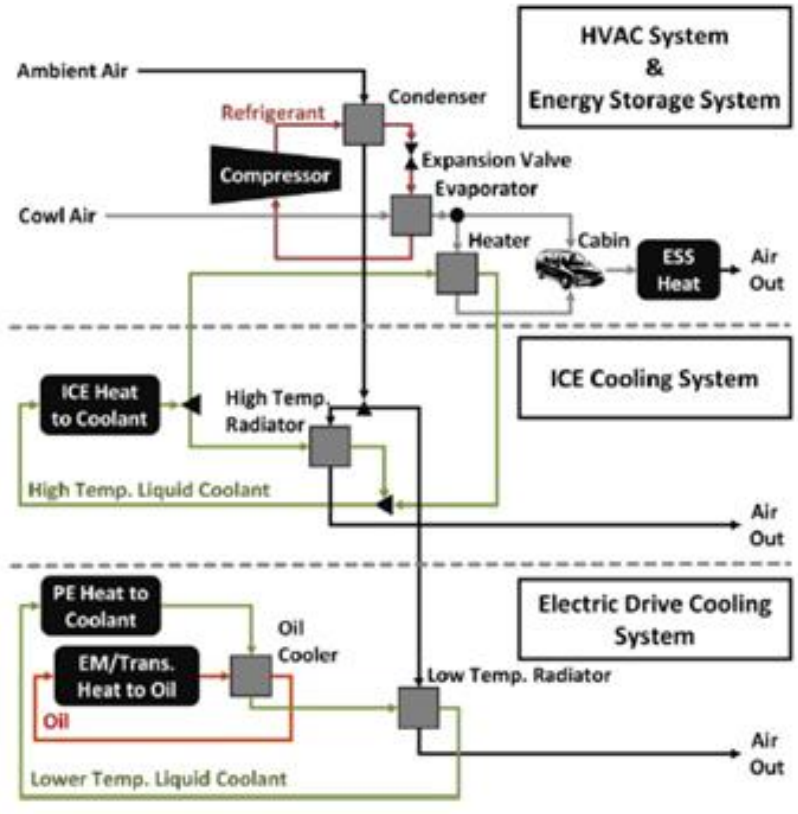

Figure 5: general schematic of a plug-in hybrid cooling system

However, nowadays the circuits are generally separated and the only integration is between air conditioning and battery. The architecture with three separated circuits, air conditioning and PTC heaters is the most common in new plug-in hybrid cars. The main problem is the high-energy consumption for cabin climatization, this is particularly important in the battery electric vehicle. In order to increase the efficiency of the system, new solutions, like the two examples presented in the following paragraphs, are studied. They are already applied in electric vehicles, and probably, they will be used in the next generation of hybrid cars.

Heat pumps

Cabin heating for electric vehicle (and partially for plug-in hybrid electric vehicle, during pure electric mode) is critic. Waste heat from ICE is not more available and the power losses for electric motor are not enough to satisfy the thermal power request. Usually, PTC heaters are used but they cause a significant decrease of the all-electric range. In *figure* 6, an example of the range reduction for an electric vehicle due to cabin heating is reported.

While the efficiency of the PTC heaters is limited to one, heat pump systems can have better performance, thanks to Coefficient Of Performance (COP) greater than one. The efficiency of the heat pump is so high because they use heat from ambient air (or waste heat from other heat sources). The technology is already used in the Nissan Leaf, first mass-produced electric vehicle to employ a heat pump as cabin heater, and also on the Audi Q7 e-tron, first on the plug-in hybrid vehicle class.

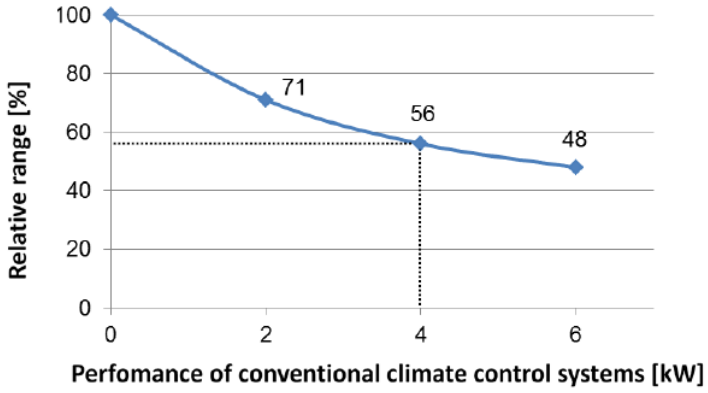

Figure 6: Range reduction of a BEV as function of cabin heating power [6]

Thanks to the heat pump, that can work both as a heater and as a cooler, existing power unit (electric motor, generator) can be included in the vehicle's heat balance.

Improving AER with no comfort reduction is not the only advantage of this system: controlling the temperature promotes better durability and less de-rating effects, reduction in refrigerant losses into the environment (greenhouse gases). The main disadvantage is the higher cost.

Layout of the heat pump includes compressor, evaporator, expansion valve and condenser. It also features accumulator, directional control valve and tubes. The directional 4/2 valve (four ports and two positions) is the key component that allows the redirection of the coolant, making both heating and cooling possible. [6]

After the compressor and the condenser, the refrigerant passes through the expansion valve (ideally isenthalpic transformation) in which high temperature and high pressure drop to lower values. The fluid moves on to the evaporator and cool down the refrigerant. The evaporator is a plate exchanger identical to the condenser, so the heat transfer is the same. Thanks to this and to the directional valve, reverse circulation is possible.

In some cases, the PTC heater is present in this architecture as well. If the heat provided by the heat pump is not sufficient, it supplies the supplementary heat required. In addition, more complex solutions are studied. The system here explained is a direct system, but also indirect systems are developed,

Indirect systems do not exchange heat directly with the external air but with the battery (or electric components) cooling circuit. Among the advantages of this solution, there are the possibilities to use battery and electric components as *heat sources*. In addition, less refrigerant is used compared to the direct system. The main disadvantage is the higher difference of temperature between condenser and evaporator, due to the additional heat exchange. This means higher pressure ratio and more power consumed by the compressor.

Indirect systems are very promising, since the reuse of dissipated heat for the cabin heating could improve the efficiency significantly and decrease the impact of cabin climatization on the AER reduction.

The *figure* 7 shows an example of indirect heat pump system with two 4/3 bidirectional valves built by VOSS. [7]

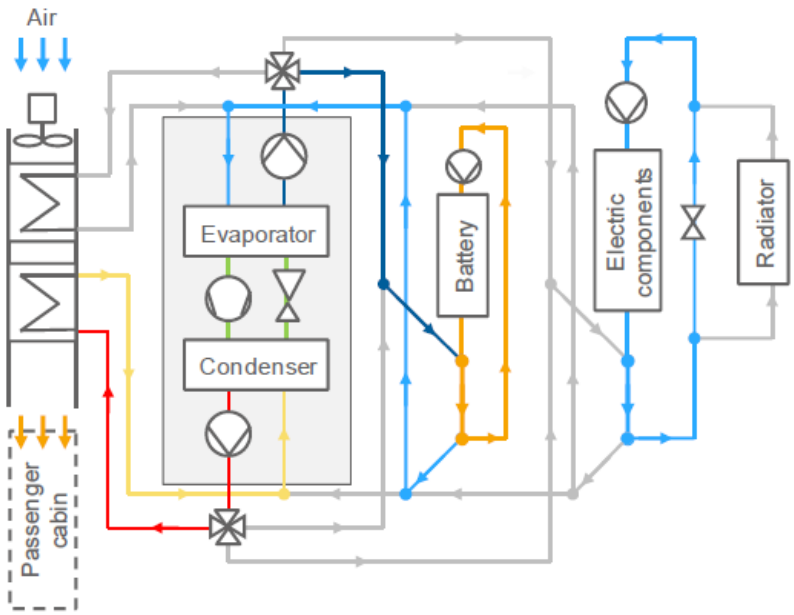

Figure 7: indirect heat pump system with HV battery as heat source [7]

Thanks to the valves, the battery can be used as heat source for cabin heating in a winter scenario. In the same way, the electric components can be used as well. The temperature and the pressure in the evaporator should be higher than the case in which ambient air is used, and so the efficiency. In addition, the system can prevent problems of ice formation on the evaporator (possible in other heat pump systems). The battery can be used as heat source only when its temperature overreaches the low limit, since in this condition it has to absorb heat and cannot be a heat source.

In a summer scenario, the advantages of the system are less evident. The two valve force the flow out of the evaporator to the cabin and to the battery (when necessary). They can regulate the flow in order to maintain the desired temperature, like the thermal expansion valve does in a conventional air conditioning system. On the other hand, the refrigerant must release the heat to the coolant in the condenser. Then, the coolant is cooled down by the external air in the radiator.

Phase Changing Material thermal energy storage (PCM)

Another solution to improve the heating of electric vehicles is Phase Changing Material (PCM) thermal energy storage. They are materials with a specific melting temperature and a really high heat of fusion. Like heat pumps, they find application in buildings to increase the thermal

mass and allow lower overheating in summer and higher thermal isolation in winter. Thanks to the melting process, these storages reach very high energy densities. The difference of density among liquid and solid should not be too high, otherwise the circuit would be pressurized after a phase change. In addition, the thermal conductibility should be as lower as possible to increase the efficiency of the system.

Some studies have been done, in which PCM storage are used in electric vehicle. The system can absorb waste heat from battery cooling circuit and storage the thermal energy. This energy can be gradually released in order to maintain battery and cabin warm, reducing the warm up phase and its impact on AER reduction. The solution looks promising, it manages to reuse waste heat during the most critical phase of the warm up. The limits are the costs of the materials, still too expensive to find applications in common vehicles.

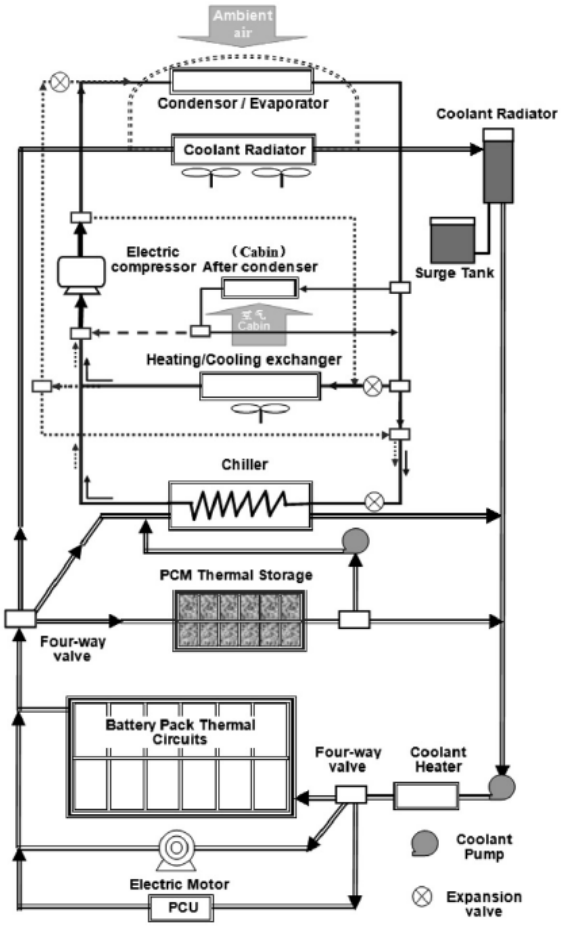

Figure 8: integrated cooling circuit for BEV with PCM storage

In *figure* 8, a BEV cooling system layout with PCM storage is reported. In [8], a long review of PCM classification and main applications is described. Different PCM storage materials can find applications in both electric and conventional vehicle. For the electric vehicle, battery and cabin can maintain higher temperature during long stops. PCM storages suitable for this application has a melting temperature of 30°C: during the last run they melt absorbing battery power losses and can maintain a temperature that is 17°C higher than ambient temperature for 12 hours. PCM thermal storage can find application also in conventional vehicles to decrease warm up times. Friction and emissions can be reduced, since oil and catalytic converter are heated up faster.

1.3 Control strategies

The previous paragraph described some examples of the hardware cooling systems and some solutions to decrease the energy consumption of cooling and climatization. Software strategies can significantly contribute, as well.

Before describing the control approach, it is important to highlight that more electrical actuators and smart valves are necessary. Substitution of the water pump and the thermostat with on-demand components is essential to obtain a more efficient control depending on the operating conditions. The rotational speed of a mechanical water pump moved directly by the driven belt cannot be controlled but it only depends on the engine rotational speed. It is evident that this kind of control cannot be optimal. But, on the other hand, mechanical water pumps are the cheapest solution (variable mechanical water pump or electrical pump). The electric pump has another advantage: since is completely independent on engine rotational speed, the pump can cool down the engine also when this is not running, avoiding overheating at the end of the run. The thermostat could be replaced with more efficient and *on-demand* components too. An example is presented in [9].

The Thermal Management Module (TMM) is a multi-circuit valve which enables variable coolant flow rate. It offers the option to control the circuits with electronical control and allows the setting of the temperature according to the component requirements to maximize the fuel efficiency.

The same is valid for the compressor, that in a conventional car is moved by a belt but in PHEV is moved by an electric motor and it can be regulated independently by the HCU.
The targets of the control strategies must be defined.
Thermal management targets are:

- Maintain the optimal temperature range for each component in every operating condition, in order to provide reliability and durability;
- Utilize as little energy as possible.

It is evident that the two targets are opposite, therefore a tradeoff must be achieved.
The energy consumption is due to pumps, fans, the air conditioning compressor and electric heaters. They should only use the optimal amount of energy to guarantee the desired temperature in each condition. The thermal management basic strategy is monitoring all the critical temperatures with temperature sensors, and only when one overtakes a limit, the control unit makes the electrical pumps move and the fans cool down that component. In the same way, cabin temperature has to be guaranteed as required by the driver and the compressor is to switch on or off depending upon the difference between real and target cabin temperature.

Pump regulation

The centrifugal coolant pump has a characteristic curve, increase of pressure as function of the volumetric flow rate, and an efficiency curve. The fundamental equations to describe a centrifugal pump are reported in the next chapter. The pumps are designed to work in a fixed point, defined by the characteristic curve and by the circuit. But to save energy, the pump has to run as less as possible. The flow rate of the pump can be regulated in different ways, with different impact on the efficiency. One option is use a valve which cause a restriction and an increase of pressure drop. The operating point shifts to the left, with a higher increase of pressure and a smaller flow rate. This method has a strong impact on the efficiency, as it can see from the efficiency curves, and it is used only when it is not possible to change the rotational speed of the pump, since the electric motor is connected to the grid.
As mentioned, regulation is more efficient in changing the rotational speed of the pump, allowing to work near the maximum efficiency area. If the motor is connected to the grid and

so its rotational speed is fixed, an inverter can modulate the frequency changing the speed of the pump.

Actually, in the cooling system, the pumps are moved by separated motors. They absorb current directly from the low-voltage battery and the rotational speed can be always modulated to regulate the flow rate. The pump has maximum efficiency at a specific rotational speed and so, generally, it always works at this point.

They always have the same flow rate and the maximum efficiency and they are switched on or off depending upon the temperature and the control strategy. Apart from the basic strategies, a more complex approach has been studied, like optimal approach based on predictive information. Some examples are described in the next paragraph.

Thermostat and fan

The conventional engine cooling system uses a wax thermostat. The function of the thermostatic valve is to maintain the desired temperature in the cooling system, that for the engine is between 80°C and 90°C. Below this temperature, the wax is solid and the valve is closed due to a spring force. Once this temperature is reached, the wax starts to melt and expand, overtaking the spring force and opening the valve. It works well, but the sensible element has a thermal inertia and so the response can be quite slow. Electric thermostat can be also applied and guarantees faster response time.

While for the engine cooling system the thermostat allows good control, for the battery cooling circuit more complex valves are necessary. As described in the example of the previous chapter, the battery cooling system has a higher degree of freedom since it can heat up the battery, cool down it with the radiator or cool down it with the chiller. A mechanical valve cannot manage this system, therefore an electric, and more expensive, valve has to be employed. For this situation, a 4/3 (4 ports and 3 positions) valve has to be foreseen.

Another electric controlled device in the cooling system is the fan. Its control is, generally, simple: a temperature sensor measures the coolant temperature and sends the information to the ECU. Depending upon this value, the control unit electrifies the fan with a linear, or a more complex, response. The position of the temperature sensor can be downstream the radiator or near the thermostat, but other solutions are possible as well.

Cabin climatization and battery thermal management

As described in the previous chapter, cabin climatization is critical for its strong impact on the state of charge of the battery and many solutions have been adopted.

Not considering heat pump solutions for the moment, the typical HVAC system for PHEV includes a high voltage compressor and an air conditioning system integrated with the battery cooling system (through the chiller heat exchanger), plus the PTC heaters (air and liquid) and eventually a heater core of the engine cooling system.

It is evident that a lot of control strategies can be applied and they play an important role in the energy impact of cabin climatization.

Considering a summer scenario, the thermal management control unit has to guarantee the driver-imposed cabin temperature and the battery temperature employing the HV compressor. The refrigerant flow rate through the evaporator and through the chiller is regulated by the thermal expansion valve (TXV) that divide the high and low pressure sides. The lamination valve allows that the refrigerant flow rate is the exact amount to satisfy the evaporator thermal request. It guarantees an increase of efficiency, since the compressor only works when it is strictly necessary. The thermal sensitive element (bulb) is connected to the diagraph by a capillary and it is located after the evaporator, monitoring the temperature change. This change of temperature is also a change of pressure and it is received by the diagraph. When the pressure of the bulb overtakes the preload of the spring, the valve opens and the refrigerant flows through the heat exchanger. When the temperature of the evaporator, and so its pressure, becomes lower the valve starts to close.

The thermal expansion valve does not need any electric connections, since, like the thermostat, it is the sensitive element that allows the flow regulation.

The HCU controls the rotational speed of the HV compressor, in order to satisfy the aforementioned thermal demands. The basic idea is that the cabin and battery temperatures are monitored, and when they overtake the target, the compressor begin to run and the refrigerant absorb heat from the evaporator or from the chiller. The relationship between the difference of temperature and the increase of rotational speed can be linear or more complex.

In a winter scenario, the PTC heater and the heater core has to provide the heat requested by the cabin and, eventually, by the battery. Not considering heat pump solutions, the battery could be heated up only by the PTC heater. The electric heater can heat the air near the battery

or, more frequently, the battery coolant. In this configuration, there is not a degree of freedom, the heater absorbs the necessary current until the battery overtakes the lower operating temperature limit.

For the cabin, the control is more complex, since both the devices could satisfy the thermal request. It is clear that it is more efficient to use the waste heat of the engine as much as possible and save battery energy, but if the vehicle is driving in pure electric mode, this is not possible. The choice is complex since different constraints have to be considered. Like for the pump regulation, optimal approaches are studied and some examples are reported in the following paragraph.

1.4 Predictive thermal management

After the description of some basic thermal management strategies, a predictive approach is considered. A predictive strategy means a control system which can know different kinds of information from external sources, and use these to improve the vehicle management. Predictive strategies could be applied in both energy management and thermal management, and can contribute to reduce the fuel consumption but also to the improve components' lifecycle expectancy.

ADAS

New vehicles are able to communicate with the external environment thanks to the ADAS (Advanced Driver Assistant Systems).

The systems are equipped with new sensors, like cameras and GPS. The technologies are divided in V2V (Vehicle to Vehicle) and in V2I (Vehicle to Infrastructure). The second ones are long- or medium-distance communication systems. The connected vehicle become can know navigation data and route conditions, and allow the implementation of predictive strategy.

For what concerns hybrid vehicle control strategies, route conditions info can be applied in energy and thermal management. A typical situation is the traffic light: the car is at a constant speed, the control unit receives information of red light phase in a known time, and calculates, depending upon the known distance, if the vehicle, without accelerating, can pass the traffic light in time. Therefore, it can decide not to interfere (if the vehicle manages to pass) or decide

to switch off the engine and start to recover energy with breaking (coasting). The earlier information is known, the less is the energy consumption. [10]

Navigation data and preconditioning

Predictive control of the temperature is highly attractive because, due to the high thermal inertia of both ICE and battery, the thermal response is always quite slow. The possibility to know the temperature behaviour in advance gives a great gain comparing to the common situational approach. The main idea is, once the driving cycle is known in terms of split factor, the control unit can begin to precondition either the ICE or the battery. In this way, it is possible, for example, to increase the all-electric range since the battery will reach its maximum temperature later than in a common strategy.

The navigation data used in thermal management are map data, including speed limits, built-up areas and slope, and traffic situation. They are obtained rearranging GPS and traffic info.

Like for energy management, many studies are made on thermal management optimal strategies and the fuel saving advantages have been demonstrated. The problem is clearly the too high computational data and so an optimal approach is not possible on-board. ADAS allows a partial knowledge of the driving cycle (generally, only a few kilometres) and these strategies are called sub-optimal.

To optimize the thermal management, data must be collected and organized very well. The scheme here considered is reported in [11].

Data is transmitted via the controller area network (CAN) to the engine control unit (ECU). A horizon reconstructor (HRC) should create the electronical horizon. Only the relevant navigation events are saved and organized in array, fundamental to save computational memory.

After data preparation, several detection algorithms analyse the data in order to find relevant events for the thermal system. Example of events are the beginning of a city area or a high load cycle with a relevant slope. Algorithms do not only consider data from ADAS sensors, but also from conventional cooling system ones (actual temperature of the coolant). They calculate the distance and the length of the event and send information to the application function, that finally decide which strategy is the best.

Figure 9 shows the function and sensors involved in the predictive thermal management.

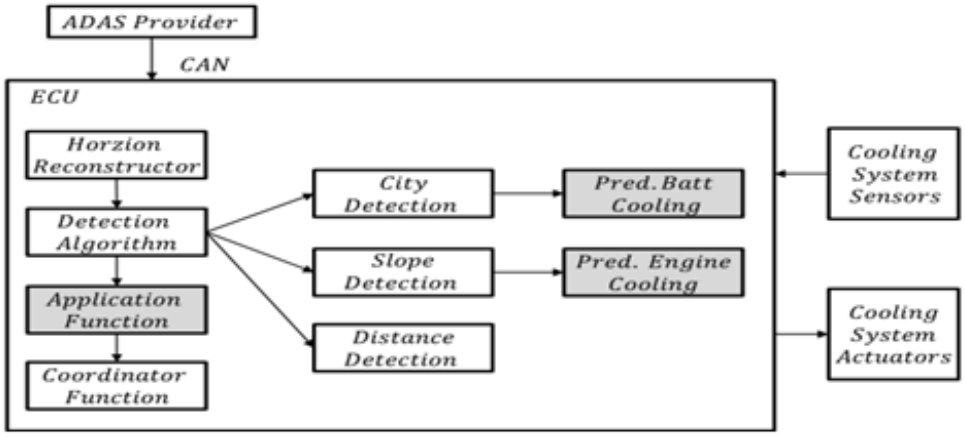

Figure 9: ADAS-ECU communication system [11]

As mentioned above, several events are provided by the horizon reconstructor: speed limits, slopes, built up areas. All the data is stored by a value and a position. That means each speed limit has a value in km/h and a position in m. The ADAS specification imposes a limit in the counter of the position, that means every time the limit is reached the counter is reset. A trade off must be done to save memory and not lose relevant information.

After the distance and the length of the event are known, the application function has to choose a strategy. In a predictive strategy, it is not sufficient to know the coolant temperature from the sensors but it should be important know the temperature behaviour in the next future. In this way, the system can react in advance if it is suitable.

A cooling circuit model, real time and implemented in the HCU, can be developed. The control-oriented model is presented again in [11], considering the cooling circuit model for battery temperature prediction and preconditioning.

In the same article, a detection algorithm is used to detect city areas. Speed limits and built-up areas data is provided by the horizon reconstructor. When the speed limit is 50 km/h and the built-up area signal is true, the HCU detects a city area event. Then, the application function has to decide from environmental conditions, battery temperature and length of the event, if a predictive cooling is suitable. Another degree of freedom is present, since the battery can be cooled either with the radiator or with the chiller and the air conditioning circuit. Therefore,

not only the application function has to decide to cool down or not, but also how heat sink should be used.

The predictive strategy cool down the battery before the city area starts, maintaining the battery temperature at lower values and, potentially, increasing the all-electric range. The system can also predict the battery temperature at the end of the event and can decide that cooling via the chiller is not necessary, use only the radiator, and save significant value of energy.

Optimal approaches

Another study is done in [12], where a non-linear model for predictive thermal management, in particular for the HV battery and for Power Electronics, is developed. The method presented, Model Predictive Control (MPC), is based on an optimal/suboptimal control and is recommended for finding optimal solutions in complex multi inputs and multi outputs problems. The main idea is to use the control-oriented model to predict the future behaviour of the system within a time horizon and the optimization algorithm to find the best control strategies in order to satisfy the constraints.

The model must be accurate while also being fast enough considering the computational capacity of the HCU.

Once the model is developed, the optimization begins. The target function, the model equations and the physical constraints must be provided. In the present case, the target function is the optimal temperature for the battery, that is 28°C. The constraints impose values that the mathematical optimizer cannot exceed. They are, for example, a maximum and a minimum coolant temperature, maximum energy of the battery, torque of the electric motor, and so on.

The model is then validated and the optimal strategy is compared to the standard one.

The results are very promising, a significant energy reduction is feasible with an optimal strategy. In *figure* 10, the battery temperature for the predictive and standard strategies is reported. The energy consumption reduction due to the coolant pump is reported as well. The optimal strategy manages to have a higher final temperature but inside the desired window, allowing to consume less energy.

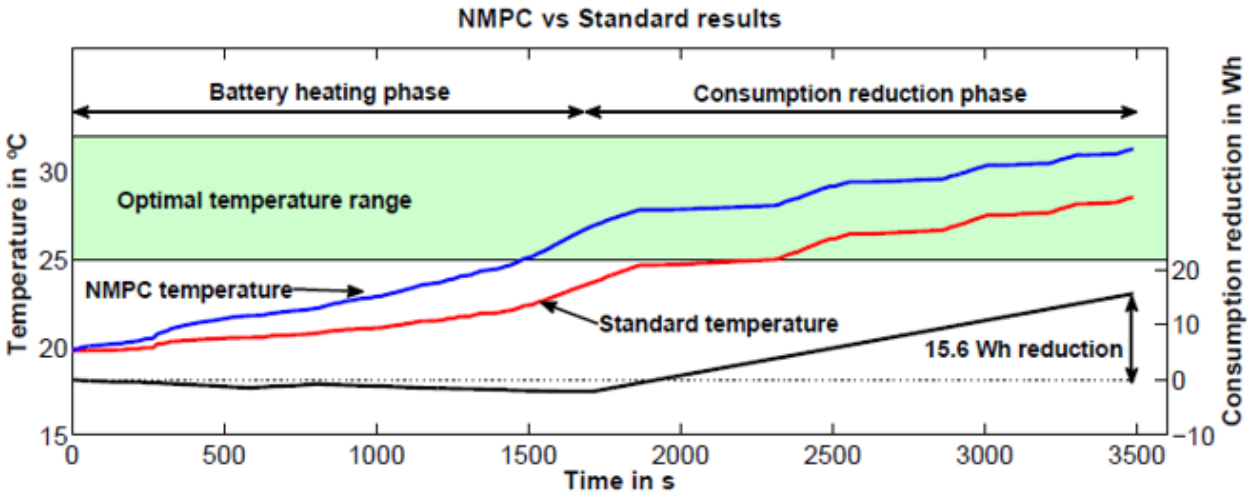

Figure 10: Comparison of battery temperature for a predictive and non-predictive strategies in a RDE cycle [12]

Another example of optimal approach towards thermal management problem can be found in the cabin heating, like in [13]. As mentioned, the cabin can be heated up either by the heater core, using engine waste heat, or by the PTC electric heater, using battery energy. A predictive model control is developed considering the start and stop of the ICE. The goal functions are: providing the thermal power requested, maintaining the battery's state of charge within the desired limits and minimize the fuel consumption. The output of the algorithm is the optimal split of the thermal power between the two heaters. The results show an improvement of 3% of fuel savings, compared to the standard control strategy. To sum up, different studies demonstrate the advantages of predictive strategies. The next step of development will be a better integration of this approach in a real vehicle, optimizing data from ADAS and models to temperature prediction in HCU. Predictive thermal management will be also integrated with predictive energy management, realizing a global optimal control and important fuel consumption/CO_2 emissions reduction. Thermal requests have to be taken into account in order to have a globally optimal control strategy and find the optimal split power factor. For example, turning on the ICE should not be decided only by the energy management strategy (EMS) but also by the TMS. If the cabin has to be heated up, it could be globally better to turn on the engine and use its waste heat and not the electric heater, also if the EMS had decided on pure electric driving.

2.Introduction to the thermal model and system description

Before starting the presentation of the cooling circuits and how these were designed in AMESim® environment, a description of the fundamental equations for hydraulic and thermal simulation is reported.

As mentioned above, the system is considered divided in three circuits with three levels of temperature: high temperature for the engine, medium temperature for the electric motor, ISG and the power electronics components and low temperature for battery cooling and air conditioning.

For each circuit, a hydraulic description has been done. The pressure losses for each component are calculated and the total pressure increase of the circulating pump has been imposed. From its characteristic curve, the volumetric flow rate has been determined. Prior to considering the model, a general mathematical description of pressure drops and pumps is reported in this chapter.

For what concerns thermal generation modelling, the problem has been simplified considering four types of heat sources: ICE, electric motors, power electronics and battery. In order to model the thermal behaviour of each component, we need to understand the amount of heat produced as function of the different operating conditions. As it will be better described, the thermal generation is based on a map of efficiency. So, a detailed physical description is not included. The heat produced will propagate inside the material and it will be transferred to the coolant and to external air. Both conduction and convection are modelled in order to predict material temperature. It is really important to know how these heat sources interact with the coolant and understand how the heat exchange is calculated using heat transfer theories. In this chapter the fundamental equations for heat transfer are discussed, since they are the base for the simulations that include thermal masses.

2.1 Hydraulic modelling background

Pressure drops

In order to simulate the hydraulic circuit, we have to know the pressure drops in the ducts and in the components. They are important to size the pumps and to understand the efficiency of the entire system.

The pressure drops are the sum of concentrated and distributed drops. The concentrated pressure drops are caused by an obstacle, such as a deviation or a bend of the pipe. They are calculated with fix adimensional coefficient, functions of geometry of the obstacle and of Reynolds number, as

$$R = \beta(Re)\frac{W^2}{2}$$

where R represents the losses, β is the adimensional coefficient and W is the velocity of the fluid.

The distributed pressure drops are expressed as

$$R = \lambda\frac{l}{D}\frac{W^2}{2}$$

where λ is another adimensional coefficient, l and D are the length and the diameter of the pipe.

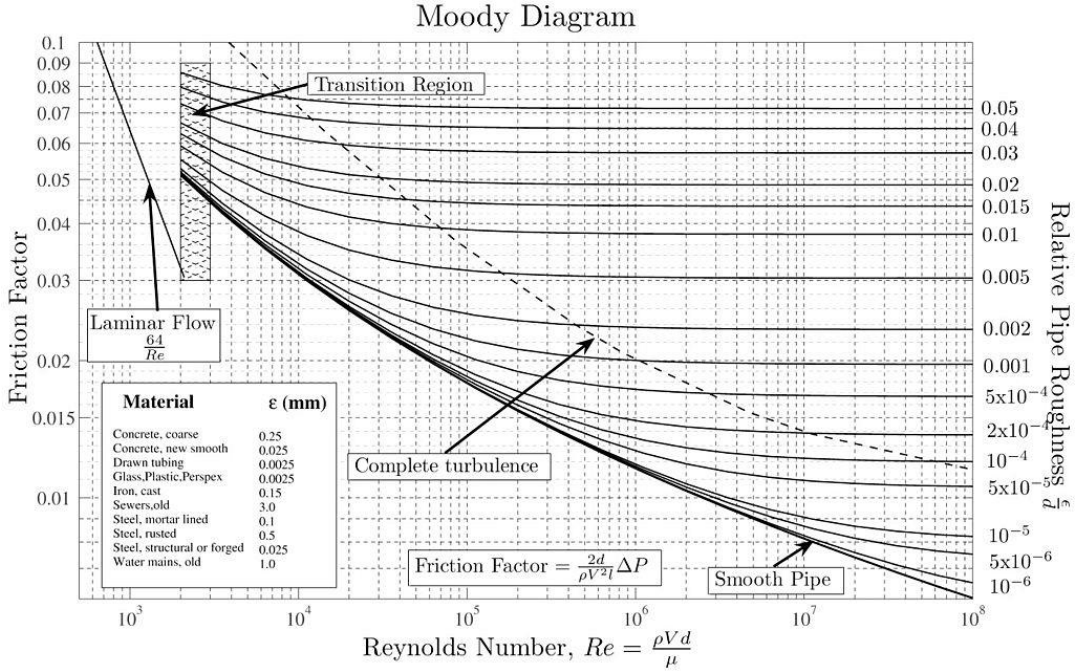

Figure 11: Moody's diagram for friction factor calculation

The coefficient λ is called friction coefficient and has different expressions depending on whether the flow is laminar or turbulent. For laminar flow the coefficient is constant and its value only depends on the geometry. For circular pipe the friction factor is

$$\lambda = \frac{64}{Re}$$

For turbulent flow λ is function of the Reynolds number and of the relative roughness. For circular pipes, we can use the Moody diagram to calculate the friction coefficient (*figure 11*). Once its value is known, the distributive pressure drops are determined by the geometrical characteristic of the pipe.

Centrifugal pumps

To circulate the fluid in the cooling system, centrifugal pumps are employed. The characteristic curves of these machines show the pressure increase and the efficiency as function of the volumetric flow rate.

The hydraulic head indicates the work done by the pump on the fluid. It measured in meters and it is derived from the general fluid equation, as reported in [14]. It is:

$$H = \frac{\Delta p}{\rho\, g}$$

where the difference of velocity (kinetic contribution) and of height (gravitational contribution) between inlet and outlet are neglected.

The net power transferred to the fluid is

$$P = \rho\, \dot{V}\, gH$$

The efficiency of the pump is the product of three contribution:

- hydraulic efficiency, which consider the fluid dynamics losses in the impeller
- volumetric efficiency, which consider the losses due to leakage along the seals
- mechanical efficiency, losses for friction in the bearings.

The total power absorbed by the pump is

$$P_a = \frac{\rho\, \dot{V}\, gH}{\eta_h \eta_v \eta_m}$$

with the obvious meanings of the symbols.

The characteristic curve (QH graph) can be obtained as difference of the work made on the fluid less the total pressure losses in the pump. For each rotational speed, a different characteristic curve is defined.

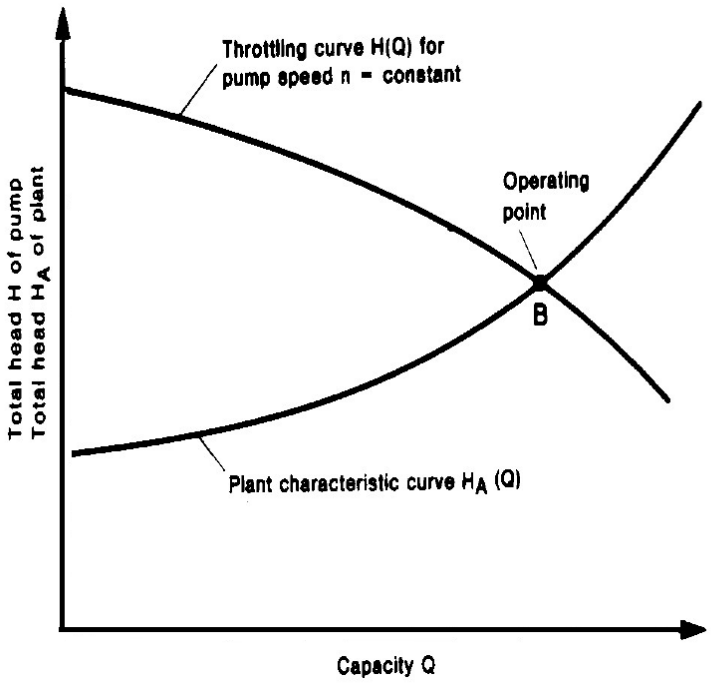

Figure 12: pump and plant characteristic curves

The curve has to be put on the same chart with the total pressure drops of the circuit and the intersection becomes the operating point, as shown in *figure* 12. The choice of the pump should guarantee efficiency when the operating point is near the maximum. In addition, cavitation must be avoided in every possible operating condition.

The hydraulic efficiency is function of the flow rate as well, as reported in *figure* 13, and has a maximum at the operating point. In this chart, due to [15], the losses contributions as function of the specific speed are reported.

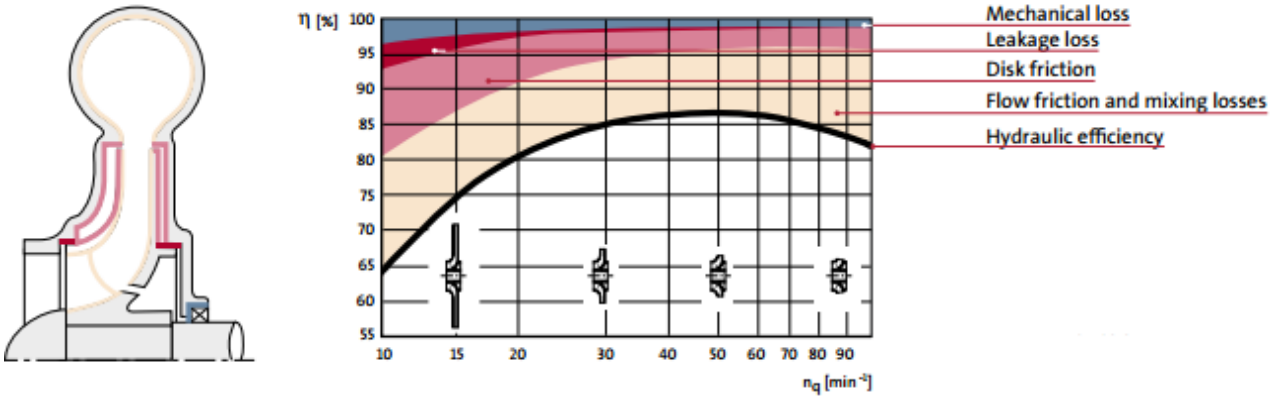

Figure 13: pump losses distribution as function of the specific speed [15]

The regulation of the flow rate can be done in different ways, as described in the chapter 1. The use of a restriction to decrease the flow rate increase the pressure drops of the circuit, therefore the operating point moves to left in the chart. But the efficiency reductions are significant if the variation is higher than a few percent. A regulation on the rotational speed is more efficient, since the characteristic curve and the operating point change allowing to remain in the maximum efficiency zone. It is possible to predict how the flow rate, the hydraulic head and the power change as function of the rotational speed, using the affinity rules. These rules are all derived under the condition that the velocity triangles are geometrically similar.

$$Q_2 = Q_1 \frac{n_2}{n_1}$$

$$H_2 = H_1 \left(\frac{n_2}{n_1}\right)^2$$

$$P_2 = P_1 \left(\frac{n_2}{n_1}\right)^3$$

More specific control strategies are used, like proportional-pressure control or constant-pressure control. They allow a more efficient use of the energy available.

The proportional-pressure control try to maintain the hydraulic head linear with the flow rate. This is done changing the rotational speed and moving to other characteristic curves. The regulation is done until the maximum speed is reached, then the pump remains in the same curve. The strategy allows to keep the same differential pressure with different thermal request. If a thermostatic valve is present, this control allows to avoid to leave the valve partially closed,

and to produce noise, reducing the flow rate with the pump. The constant-pressure control is done to maintain the hydraulic head constant for every flow rate, until the maximum speed is reached. This finds application in open circuits, like in a water supply system where a different consumption does not affect the pressure of the fluid.

2.2 Heat transfer theory

Conduction

The conduction governs the heat exchange between solid materials. The general approach for a thermal model is to consider the thermal losses concentrated in a single thermal mass and link them together using thermal resistance. The heat source, as the electric motor, can be divided in more thermal masses and the heat spreads from one to another following conduction law. For example, the losses of the rotor propagate to the stator and then to the cooling plate. In literature, very complex models of electric motor are studied, like in [16]. In the present work, a simple approach has been used to determine the temperature of the motor (or other heat sources) and the conduction effect are not modelled in a rigorous way. However, it is interesting to report and keep in mind the heat transfer general laws, also for future developments of the thermal model.

Inside a solid material, the heat power is equal to minus the temperature gradient multiplied by a constant value, function of the physical properties of the solid considered. This law is called Fourier's law.

$$q = -k\,\nabla T$$

the constant value k is the thermal conductibility and is measured as $[\frac{W}{m\,K}]$.

To describe a general problem of conduction we have to consider a closed system in which heat could be generated. Fourier's law and the conservation energy equation allow to write the Heat equation (or Fourier's equation) that describe different kinds of heat transfer problems.

$$\frac{\partial T}{\partial \tau} = \alpha\,\nabla^2 T + \frac{q_g}{\rho\,c_p}$$

where α is the thermal diffusivity and is equal to

$$\alpha = \frac{k}{\rho\, c_p} \quad [\frac{m^2}{s}]$$

q_g is the heat generated inside the closed system, ρ is the density, c_p is the specific heat capacity.

With this equation, it is possible to determine the curves of temperature and heat flux along the solid. For problems in which the temperature is function of only 1-D and no heat generation is present, an analytical solution is possible. But in general, numerical solutions are required.

As an example, we consider a stationary problem with heat generation and cylindrical geometry. The problem describes the electric resistor heated for Joule effect when the current flows. The temperature is function only of the radius of the cylinder, and the heat flux is only radial too. Using the heat equation, we can find the behavior of the temperature along the radius r.

Heat power generated per volume unit is

$$q_g = \frac{V\, I}{\pi\, r^2 l}$$

Where V and I are the voltage and the current of the resistor, r the radius and l the length.

Since the problem is stationary, the first term of heat equation is equal to zero. So we can write

$$\nabla^2 T = -\frac{q_g}{k}$$

Expressing the Laplace operator in cylindrical coordinates and integrating we find

$$T(r) = -\frac{q_g}{4k} r^2 + B$$

We can find the constant B imposing the boundary conditions, i.e that the external surface is at a fixed temperature T_0.

$$B = T_0 + \frac{q_g}{4k} {r_{ex}}^2$$

$$T(r) = T_0 + \frac{q_g}{4k} ({r_{ex}}^2 - r^2)$$

Finally, we find the temperature has a parabolic behavior with a maximum for $r = 0$. It is necessary to control that this temperature does not exceed a pre-fixed value. To maintain the temperature of the external surface constant, the heat is exchanged with external air.

This problem could be generalized for more complex geometry and could be applied to describe the heating of an electric motor as well as the heating of the battery.

Convection

The analytical description of convection problem is very complex. Fluidynamics and heat transfer equations have to be resolved at the same time in order to completely describe the physical system, such as finding the function of velocity and temperature.

A physical approach is out of the scope of this thesis and only the most important relationships are reported.

The heat exchanged between the wall and the external fluid can be expressed as:

$$Q = h\,S\,(T_w - T_f)$$

where h is the heat exchange coefficient, T_w is the temperature of the fluid and T_f is a reference temperature of the fluid and it has to be defined according to the kind of convection.

A series of adimensional parameters are introduced. The Nusselt number is

$$Nu = \frac{h\,L}{k}$$

where L is a reference length and k is the thermal conductivity of the fluid.

Different problems of convection exist. We speak of external convection when the fluid has no space limits, of internal convection when the fluid is inside a pipe or a duct. In the first case it is easy to define a reference temperature as the temperature of the fluid far enough to not be influenced by the heat exchange. In the second case, the reference temperature is considered the bulk temperature. This is defined as the temperature that the fluid would have if the temperature was uniform in the duct and the enthalpy was the same.

The convection is also classified as forced or natural. In a forced convection problem, there is an external machine to generate the motion of the fluid and to create a difference of pressure (pump or fan). Instead if it is only the difference of density due to temperature the cause of the

motion, the convection is natural. If both the conditions are true, the convection is mixed. For our purpose only forced convection is considered and all the following correlations are valid in forced conditions.

In literature, we can find special correlations to express the Nusselt number (and so the heat exchange coefficient) for different boundary conditions and both for laminar and turbulent flows.

The correlations for the most common situations are reported. They are also used by AMESim® to describe the external convection heat exchange as predefined correlations.

In the fully developed region, such as when a stationary thermal situation is reached, the Nusselt number is constant and depends only on the geometry.

For a circular pipe, with laminar flow and uniform surface heat,

$$Nu = \frac{h\,D}{k} = 4.36$$

In the entry region, before a thermal balance is reached, the flow is turbulent and quite complex correlations are used. For flows characterized by large property variations, the following equation, due to Sieder and Tate, is recommended [17]:

$$Nu = 0.027 Re^{0.8} Pr^{1/3} \left(\frac{\mu}{\mu_s}\right)^{0.14}$$

where Re is the Reynolds number, Pr is the Prandtl number and μ is the kinematic viscosity.

The description of the convection is really complex and difficult to simulate. The Sieder and Tate correlation are easily implemented in the commercial software, but errors as large as 25% may result from its use [17].

3. PHEV thermal management modelling

3.1 Scope of the model

The developed model represents the three cooling circuits of a plug-in hybrid vehicle. The problem is quite complex and multi-physics software have to be used.

It is important to point out the scope of the model from the beginning, in order to understand what is necessary to model as best as possible and, on the other hand, what is possible to neglect in order to save computational time.

The main purpose of this work is build up a model to implement and validate new control strategies. As mentioned in the first chapter, energy consumption becomes more and more important in hybrid and electric vehicles. In such a perspective, the cooling of thermal sources plays a key role in saving energy and increasing battery autonomy.

The cooling system of the investigated car includes four electric pumps, one HV compressor and the engine centrifugal pump. In addition, the fans of the different radiators increase the current absorbed, as well as the PTC heaters. Clearly, the system has to guarantee an optimal cooling of all the critic components (also in term of aging); but on the other hand, it should minimize the energy consumption. This could be done both with an optimal design as well as with an optimal control strategy.

Thermal management becomes so crucial for hybrid/electric cars both for the general limited energy on the ‘tank’ and since the energy used for cooling and climatization is higher than in a conventional car.

The vehicle’s cooling system has already been tested and validated and so it is not the primary objective of the model to verify or design a new layout. Instead, the scope is having a platform in which it is possible to implement new strategies. The basic strategy used for thermal management is to switch on or off the electric pump when the temperature, for example of the electric motor, overtakes a threshold (start and stop). The same is done for the activation of the fans. Instead, the battery control is generally more complex and has a great influence on its life expectancy and aging effects, and so specific controllers are used (so called BMS, battery management system).

The development of a new model is strictly linked to the data available. For most of the components, the prediction of temperature, pressure and volumetric flow rate is based on external maps. The pump characteristics, the pressure drops, the heat exchanged with the components and along the pipes are some of the information that have to be provided.

This data could be provided either from suppliers or from experimental activities. One of the first activities was the analysis of the data available to understand what was ready to be implemented, what could be calculated and, on the other hand what was missing. If a components info is not available, the maps are estimated or extrapolated as it will be better explained in the following pages.

3.2 Description of the circuits and data available

As mentioned before, the thermal management model of a plug-in hybrid car includes, at least, three different circuits. They are classified as high temperature (internal combustion engine and oil cooler), medium temperature (electric motors and power electronics) and low temperature (battery and air conditioning). The cooling systems are now briefly described one more time in order to point out the information available.

For the high temperature circuit, the coolant is moved by a centrifugal pump driven directly by the belt. A map of fuel consumption of the engine was available. From this, It is possible to calculate the efficiency, but it was not known how the thermal losses are divided in heat exchanged with the coolant, enthalpy of exhaust gases, convection and irradiation. It is necessary to estimate the real heat exchanged with the coolant, as it will be explained. The pressure drops of the water along the engine are calculated from experimental data. Instead, the radiators are completely characterized for what concern the heat exchanged, the pressure drops and the fan influence.

The medium temperature circuit includes two separate parts, one for the front axle and one for the ISG in the rear axle. The vehicle considered is a parallel plug in hybrid with a P1-P4 architecture, so it has two electric motors directly connected with the wheels and an integrated starter generator directly connected to the internal combustion engine. The cooling circuit uses two identical electric pumps and a radiator in the front of the car, the same is for the ISG circuit (with only one pump). The data available include the efficiency map of the e-motors, the e-

pump characteristics and the heat exchanged by the radiators. As for the high temperature circuit, the pressure drops are calculated from pressure measurements.

Finally, the low temperature circuit includes battery cooling system (battery, pump and chiller) and air conditioning circuit (refrigerant compressor, condenser, evaporator and TXV valves). In addition, PTC heaters are used to heat the cabin. Air conditioning is partially modelled and not validated; cabin and PTC heaters are not modelled at all.

The three circuits are independent and they are modelled as three different models. The frontal axle circuit is completely independent and it is not affected by the other systems at all. There are a few interdependencies mentioned in the previous chapter:

- The A/C condenser affects the engine radiator since it heats up the air,
- The battery circuit is integrated with the A/C system through the chiller heat exchanger.

The experimental data available comes from real tests when the car was equipped with many sensors. Coolant temperature, pressure and flow rate were measured in different points of the cooling systems (like inlet and outlet of the electric motor) and in various driving situation. The tests were done to validate the global cooling system, and the results were made available to the present work. In addition to the experimental measurement, data from the different control units were available as well.

The calculation of the various pressure drops for different temperature, as well as the heat exchanged by water with each single component were used for the model calibration.

The procedure followed for the development of the model can be divided in three steps:

- First hydraulic validation, so only pump and pressure drops are included and temperature changes are not taken into account.
- Second, the thermal models are implemented and the temperature are calculated but only map based model are used in these parts. The power losses of the electric components are estimated from efficiency maps or directly from the heat exchanged with the water (calculated as mentioned above) has been used.
- Third and last, a more physical model is developed. In this last part, thermal masses are used and the heat exchange coefficient is also imposed through convection correlations.

The reason for this step-by-step procedure is that allows the calibration of the different parts separately and independently. Otherwise all the parameters are dependent from the each other's and the validation would become too complex.

The procedure followed to develop the model is now described in detail, dividing it in the three parts just mentioned.

3.3 PHEV thermal management model

3.3.1 Hydraulic model

After the data analysis, the hydraulic model has been developed. A short description of the AMESim® components used is reported.

Pump

Different blocks represent a hydraulic pump in AMESim®, The most suitable of this case, also considering the data available, is the centrifugal pump that belongs to the hydraulic resistance library.

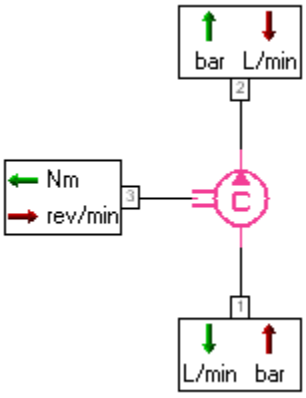

Figure 14: centrifugal pump component

The pump receives a value of pressure from the inlet port (1) and from the outlet pressure (2) a value of flow rate. The other port (3) is connected to the mechanical library and receives the value of the rotational speed. The characteristic curve and the reference parameters are used to

calculate the pressure increaseThe flow rate is transferred to the inlet port and the calculated torque to the port 3 (linked to an electric motor or combustion engine).

The calculation of the pressure increase is calculated using similarity laws [18]. The user has to provide the characteristic curve, such as the pressure increase as function of the volumetric flow rate, and the reference condition in which this curve is obtained. The curve could be referred to a single rotational speed or also at different speeds. Also, the efficiency could be specified as a constant or with a table as function of the volumetric flow rate. As mentioned in the previous chapter, the similarity (or affinity) laws allow to calculate pressure and flow rate for different rotation speeds, for different diameters of the pump and different densities of the fluid (the user has also to provide the reference diameter of the pump and the reference density). In order to use these laws, adimensional coefficients have to be used. The values of volumetric flow rate, power and rotational speed are respectively multiplied by the following coefficients:

$$C_q = \frac{1}{N\,D^3}$$

$$C_P = \frac{1}{\rho\,(N\,D)^2}$$

$$C_W = \frac{1}{\rho\,N^3\,D^5}$$

where N, D and ρ are respectively the reference speed, diameter and density.

The curves are rescaled with these parameters. The recommendation is that similarity laws are valid within a 10% of the original curves. The pumps of the system are five: four are identical and they are electric centrifugal pump with characteristic curve (at the speed reference) and efficiency available, the other one is the water pump of the engine. The characteristic curve of the electric pump is reported in *figure 14a.*

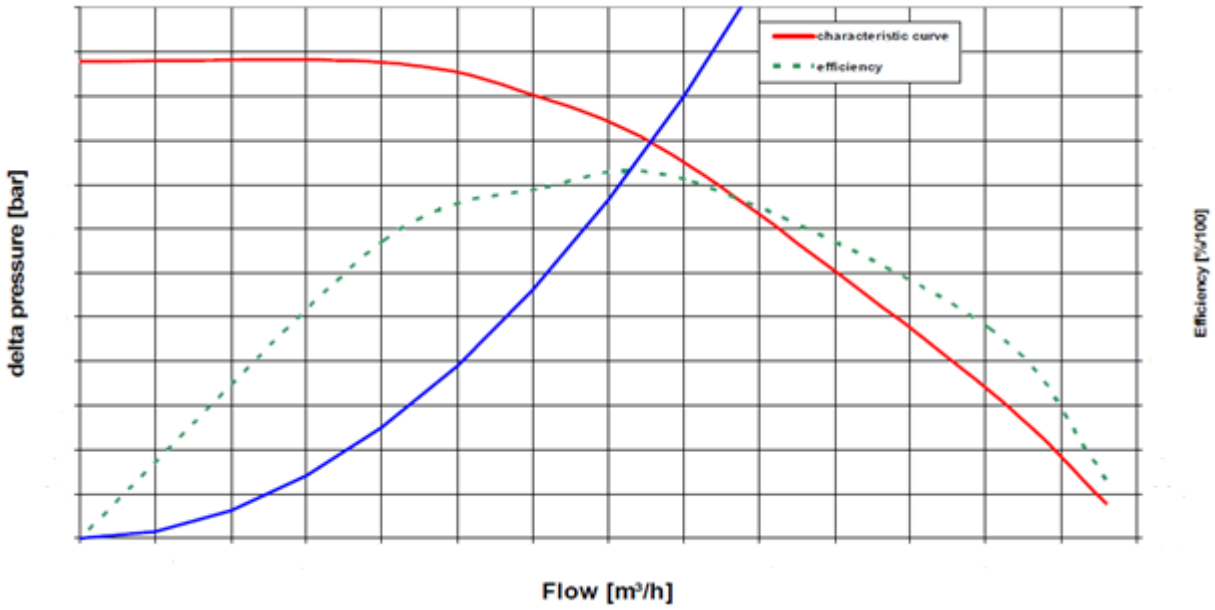

Figure 14a: electric pump characteristic curve

For the engine pump, the characteristic curve was not available and another AMESim® component had to be used. This is the ideal fixed displacement hydraulic pump: as it can be seen from figure 15, the outlet port 2 receives a pressure information and gives a flow rate value.

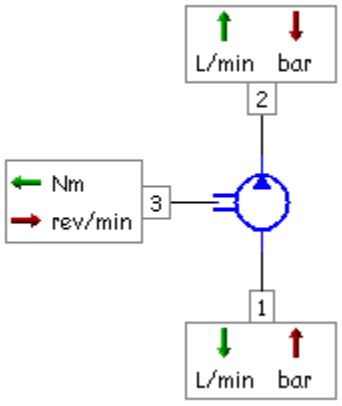

Figure 15: ideal fixed displacement hydraulic pump

Basically, this component only calculates the flow rate as

$$\dot{V} = \frac{displ * speed}{1000} \quad [\frac{L}{min}]$$

where the displacement is provided by the user and the speed is received by port 3. In this case, the engine rotational speed multiplied by the pump ratio is the input signal. The pressure increase is not calculated and is determined by the global pressure drops of the circuit. The displacement value of the pump is calibrated to match the experimental data of the flow rate.

Pressure drops

For what concerns the pressure drops, they should be divided in distributive and concentrate. The first problem is the lack of knowledge about the cooling pipes inside all the components. Only the diameter of the pipe is noted, neither the length nor the number of bends are known. So it is not possible a model with distributive pressure drops. The idea is to convert all the distributive pressure drops that cannot be modelled to a concentrated pressure drop that should cause the same difference of pressure. This is could be done using the experimental measurements and calculating the difference of pressure between the inlet and the outlet of a component.

The hydraulic resistance library of AMESim® allows to choose between different blocks and sub-models to model concentrated pressure losses. The most suitable block in this case is the '*hydraulic orifice with user table or equation q= f(dp)*'.

Figure 16: hydraulic orifice component

The pressure loss is function of the flow rate and a table or an equation has to be provided for each of these blocks included in the model.

The distributive pressure losses are not modelled for more than one reason. Considering the length and the diameter of the different pipes it has been calculated that they are not really significant compared to the pressure drops through the motors or the radiators. These values

are calculated using Moody's diagram evaluating the different tubes in their maximum flow rate condition. The distributed pressure drops are expressed as

$$R = \lambda \frac{l}{D} \frac{W^2}{2}$$

where λ is the adimensional coefficient calculated from Moody's diagram, l is the length of the pipe, D is its diameter and W is the velocity of the fluid. The concentrated pressure drops are calculated as:

$$R = \beta(Re) \frac{W^2}{2}$$

where β is the adimensional coefficient, function of the geometry of the obstacle and of Reynolds number.

The values are reported in *table 1*. A length of one meter is considered as example. The fluid used is 50% water and 50% glycol, density and dynamic viscosity are function of the temperature. As it can be noticed, the flow is turbulent and so the pressure drops are function of the relative roughness. The value of roughness used is the typical value for the material of the pipe. The numerical values considered are from [1].

The total length of the circuit (precise data not available) should not be more than some meters, and so the total drops should stay in tens of mbar, order of magnitude.

The pressure drops due to motors or radiators, are hundreds (until thousand) mbar. This approximate estimation highlights that the neglection of the distributive pressure drops is not so significant considering the pressure drops due to heat sources and heat sinks.

In addition, the distributive pressure drops, are partially taken into account in the restriction block tables, In fact, as it will be described below, these tables are obtained from measurements, so the pressure difference between two sensors is considered. Obviously, the position of the sensor was not exactly out of the different components and so some pressure drops are included in these differences.

Estimation of the distributive pressure drops along the pipes for the three circuits												
	Max Flow rate	Diameter	Area	velocity	Temperature	Density	Viscosity	Reynolds	lambda	Length	R	Pressure losses
	l/min	mm	mm2	m/s	degC	kg/m3	kg/m/s	-	-	m	J/kg	mbar
High T	90,00	50,00	1963,50	0,76	90,00	1031,23	0,00	47506,90	0,02	1,00	0,13	1,37
Medium T	27,00	30,00	706,86	0,64	40,00	1063,74	0,00	8302,01	0,03	1,00	0,22	2,34
Low T	27,00	25,00	490,87	0,92	30,00	1068,80	0,00	7838,41	0,03	1,00	0,54	5,67

Table 1

The same approach is valid for the concentrated pressure drops due to bends and three way valves. Their estimated values are low, compared to the one of the heaters or coolers, as reported in *table 2*. They are also partially taken into account in the tables used for the restriction block. For the estimation of the concentrated pressure drops, the beta coefficient has to be chosen. Different types of losses are present in the circuit (bends, valves, change of section) and so the maximum value of beta, that is 1, is considered as example. The results show that a single obstacle does not have a great impact in the total balance, but if they become a remarkable number, the value of pressure losses it is significance. It has to be underlined that the losses due the bends are probably overestimated because the beta coefficient is lower than one, function of the ratio between the bend radius and the diameter.

Estimation of the concentrated pressure drops along the pipes for the three circuits									
	Max Flow rate	Diameter	Area	velocity	Temperature	Density	beta	R	Pressure losses
	l/min	mm	mm2	m/s	degC	kg/m3	-	J/kg	mbar
High T	90,00	50,00	1963,50	0,76	90,00	1031,23	1,00	0,29	5,66
Medium T	27,00	30,00	706,86	0,64	40,00	1063,74	1,00	0,20	1,41
Low T	27,00	25,00	490,87	0,92	30,00	1068,80	1,00	0,42	2,04

Table 2

However, the modelling of every single pipes is too complex and it is also out of the scope of the model because, in general, the effect are not so relevant, as demonstrated.

Definition of the pressure losses maps

All the pressure drops are included in the restriction blocks, and a map of volumetric flow rate and difference of pressure has to be provided. The building of the maps could be done in two ways: using the information available from the suppliers or the results of measurements done on the same circuits. The data from the suppliers were available for only a few components. In addition, the comparison of the curves with some experimental points shows that the pressure losses are too underestimated. In *figure 17*, it is reported the comparison of inverter pressure drops from datasheet and calculated from measurement value. The difference is roughly 100 mbar. This is probably due to the different position of the sensors in the two measurements.

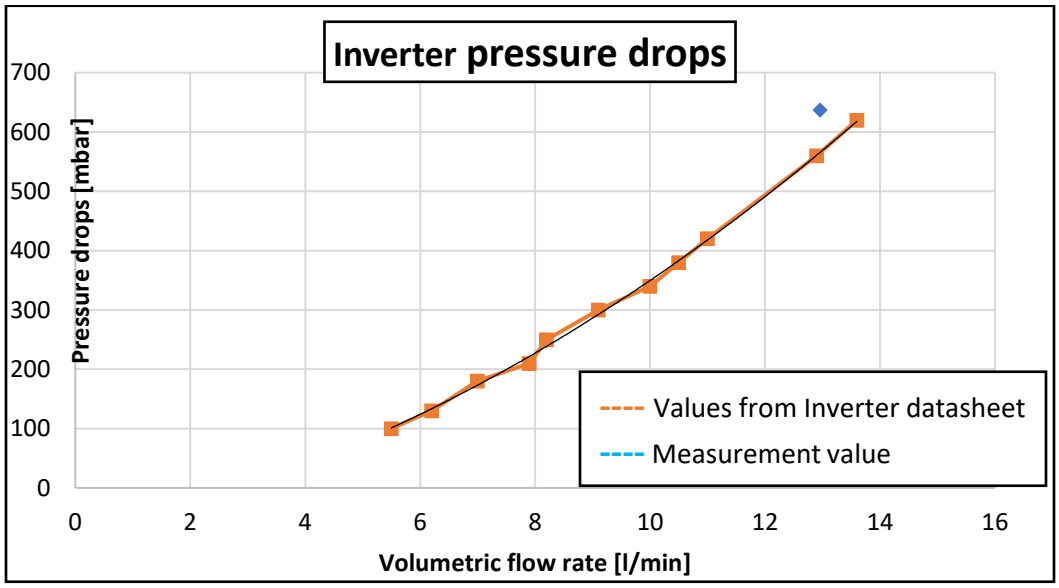

Figure 17: inverter pressure drops, datasheet and experimental value

The attempt is to build maps as 1-D table for each component (pressure drops as function of the volumetric flow rate). The pressure drops are function not only of the flow rate but also of the temperature, and this dependency will be taken into account in the next parts, when temperature is considered. In addition, the pressure losses are function of the square of the velocity and so of the square of the flow rate (Bernoulli's equation)

$$\dot{V} = C_q \, A_{eq} \sqrt{\frac{2 \, \Delta p}{\rho}}$$

where C_q is called flow parameter, A_{eq} is the equivalent area of the pipe and ρ the density of the fluid. This formula cannot be directly implemented because flow parameter is not known, In addition also the diameter and so the equivalent area of the pipes are not always known.

The limit of the table approach is that the electric pump always work at the same point. This means that when the pump is switched on, the flow rate and the difference of pressure between inlet and outlet are constant. Only one point can be calculated, one other is [0;0] and, knowing that a parabola should be built, one other point misses. Attempts to extend the maps with extrapolation or from curves found in literature are a possible further development of the model. The idea is to consider A_{eq}, ρ and especially C_q as constant and calculate the ratio K from the experimental point as

$$K = \frac{\dot{V}}{\sqrt{\Delta p}} = C_q \; A_{eq} \sqrt{\frac{2}{\rho}}$$

and substitute the table with this relationship.

Summary of the hydraulic validation

The three circuits built up are quite similar in this first step and so only the hydraulic model of the front axle circuit (electric motors, inverter and DCDC converter) is reported in *figure 18*, as an example.

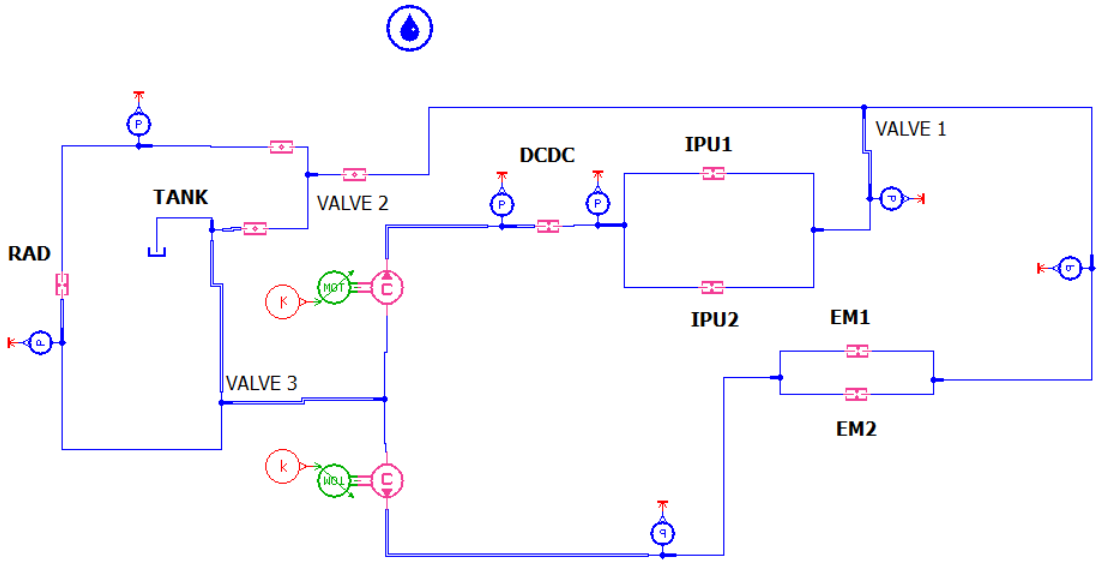

Figure 18: hydraulic model for front axle circuit

First, the pumps are calibrated with their characteristic curves and with the control signal of the rotational speed. In this case, the pumps always work at the same point (maximum efficiency), therefore, the velocity is the typical rotational speed or zero. Then, the pressure drops of all components are provided as function of the flow rate. Due to the control strategy of the pump, only two experimental points were available (zero and the typical flow rate). Once all the pressure drops are provided, the total losses of the circuit are known, and the pressure increases of the pumps are calculated to obtain a balance. The pressure and the flow rate are known for each branch. The next step is to convert the hydraulic library into the thermal hydraulic library, including the temperature effect.

3.3.2 Thermal model map-based

After the hydraulic validation, the development of the model can proceed with the thermal part.

The conversion of the hydraulic model to a thermal-hydraulic model, using the appropriate library, is the first step. The blocks (pump and 'restriction') of the hydraulic resistance library are also included in the 'thermal hydraulic resistance' library, with the addition of the temperature description.

The settings of this blocks is easy, once the model is calibrated in the hydraulic part. This is one of the main reasons that justify the procedure step by step.

The pump block can be directly copied from the previous step without any modification. It is possible to implement a map of pressure increase that is not only function of the flow rate but also of the temperature, but this information was not available and so the same map was used. The map of efficiency is reused without modification as well.

For the restriction block, the map of pressure drops has to be converted from volumetric to mass flow rate, and influence of temperature should be taken into account as well. The Bernoulli's equation become

$$\dot{m}(p,T) = C_q \; A_{eq}\sqrt{2\,\Delta p} * \sqrt{\rho\,(T)}$$

The temperature changes the density of the fluid, and so the mass flow rate. For the coolant considered, water/ethylene glycol 50%, the density can be expressed with a second grade polynom, as reported in [18].

$$\rho(T) = 0.024\,T^2 - 0.3381\,T + 1081.1$$

Like for the hydraulic model, only a couple of points were known from the experimental data. So the map was built only using the information available. This is quite a strong estimation, in particular in order to predict the temperature effect on the pressure drops more points are necessary. The model has only been calibrated in a few test cases and due to this, its general validity is not guaranteed. However, the block used is the equivalent of the hydraulic resistance in the thermal hydraulic resistance library. The pressure drops are not not function of the volumetric flow rate but of the mass flow rate, so the previous tables were multiplied by the density of the fluid.

The 1-D table could be substituted with equations that express the relationship of the mass flow rate versus pressure and temperature. Like for the hydraulic part, if we consider C_q and A_{eq} constant, Bernoulli's equation can be used and implemented in the AMESim® block as

$$\dot{m}(p,T) = K_1\sqrt{\Delta p} * \sqrt{(0.024\,T^2 - 0.3381\,T + 1081.1)}$$

after that the ratio K_1 has been calculated from the experimental measurement.

Once the hydraulic parameters are set, the calibration of the heat flows can begin.

The procedure followed is organized in three steps.

- Firstly, only calculated experimental heat flows are provided (both for the heat sources and for the heat sinks). This allows the calibration of the thermal losses along the pipes.
- Then the radiators are inserted and the real heat exchanged calculated by AMESim® is compared with the experimental results.
- Finally, also the experimental results of the heat sources are substituted with the AMESim® results.

In this first step of thermal model, thermal masses are not used. Only coolant temperatures are calculated, but not component temperature. They will be considered in the next and last step.

Thermal losses along the pipes

As mentioned, whether the distributive pressure drops along the pipes could be neglected for hydraulic validation, in the thermal model the pipes play a determinant role in the model description. The heat exchange between the pipe and the external air has to be considered. This

is evident studying the experimental data: in test cases in which the temperature of the water is roughly constant, the total heat exchanged should be zero. But this is not true and it is always greater than zero. This means that an additional contribution (losses along the pipes) is present and cannot be neglected in order to obtain a correct prediction of the coolant temperature.

This heat loss is function of the car velocity and can be described as external convection. The convection is mixed, both natural and forced, and the heat exchange coefficient increases with the speed of the car.

Instead to model each single pipe with its own heat exchange coefficient, the idea is to include all the heat exchanged along the pipes in a single block. In this block an amount of thermal power is removed from the water and this amount is function of the car velocity.

There are different ways in AMESim® to model like that. The thermal hydraulic library includes a piloted external convection block in which the air speed is input and a heat exchange coefficient is calculated using predefined correlations. Some attempt has been made using this block, but the results are always really different from the experimental values.

After these attempts, it has been decided to use the other way and relate the losses along the pipes only to car velocity. There is not information available about the air velocity and so a parameter has to be calibrated. The block used is shown in *figure 19*, it is a thermal chamber and allows to calculate directly the thermal power absorbed. As mentioned above, the signal used is the car velocity and must be converted with a gain, or a more complex function, to the heat exchanged. The component receives a thermal power amount (from port 3), that in this case is negative since the heat is removed from the system.

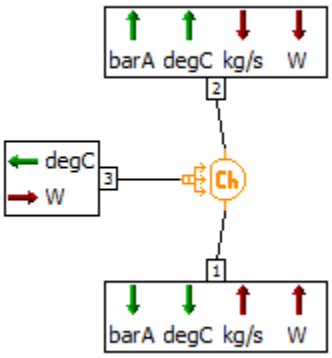

Figure 19: thermal hydraulic capacity

The calibration of the gain is done using constant speed and constant water temperature test cases. After the net heat exchanged is calculated, it is divided by the speed of the car and so we obtain a linear relationship. Like for the pressure drops, due to lack of information, the validity of the model is guaranteed only in the 'points' available and not in every condition. In fact, we know that the heat exchange coefficient is not linear with the air velocity but has more complex relationship that depends on convective heat exchange coefficient and that has not been considered.

Heat sinks

Radiators

After the calibration of the gain for model the heat exchanged along the pipes, the thermal model proceeds with the calibration of the radiators.

There are two ways to represent a radiator in AMESim®: one is with the *cooling library* and one is with the *heat exchangers assembly tools*. The first one is simpler and the heat exchanged is calculated from a map, function of air velocity and coolant flow rate. The second one is more complex and the heat is calculated using convection equations and Nusselt number relationships. Considering the scope of the model, it is preferable to use the simpler block in order to not complicate the model calibration and save computational time. The heat exchangers assembly tool is very detailed and it should be used, for example, to test and validate a new cooling layout. The tool is really interesting, thanks to the regression tool: it allows to obtain Nusselt number relationship starting from experimental data (difference of temperature of water and air). In addition, the influence of the different components on the air and its pressure drops could be taken into account in a very detailed way. In a future development, it would be interesting the use of this block in the model and the comparison with the cooling library block. The decision was to use the map based block, belonging to the cooling library. The input and output of the different ports (external variables) are reported in *figure 20.*

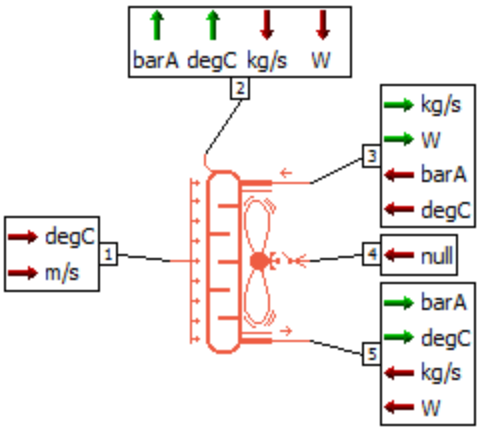

Figure 20: AMESim® *radiator block (cooling library)*

Port 1 brings information of temperature and velocity of the external air, port 3 and 5 are the inlet and outlet of the coolant, port 4 is the signal of the fan. Different sub-models can be used, according to the data available. For a good description of the air pressure drops, an under-hood model could be used, but it was not available in this case. The sub-model chosen has been the radiator with prescribed air velocity and table or expression for the pressure drops.

The external air velocity input at port 1 is 10-20 % of the vehicle speed. This reduction is attributed to the cooling duct opening (if the duct opening is made larger it increases the drag and hence a trade-off is made between aerodynamic coefficient and cooling performance). [18]

This gain between the car velocity and the air velocity has been calibrated for each radiator. The table for the pressure drops is the same used in the hydraulic validation. The map of the heat exchange between air and coolant for different conditions was available for experimental data. The 3-D map is reported in *figure 21*.

The heat exchanged increases both with the air velocity and with the coolant flow rate. The geometrical parameters are specified as well. The map is obtained with a difference of 70 degrees between coolant and air. The heat calculated with the map is scaled on the real difference of temperature.

The influence of the fan is considered as well. The control signal of the fan is converted (with a table or an equation) to an increase of air velocity. In order to calibrate the radiators, the heat calculated by AMESim® and the results of experimental data are compared. Inlet and outlet

temperatures of the radiators, as well as the flow rate, were available for different driving cycles. The heat exchanged is calculated using density and specific heat function of the temperature. The expression for the density has already been reported, for the specific heat, always in [18], it is:

$$c_p(T) = 2.64 * 10^{-9}\, T^2 + 3.86 * 10^{-3}\, T + 3.203$$

The calibration is done changing the gains of the air velocity and of the influence of the fan. The other parameters are known and constant. An example of comparison for the radiator of the frontal axle is reported in *figure 22.* The car velocity is also reported to better understand the results.

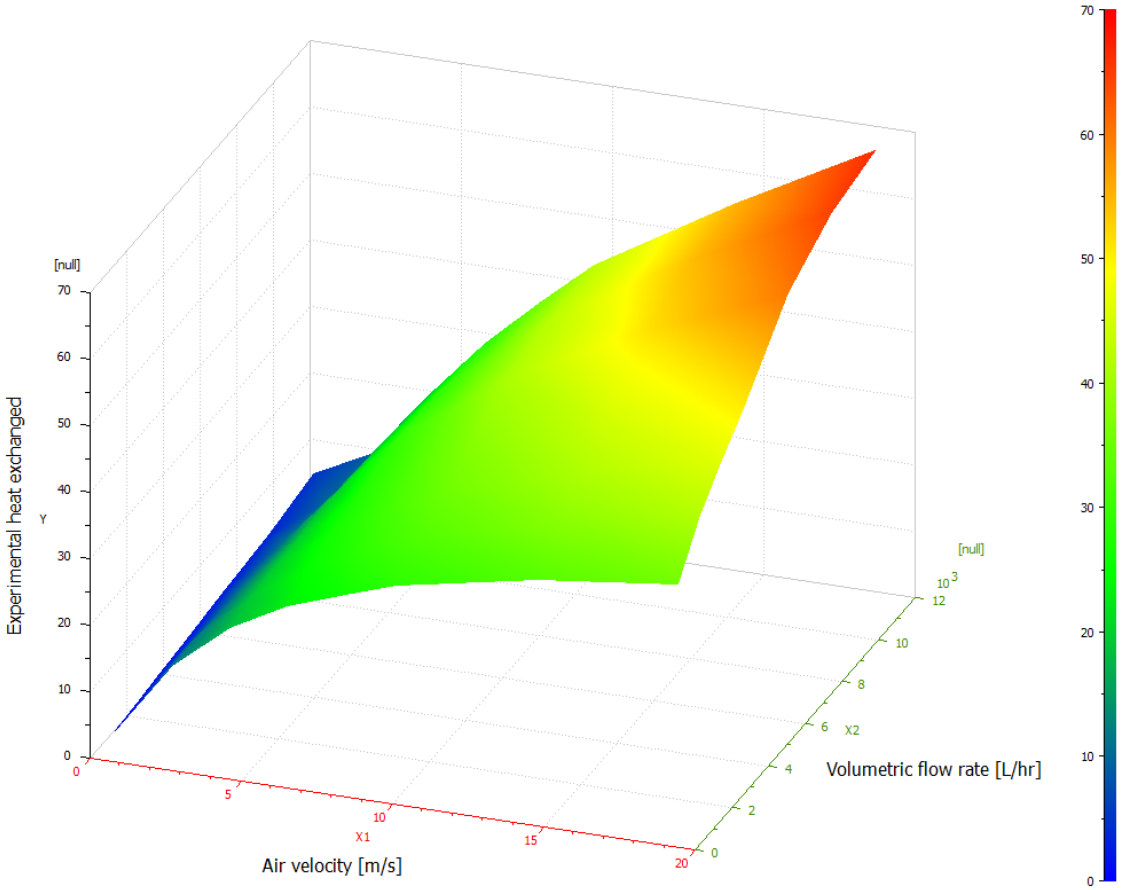

Figure 21: radiator heat exchanged map, function of coolant flow rate and air velocity

As it is possible to notice in *figure 22*, when the velocity is stable at the maximum value, the calibration is correct (the red and the green lines are similar). The air velocity is only the 8% of the car velocity.

The problem is when the velocity is in the other stable region, from 200 to 400 seconds. In this situation, the heat calculated by AMESim® is too high. We know that the coolant flow rate is constant because the electric pump works always at the same point (max efficiency), so is the air velocity that is too high. This suggests that the relationship between the car velocity and the air velocity through the radiator is not linear but it is at least a second-grade polynomial.

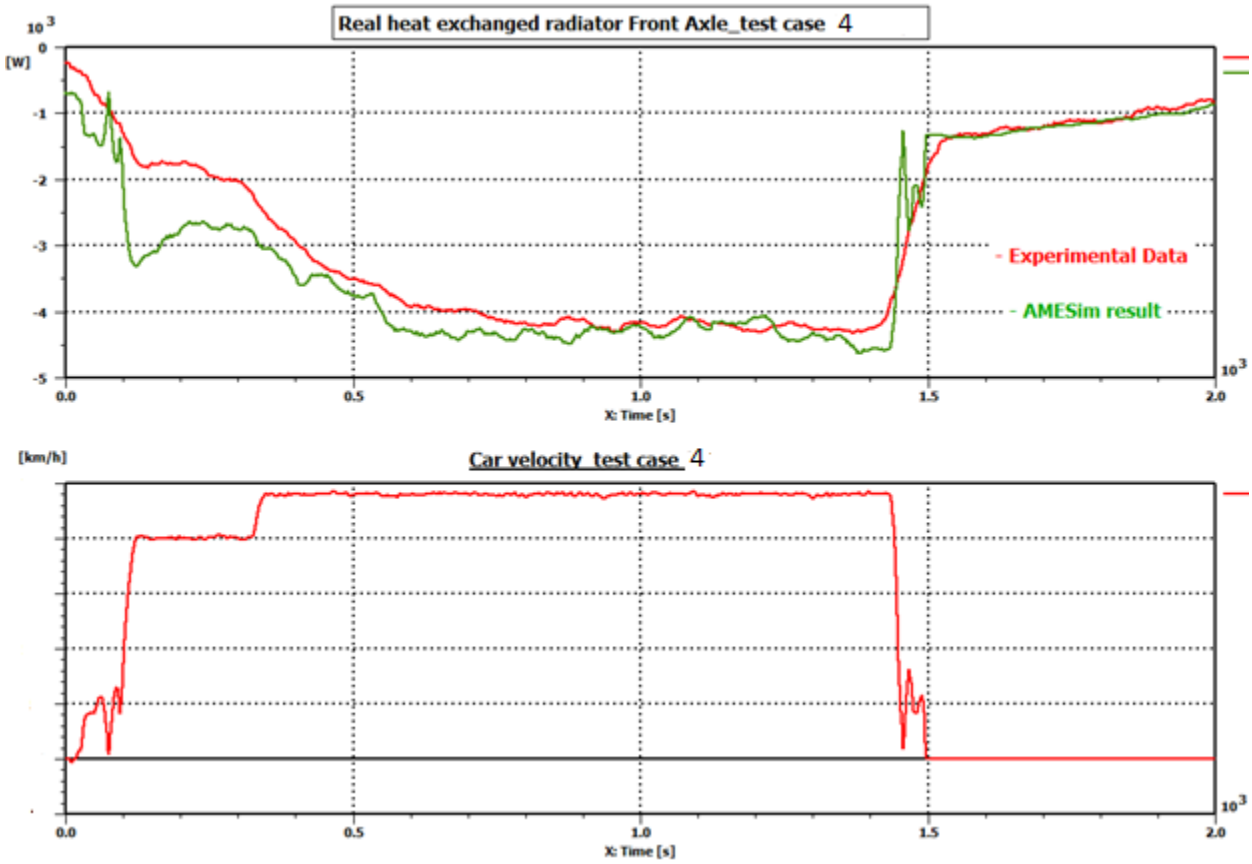

Figure 22: power losses electric motor estimation

Another reason is probably that the map is obtained in different conditions and so the experimental data can be not completely in accordance with it. The influence of the fan is calibrated thank to the last seconds, when the car is at standstill: the air velocity at that moment is only due to the fan. When we obtain that the two heat exchanges are equal, we have found

the right gain for the increase of air speed. The relationship is linear and the control signal (that is a 0 – 1 signal) is multiplied by 4 (AMESim® default file use the same value).

This procedure is repeated for the two radiators of the ISG circuit (which have only one fan) and for the two radiators of the ICE circuit. The vehicle has one other radiator for oil cooling, but no information was known about this circuit and so it was decided not to model it in this work. Comparison between model and experimental data for one of the engine radiator is shown in *figure 23.* The test is the same and, like in the front axle radiator from 200 to 400 s, the heat exchanged calculated by the model is higher. The gain to convert car velocity to air velocity has been calibrated to 10%.

The values of thermal power are completely different between the two circuits: the engine radiator absorb almost ten times the amount of power absorbed by the electric motor radiator. Of course, it depends on the driving condition and of the split factor: in this situation, the power to the wheel is provided mostly by the engine but, anyway, it is significant to highlight the ratio between the two contributions.

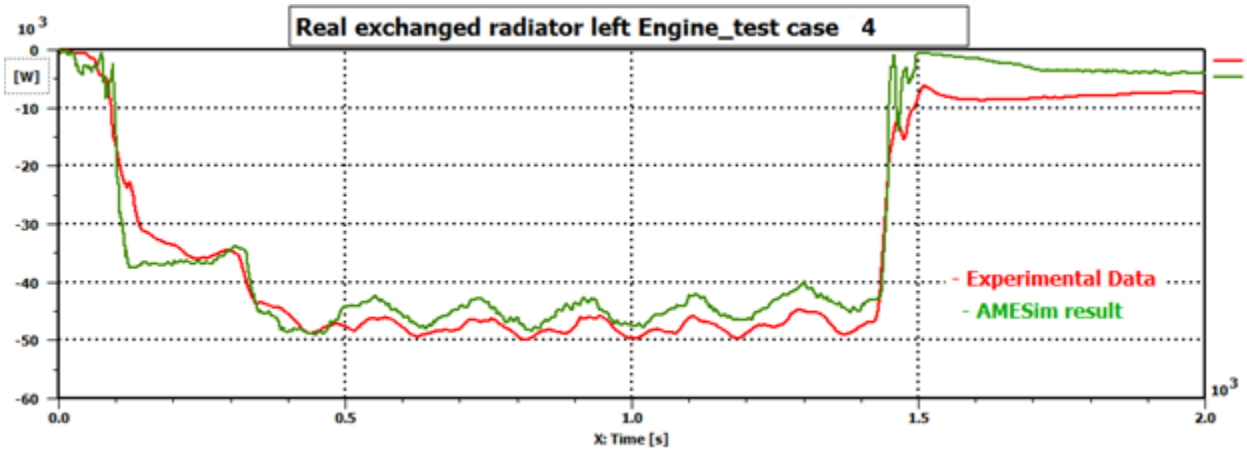

Figure 23: engine left radiator, model and experimental data

The tests at constant speed are used to calibrate the numerical values (air velocity and fan influence) in order to match the experimental heat exchanged. Some other tests are used to validate the model in different driving condition. This will be reported in the following chapter.

The two radiators of the high temperature circuit have the same size but the heats exchanged are different. This is since the condenser of the air conditioning system is in front of only the right radiator. The air is first heated by the condenser and the higher inlet air temperature the

lower the heat exchanged. In order to impose a higher inlet temperature of the air, the condenser block, belonging to the cooling library, should be used. Port 3 and 4 have the information on the air (temperature and velocity), the control signal at port 2 says if the air conditioning is on or off, and port 1 calculates the power absorbed by the compressor. When the air conditioning is on and the condenser has to remove heat from the refrigerant, the air is heated, typically around 10-15 degrees and this limits the performance of the radiator.

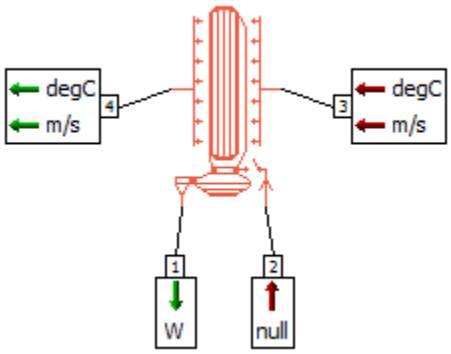

Figure 24: condenser block (cooling library)

Chiller

The radiators are not the only heat sinks, since the battery circuit uses a chiller. The temperature of the battery must stay below 40°C and, consequently, the external air cannot always be used. As described in the first chapter, the battery circuit is linked with the air conditioning system through a heat exchanger, which is like an additional evaporator, and a thermal expansion valve.

A map of heat exchange for the chiller was available. This is function of the coolant flow rate, coolant inlet temperature and refrigerant outlet pressure. A specific component is not present in the cooling library. Another possibility was to use the air conditioning library which include particular heat exchangers, but it is too detailed for the scope of the model. Therefore, the solution used was to calculate the heat exchanged using the map, and use a thermal capacity of the thermal hydraulic library to cool down the coolant. The built model is reported in *figure 25.*

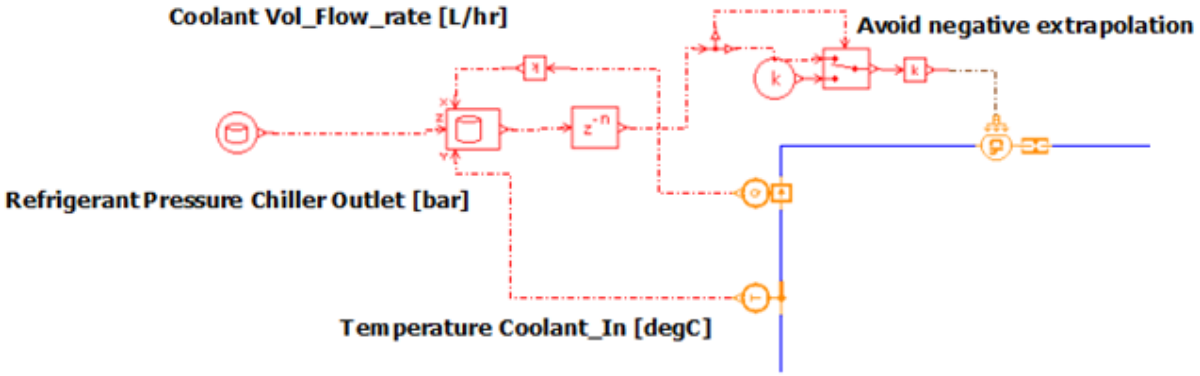

Figure 25: simplified map-based chiller model

The coolant inlet temperature and the coolant flow rate which enter in the map, are calculated by the model, so no additional data is necessary. Instead for the refrigerant pressure, the ECU signal is used. The air conditioning circuit has not been modelled yet and for a first validation it was preferable have a correct value. This signal cannot always be available and it will be switched with an internal AMESim® parameter in the following step. The map is defined only for coolant temperature over 20°C, but typically the coolant could reach lower temperatures. In this situation, it is necessary to extrapolate data from the table. The problem is that when the coolant temperature is really low, the extrapolation gives negative values of heat exchanged which are not physical (the coolant cannot cool down the refrigerant). To avoid negative extrapolation of heat exchanged, a switch is added: when from the table a negative value is calculated, this is converted to zero. The experimental heat exchanged for the chiller was not available because during the test the sensors of temperature were only in the battery side. To be able to validate the model, the idea was to use the experimental value for the battery and the calculated one for the chiller, and to compare the two coolant temperature values (experimental and of the model).

Heat sources

After the validation of the radiators it is time to substitute the heat exchanged by coolant with the real heat produced by the different components (and estimate an appropriate heat exchange coefficient).

Power electronic and electric motors

For the medium temperature circuit, the thermal sources are power electronic components, they are DC/DC converter, inverter and electric motor. The model has to predict the heat generated by each component in the different operating conditions.

Usually they have very high efficiency, however their power losses produce a significant amount of heat. All the power losses become heat and increase the temperature of the component. The maximum limit of temperature is linked to silicon properties. A temperature limit for the coolant is specified as well. This is around 80°C for the inverter and around 60°C for the electric motor. They are quite preventive because, like in the batteries, the thermal cycles and the maximum temperature have an important effect on the derating of the power electronic components. In order to avoid premature derating, it is important to leave the temperature as low as possible.

The losses of the electric motor are divided in iron and copper losses. The copper losses are due to Joule effect, the iron losses are more complicated to estimate and are due to hysteresis and eddy currents. The thermal models of electric motors are quite complex and the topic is out of the scope of the present work. It would be necessary to model all the electric connections using specific libraries. The software used allows this approach since an electric library is included and most of the other component can be connected to this. However, this is not considered in the present work. Luckily, it is possible to have a simple thermal model using the map of efficiency (map-based thermal model).

For the two electric motors (three including also the Integrated Starter Generator) the efficiency map was available. The efficiency is function of rotational speed of the motor and torque, obtaining a 2-D table. For the inverters, a map of efficiency was not available, but it has been obtained starting from a map of global efficiency of the system (including both the inverter and the motor). For the DC/DC converter a constant efficiency, around 90%, is implemented.

In order to enter in the efficiency map of the electric motor, torque and rotational speed have to be calculated. For what concerns the rotational speed, the hybrid car has a P1-P4 configuration. This means that the speed of the two frontal electric motors have a constant ratio with the wheel rotational speed, and so with the car velocity. Instead the generator has the same rotational speed of the ICE. So the rotational speeds of the motors could both be calculated

from two known signals. On the other hand, the torque could be calculated starting from the voltage and the current of the inverters, both included in HCU signals, available after the test cases done. The calculation of the power is immediate, then the inverter efficiency has to be considered. At the end the electric power is multiplied by one less the efficiency to obtain the power losses.

The control scheme for the front electric motor is reported in *figure 26*. It has been done using the control library of AMESim® that is actually like Simulink.

The same procedure has been used for the calculation of the power losses of the ISG, the only difference is for the rotational speed, that is directly the engine rotational speed.

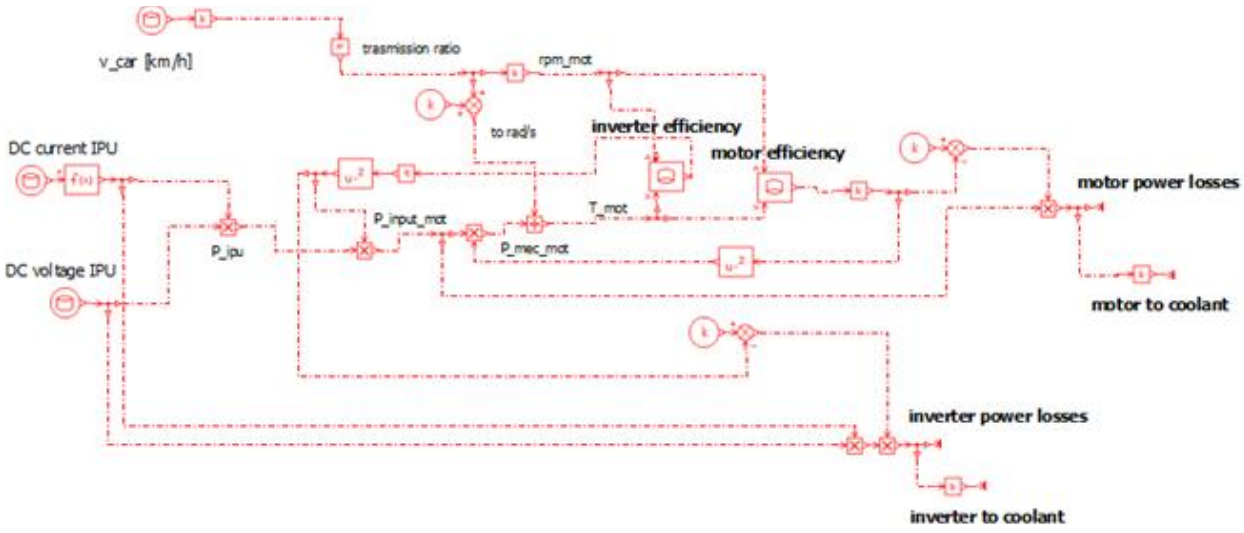

Figure 26: map-based power losses calculation for inverter and electric motor

The thermal heat flows obtained are compared with the experimental coolant heat exchanged. The results for a test case are presented in *figure 27a* and *27b* both for electric motor and inverter. The difference between the two curves is related to the heat exchange coefficient that, obviously, is limited. The heat produced and not exchanged with coolant determine the increase of temperature of the component.

As mentioned before, in this first thermal step model the components and the convection heat exchange are not included. In order to convert the power losses to coolant heat exchanged a constant ratio is estimate. This is necessary to obtain correct values of coolant temperature and

be able to validate the model. This ratio, which is around 0.7-0.8, cannot be always constant, as it can be seen from the figures. Therefore, the estimation is not rigorous but it is necessary in this first step. Two test cases were considered: one to calibrate a good value of this gain and the other to validate the model. This ratio has no physical value and it will be substituted with a physical description of convection and heat transfer in the next step.

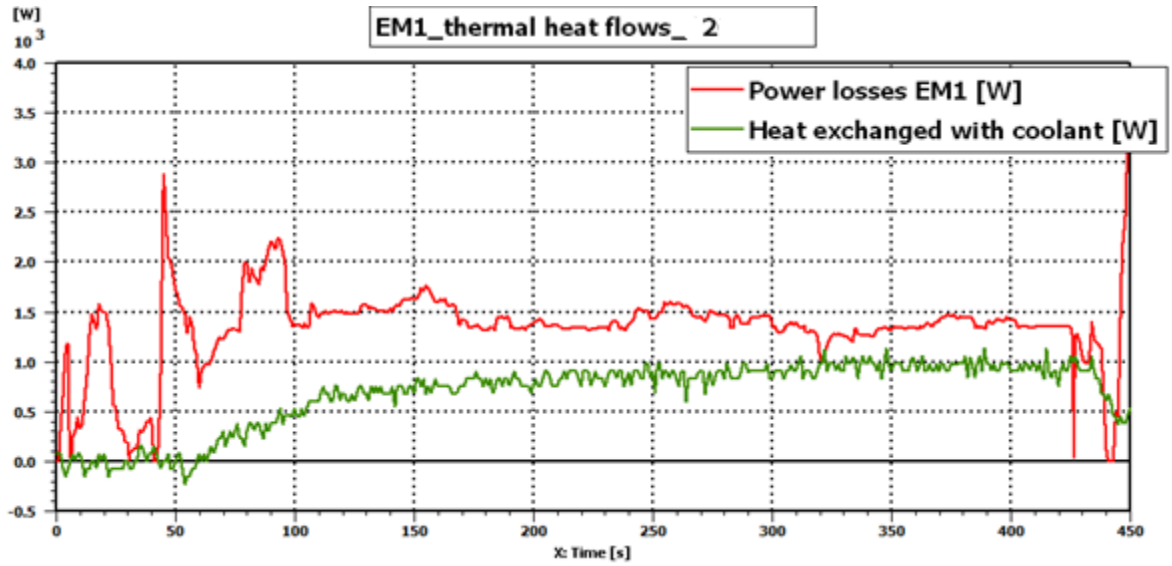

Figure 27a: thermal heat flows for electric motor

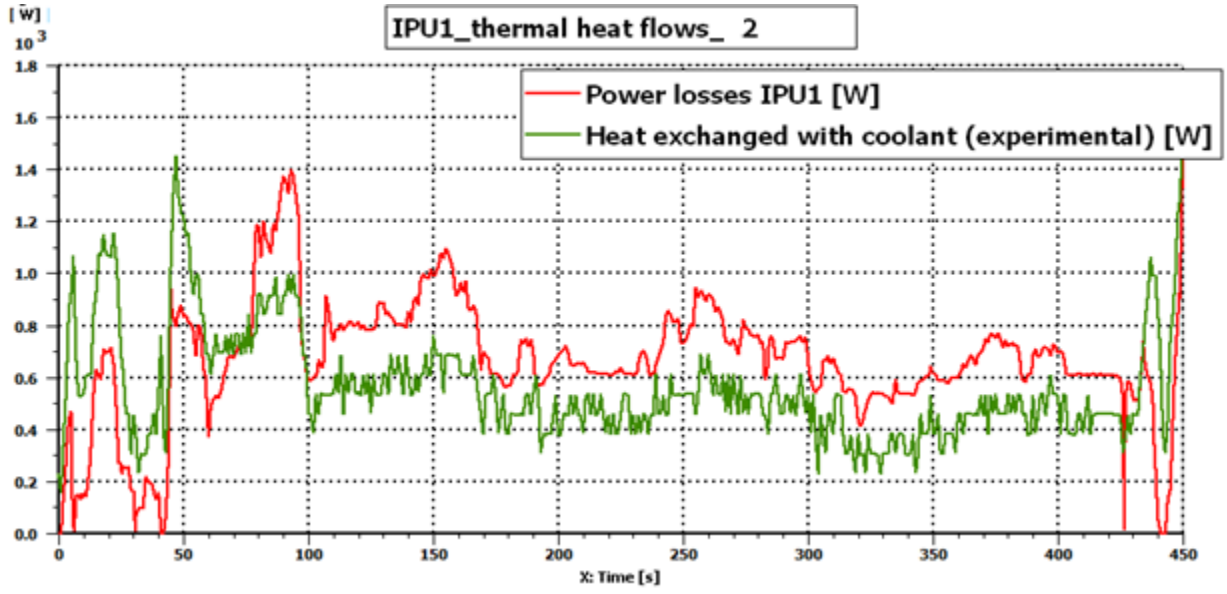

Figure 27b: thermal heat flows for inverter front axle

Internal Combustion Engine

The ICE remains the main heat source also in a hybrid car. Its power is generally much higher than the electric motors and its efficiency is much lower.

As a first estimation, it is possible to consider that the chemical power of the gasoline is divided in three equal contributions: mechanical, remained in exhaust gases and exchanged with the coolant. Actually, the problem is more difficult for two reasons:

- the various ratios are not constant but are function of the engine rotational speed
- additional contribution must be considered, such as irradiation, convection with air and losses due to combustion inefficiency

and so, the division by three cannot bring good results.

The best thing would be having a thermal map of the engine with the coolant heat exchanged as function of rpm and shaft torque. Unfortunately, only a map of fuel consumption was available.

The idea was to calculate the mechanical efficiency from the fuel consumption and then estimate the heat percentage exchanged with the coolant.

In order to go into the fuel consumption map, we need the engine rotational speed signal (known) and the engine torque. For the engine torque a throttle signal is used and it is multiplied for the maximum engine torque. Dividing the fuel consumption for the mechanical power, the brake specific fuel consumption is obtained, and considering the lower heating value, the mechanical efficiency is found. Now it is possible to calculate the total power given to the engine and from that, estimate the power to the coolant with a suitable percentage. Values suggested in literature from spark ignition engine go from 26% (at low rotational speed) to 17% (higher rotational speed). [19]

$$bsfc = \frac{fuel\ consumption}{brake\ power} \quad [\frac{g}{kWh}]$$

$$\eta_{eng} = \frac{1}{bsfc\ LHV}$$

$$Power_{coolant} = \frac{P_{brake}}{\eta_{eng}} * k(rpm) \quad [kW]$$

The scheme implemented is reported in figure.

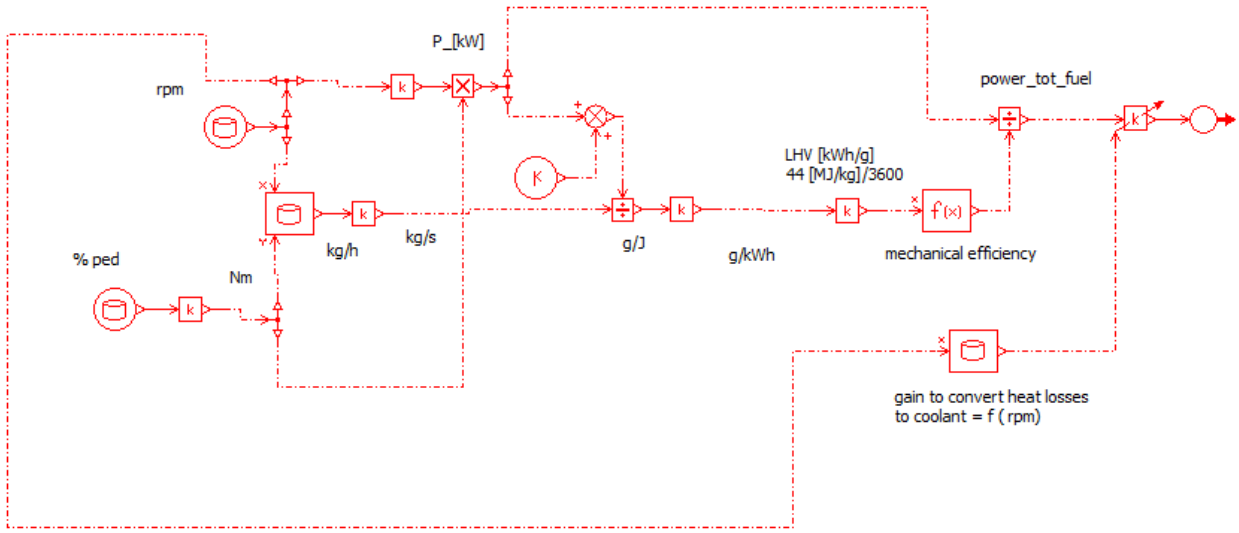

Figure 28: engine power losses

Experimental results available are used to find the correct percentage of the total heat given to the coolant and to build up the table for different rpm.

A test case is reported in figure. The engine speed is very high and the value that fits the curve at that velocity is around 0.14. It is a bit different from the ones suggested in literature, but the engine considered is different as well. The experimental data is, of course, limited; for the other rotational speed a linear interpolation is considered. In addition, with this approach thermal inertia is not taken into account. For example, if the brake power is zero and so is the fuel consumption, the calculated heat rejected is zero as well. But due to thermal inertia of the coolant and of the engine components, the experimental data could show the heat exchange is still positive. This is also the reason for the spikes and for the too high slope, compared to the experimental results, of the curve. To sum up, the approach is not the best because estimations are necessary and results are not so coherent. But, on the other hand, it is the only possible with the data available and it is allowed to have a main thermal description of the engine cooling circuit.

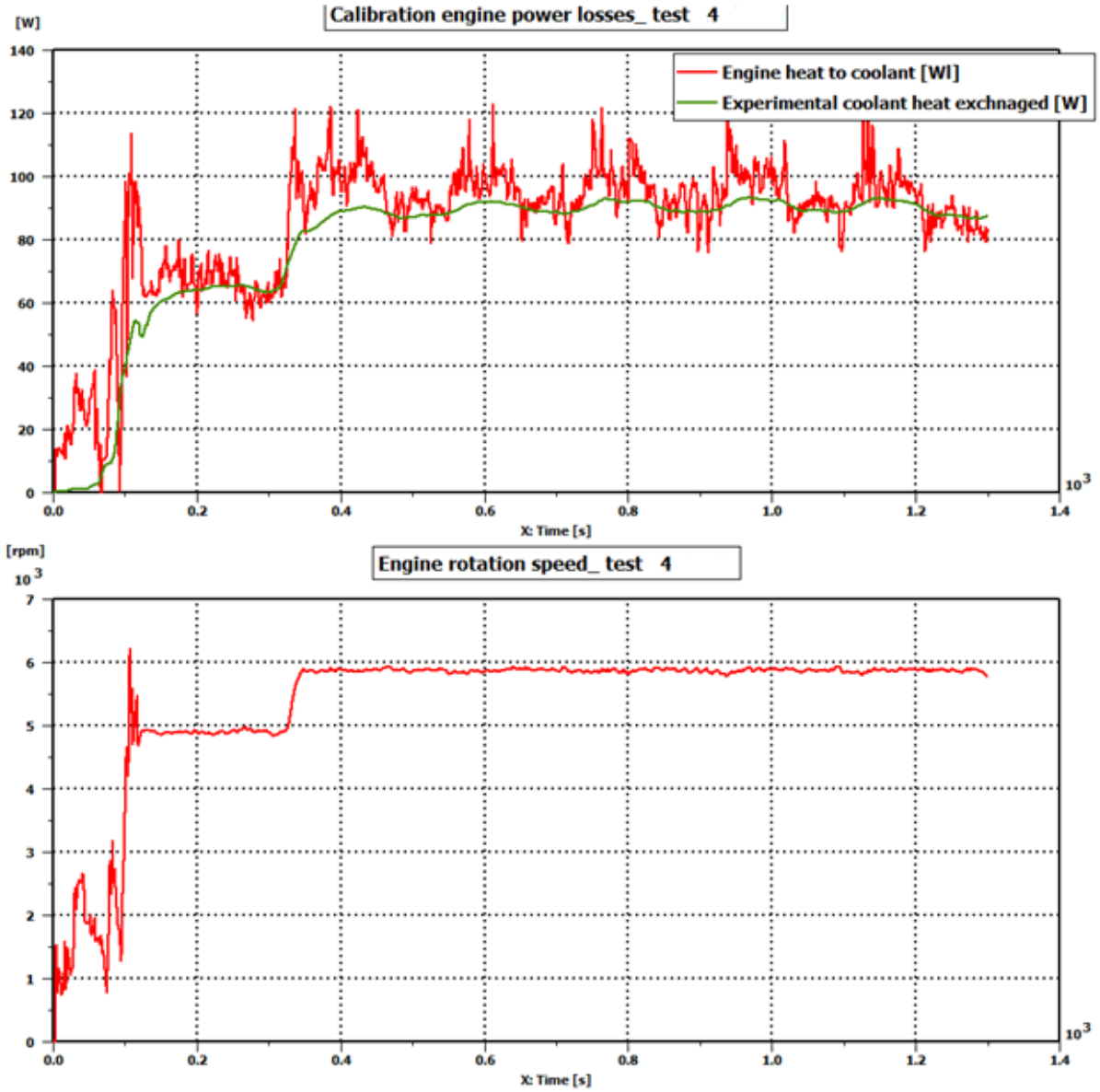

Figure 29: comparison of engine heat rejected to coolant and engine rotational speed

Thermostat

The model of the thermostat has to be included as well. The warm up of the engine has to be as fast as possible to reduce emissions and frictions (warming up post-treatment devices and oil). The thermostat allows this with a bypass of the radiator when the coolant temperature is below a threshold. Once the warm up has concluded, the thermostat opens and the coolant can go through the radiators. It allows to maintain the desired temperature during all operating conditions.

The thermostat behaves like two orifices of variable cross-sectional area and the variation of the cross-sectional areas is a function of the convective exchange between the coolant and the wax, [18], which is the thermo-sensible element. The opening and the closure laws are defined in the 'hysteresis' block and stabilize the fractional area opened as function of the wax temperature. A value 0-1 is calculated and passed to the two additional blocks. This is necessary to model the fact that when one part (line to the radiators) is partially open, the other (bypass). receives the remaining flow rate. The aperture and closure laws, generally, are different in order to take into account the thermal hysteresis effect of the wax. The sketch is represented in figure

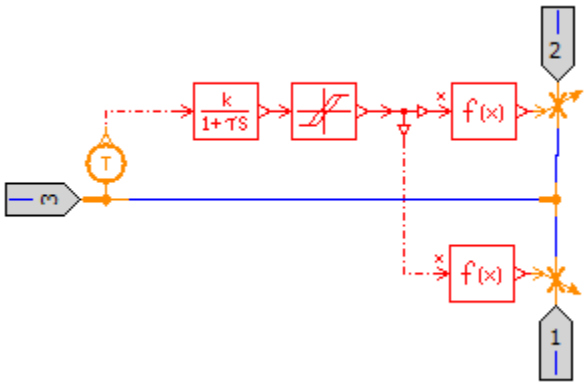

Figure 30: two ways thermostat for the engine coolant circuit

Battery

The battery is the most critical component from a thermal point of view. Its temperature has to stay between 5°C and 40°C [2]. Battery circuit is integrated with the air conditioning and, as already mentioned, a chiller cools down it. An electric heater is necessary to warm up the battery when the external temperature is below the low threshold. This can be warm the liquid or directly the battery surface. The PTC heater is not modelled in the present work.

The battery power losses are due to its internal resistance and to Joule effect. A map of internal resistance of a battery cell, function of the battery temperature, was available. Thanks to this, the heat calculation is quite simple. The internal resistance has to be multiplied by the cell number and by the square of battery current. If available, the resistance of the conductors can be added to obtain the global battery resistance.

Like for the medium temperature circuit, in this first step only the coolant temperatures are obtained. The internal resistance is function of the battery's average temperature that has to be implemented from measurement values. In the second step, battery temperature is calculated as well, and the external signal can be substituted.

A comparison of the battery power losses calculated and the measured heat exchanged with coolant is presented in *figure 31*.

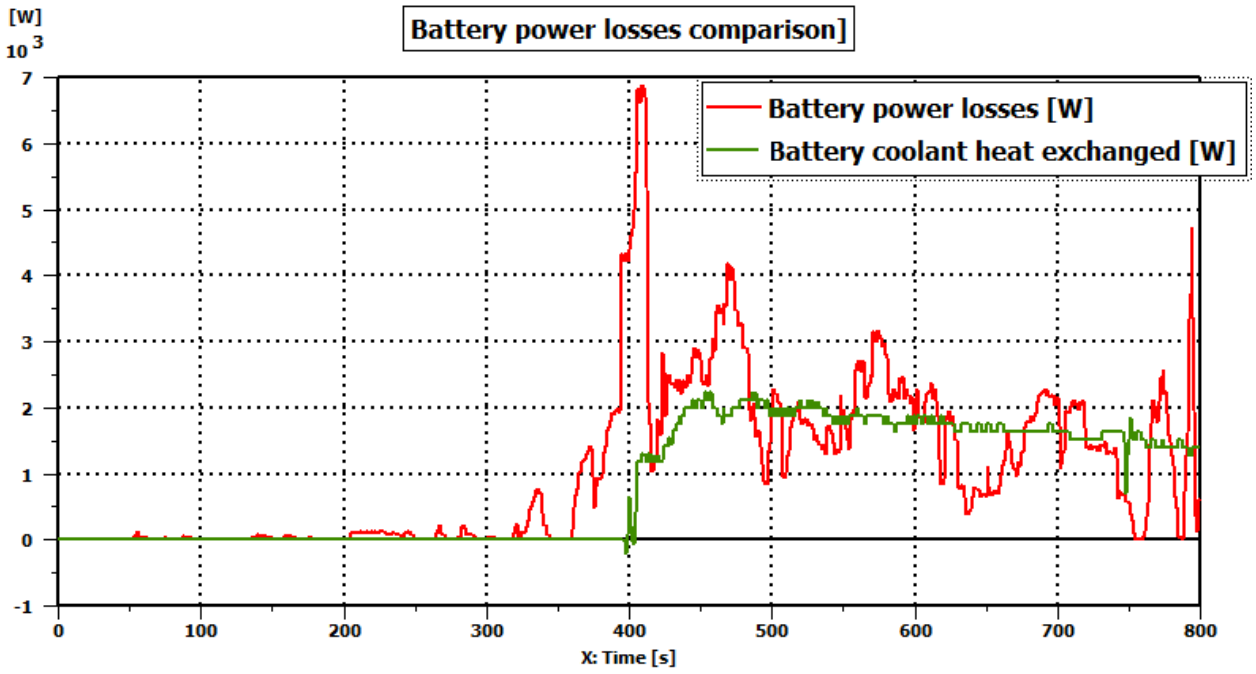

Figure 31: battery power losses estimation and comparison with experimental results

Thermal model first step summary

The hydraulic library is converted to the thermal hydraulic one. The thermal losses along the pipes are calibrated, as function of the car velocity. Then, heat sinks and heat sources are inserted: they calculate the heat exchanged with the coolant using a map of efficiency or a specific map of heat exchange.

In order to enter in these maps, different input signals are necessary and they have to be provided to the software. In table 3. There is a summary of how the heat contributions are calculated and the different external input data necessary is underlined.

Circuit	Heat source Map	External Input for heat source	External input for heat sink
HT	***Fuel Consumption***	***engine rpm and engine torque***	***car velocity***
MT	***Efficiency***	***motor rpm and motor torque***	***car velocity***
LT	***Internal Resistance***	***HV battery current***	***chiller outlet pressure***

Table 3: summary of external model input

The validation of the model was done using HCU signals from the test as external input files and comparing the coolant temperature and heat flows obtained with the ones calculated starting from experimental data.

3.3.3 Thermal model with thermal masses

In the first thermal model, only the coolant temperature is calculated. In addition, the conversion from power losses to thermal power to the coolant has been done without physical meaning but in order to fit measurement results. In the last step of the model, these two limits are overtaken.

The addition of thermal masses and thermal resistance allows to predict the temperatures of the components, like the electric motor, the battery, and the inverter. The amount of thermal power exchanged with the coolant and the remaining part, exchanged with air or that heats up the mass, are calculated using convection relationships.

The description of thermal behaviour of a component is quite complex and to obtain highly accurate results, a detailed model is necessary. The electric motor, in particular, is very complex since it has different materials, internal gap air, complicated shapes. In literature, complex thermal model are built, like the one in [16].

The thermal mass belongs to the thermal library and has four thermal ports. They are connected to other libraries, where the thermal power is calculated. The thermal properties of the material has to be specified.

The temperature is calculated as:

$$m\, c_p(T)\frac{dT}{dt} = \sum_{i=1}^{4} dh_i$$

$$T(t) = T(0) + \frac{\sum dh}{m\ c_p(T)}$$

where m is the mass, $c_p$is the specific thermal capacity and $\sum dh$ is the sum of the four thermal flows of the block. If the component is composed of different materials, more than one thermal mass has to be considered. The different thermal blocks are linked together with a block that models the conduction. The general conduction equations are reported in chapter 2. Not only the specific thermal capacity, but the thermal conductibility determines how fast the material increases or decreases its temperature as well.

The heat exchanged between solid material and external air is considered using an external mixed convective exchange. The external surface of the material, such as the surface cooled down by the air, has to be specified. The air velocity characterizes the thermal exchange and in a car, it is function of the car velocity, as mentioned in the previous pages.

The majority of the power losses are removed by the coolant through convection. This is modelled using the block in *figure 32.* Port 1 and 3 are inlet and outlet of the coolant, the port 2 calculates the thermal exchange and it is connected to a thermal mass. The heat exchange is internal convection between the fluid in the pipe and the wall of the pipe. [18]

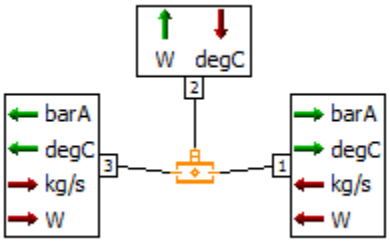

Figure 32: thermal-hydraulic pipe with heat-exchange

The internal convection can be modelled imposing a convective heat exchange coefficient or providing correlations for the Nusselt number. Neither of these options is in general available without specific investigation. A third option is to use *predefined correlations* that are generally accepted to describe the heat exchange with laminar or turbulent flows. They are described in chapter 2 and this option is the one used in the present model. Beyond

convective correlations, the heat exchange is also function of the geometry of the pipe, in particular of the diameter and the length of heat exchange.

The predefined correlations calculate the Nusselt number, and from this, it is possible to know the heat exchange coefficient as

$$h_{conv} = \frac{Nu\ k}{L}$$

where L is a reference length and k is the thermal conductivity of the fluid. The convective heat exchange is computed as

$$Q_{conv} = h_{conv}\pi Dl\ (T_{in} - T_{wall})$$

Some of these parameters were not known. The approach was to give them a physical value in the first attempt and try to calibrate this value in order to match some of the experimental results. Once a good value is found, other tests are used for the validation of the model.

The thermal masses for the electric motor and the battery are included in the respective circuit. On the other hand, the ICE circuit is not modelled anymore in this step and its final model is the one described in the previous chapter. In fact, the thermal power to the coolant has already been calculated from the fuel consumption map. It is different from the other two circuits where the total power losses have been obtained. In addition, while in the PEEM all the power losses are converted to heat, this is not true in the combustion engine, where part of the energy remains in the gas enthalpy or it is not converted at all due to combustion inefficiencies. The problem is much more complicated and more estimation are necessary. Engine thermal model need a big effort and has been deeply investigated, so is not included in the present model.

Electric motor and inverter

As mentioned, electric motor thermal model need to be complicated in order to reach a high level of accuracy. This is not the specific focus of this work, therefore the thermal model had to be as simple as possible. After some attempts using only one thermal mass, the decision was to use one more mass. In fact, it was not possible to match both the material temperature and the coolant heat flow with this approach. On the other hand, using two thermal masses is more realistic and allow to match the experimental data better. The model scheme is shown in *figure 33*, it is an extract and all the cooling circuit is cut away.

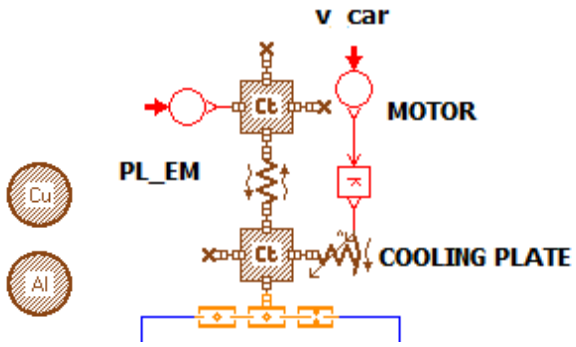

Figure 33: electric motor thermal masses for temperature prediction

The first thermal mass includes all the thermal generation. This is an important approximation but it has been considered acceptable in this easy thermal model. Actually, the electric motor thermal losses are divided between rotor, stator and bearings. Different kinds of motor have different iron and joule losses and different distribution inside the component. Another mass is used to implement the cooling plate, that absorbs part of the losses for conduction and it is cooled down by the fluid for convection. A port of the cooling plate is also connected to external convection with environmental air, to simulate its cooling effect. This contribution is function of the air velocity and so of the car velocity. The parameters specified are the mass of the motor and the thermal properties of its materials. In addition, the surfaces for the conduction and convection exchanges have to be specified. For the conduction, geometrical data was not available and the value is calibrated to match a test case and obtain a good matching with the motor temperature. For the convection exchange, the diameter of the pipe was known but not the heat exchange length and so also this value is calibrated in one test case to obtain the experimental coolant heat exchange. The thermal properties used are the one of the copper for the motor and of aluminum for the cooling plate. The total weight of the motor was known, the division between the two thermal masses was estimated. The parameters are the same both for the two motors at the front axle and for the ISG in the rear axle, since the motors are identical.

For the inverter, only one thermal mass was used, choosing aluminum as material and using the known value of weight. The inverter power losses are quite low compared to the electric motor ones, since its efficiency is higher. In addition, it is very well cooled down by this system. Due to this, its temperature maintains lower values than the motor.

Battery

For the battery, the approach used is identical to the one used for the electric motor, but only one thermal mass is used. The weight of the component was known, while its thermal properties were looked up in literature, where they are widely investigated. Experimental value of Li-ion battery thermal properties can be found in [20] and [21]. Using only one thermal mass, only the specific thermal capacity influences the results, while the thermal conductibility is important if more thermal masses are considered and determines the thermal resistance. It is difficult to calculate the specific thermal capacity and quite different values have been calculated. Starting from values reported in the papers, the parameter has been calibrated in a test case and the value used is 1100 $\frac{kJ}{kg\ K}$.

The internal resistance of the battery, used to calculate the power losses, is function of the battery temperature. In the previous step, the external signal (from the BMS) was implemented, but now it can be deleted. In order to calculate the battery power losses, only the battery current has to be provided to the model. The battery circuit model is reported in *figure 34.*

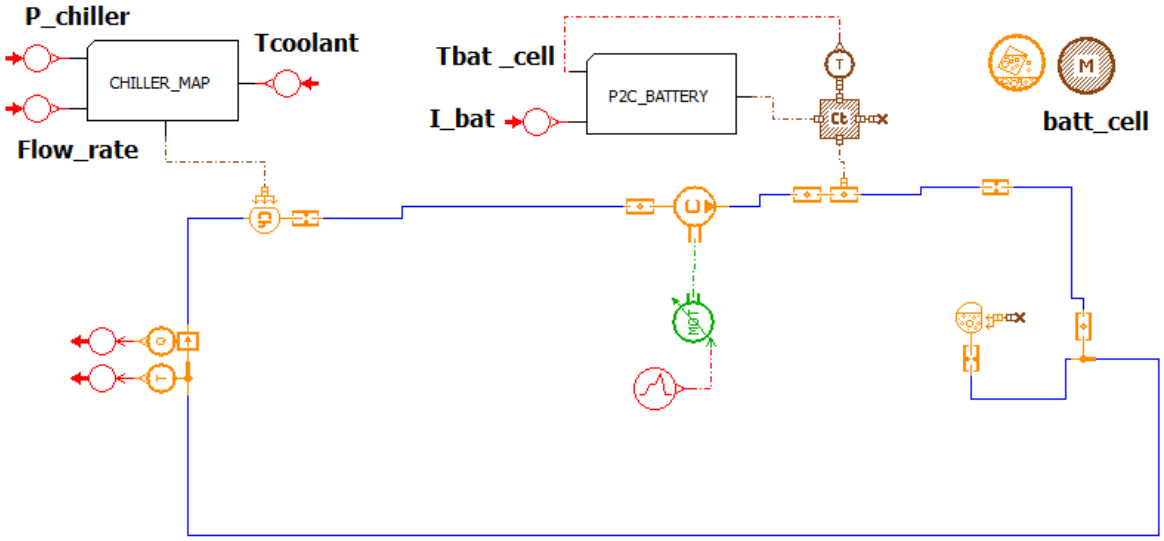

Figure 34: battery cooling circuit with thermal mass

Air Conditioning modelling

In PHEV and BEV, the A/C compressor not only has to cool down the cabin but also the battery. It is interesting to be able to model the integrated system to design it and also to study control strategies since the HV compressor has a considerable power and it has an important impact on the battery SoC.

Air Conditioning modelling is much more complicated than a cooling system, since the fluid changes phase in the condenser and the evaporator. More variables, like the gas mass fraction, have to be taken into account. The heat exchange in condenser and evaporator have to be modelled in details to ensure that the all the fluid changes its phase. Specific libraries are implemented in AMESim®: the two-phase flow library substitute the thermal-hydraulic and the Air Conditioning library allows the modelling of the four main components, compressor, condenser, lamination valve and evaporator. Since the physics of the problem is much more complex, the model becomes extremely detailed and many parameters have to be provided. Most of these parameters were not available, in addition the effort to obtain a good model was too high. For these two reasons the system has not been validated.

However, thanks to the aforementioned library, building a generic air conditioning model is not so difficult and a first attempt is included in the present work. The compressor block receives a rotational speed signal from the mechanical library and its displacement and efficiencies are required. The condenser model is really detailed and both the refrigerant and the environmental air side are modelled. For the refrigerant side, each heat exchanger tube is considered and its geometrical parameters are specified. In addition, heat exchange coefficients for Nusselt number correlations have to be provided. For the external air side, the temperature, humidity, pressure and mass flow rate are the external input. After the condenser, the fluid goes to the lamination valve, that in this system is a thermal expansion valve. As described in the first chapter, it allows a better regulation of the refrigerant mass flow rate, only an amount which satisfies the evaporator request goes to the heat exchanger and the superheat of the fluid controlled, reducing the energy consumption of the compressor. Thanks to the valve, the liquid mass fraction at the outlet of the evaporator is zero and the liquid accumulator can be omitted. After the lamination valve, the refrigerant goes to the evaporator. The air conditioning system integrated with the battery cooling circuit has two evaporators, one is for the cabin and one is

for the chiller. While the first is the classical air conditioning evaporator (liquid-gas exchanger), the chiller is a liquid-liquid heat exchanger (or liquid- two phase flow). In the present work, the chiller is not physical modelled but the calculation of its heat exchange is map-based. As mentioned, the outlet pressure of the chiller is a necessary data to enter in the map and from the A/C model can be transmitted to the battery coolant circuit.

A first attempt of model the liquid-liquid heat exchanger has been done: the idea is to use internal convective exchange, one for the coolant side and one for the refrigerant side, connected to a thermal mass that represent the chiller plates. The approach has been found in literature in [22]. The cabin evaporator is not modelled at all, since neither the cabin is included in the model. The A/C model has not been validated, only a generic model of the system has been built but most of the necessary input has not been specified. In addition, more complex models are necessary to consider heat exchange effects in more detail. However, it is interesting for this work to include this first attempt and underline that this is not difficult thanks to the specific library of the software used.

4. Results and validation

The results obtained in the three steps of the model are compared to experimental data in terms of volumetric flow rate, coolant pressure, coolant temperature, thermal heat flows of heat sinks/sources and temperature of components (e-motor, inverter and battery). As already mentioned, the experimental data includes signals from the control unit and acquisitions from additional sensors. From this data, all the information necessary to compare and validate the model was available.

To perform the simulation, the external input data listed in *table 3* (car velocity, battery current, invert current and voltage, etc..) is taken from the available data. Neither a vehicle model or a powertrain model is built, so this is the only way to be able to compare the results. In addition, the control signals for the pumps and fans must be the same. They are copied from the control unit data as well. For the three circuits, the complete list of external input to perform a test case is reported in *table 4*.

	External Input for thermal model	Control signals
HT	*engine rpm / engine torque / car velocity*	*Fan signals (2)*
MT	*motor rpm / motor torque / car velocity*	*E-pump rpm (3), Fan signals (3)*
LT	*HV battery current / chiller pressure*	*E-pump rpm (1), HV Compressor rpm*

Table 4: complete input list for simulations

During the validation, all these signals are provided from experimental data. Once the model is validated, the thermal model could be connected to a drivetrain model and different control strategies could be studied and developed. This is better point out in the next conclusive chapter. In addition, initial conditions are specified as well. Air, coolant and material temperature values are set equal to the real conditions during the test.

Like for the modelling part, the validation is divided in three steps. For each one, the main relevant results are here discussed.

4.1 Hydraulic validation

The first model developed considers only the hydraulic library and temperature is not taken into account. As described in the previous chapter, the pressure losses are calculated from experimental data. In addition, for the medium and low temperature, electric pumps are used

and they are controlled with a start and stop strategy. When they work, they have always the same flow rate, that allows to have the maximum efficiency. Due to this, only one operating point was available from data and the validation is not guaranteed for different flow rates.

From the characteristic curve of the pump and the total pressure losses, the operating point is found; flow rates and pressures in each point of the circuit are determined and compared with measurements. Flow rate and pressure results for the front axle circuit are reported, respectively, in *figure 35a* and *figure 35b*.

In *figure 35a*, also the ISG flow rate is reported. Its value is roughly the half of the front axle value, since it has one e-pump and one e-motor, while the second one has two of both.

The same results are obtained for the low temperature circuit, in which the hydraulic model is very simple. In fact, no three-way valves are present and only two thermal sources are modelled. The electric pump is the same used in the medium temperature circuit, the total pressure losses are a bit higher than the medium temperature circuits and so the operating point is found for a lower flow rate value (20 l/min against 27 l/min for the previous circuit).

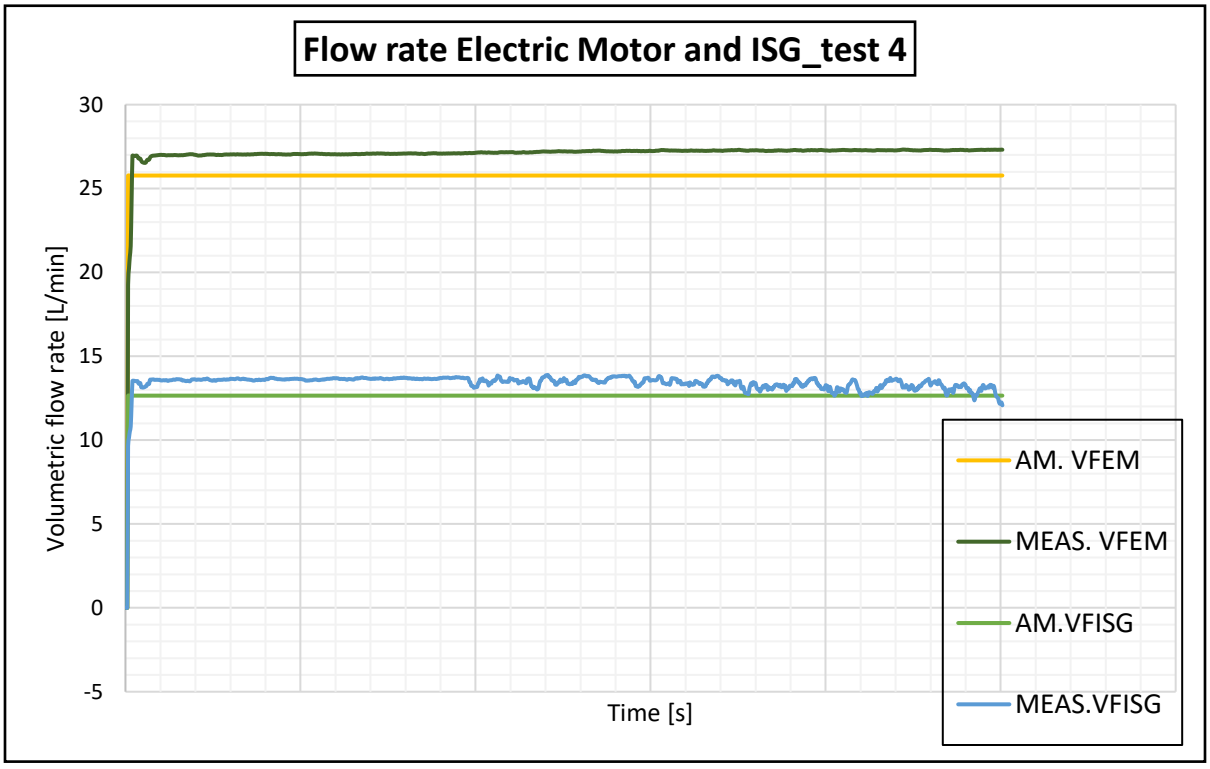

Figure 35a: volumetric flow rate validation for medium temperature circuit

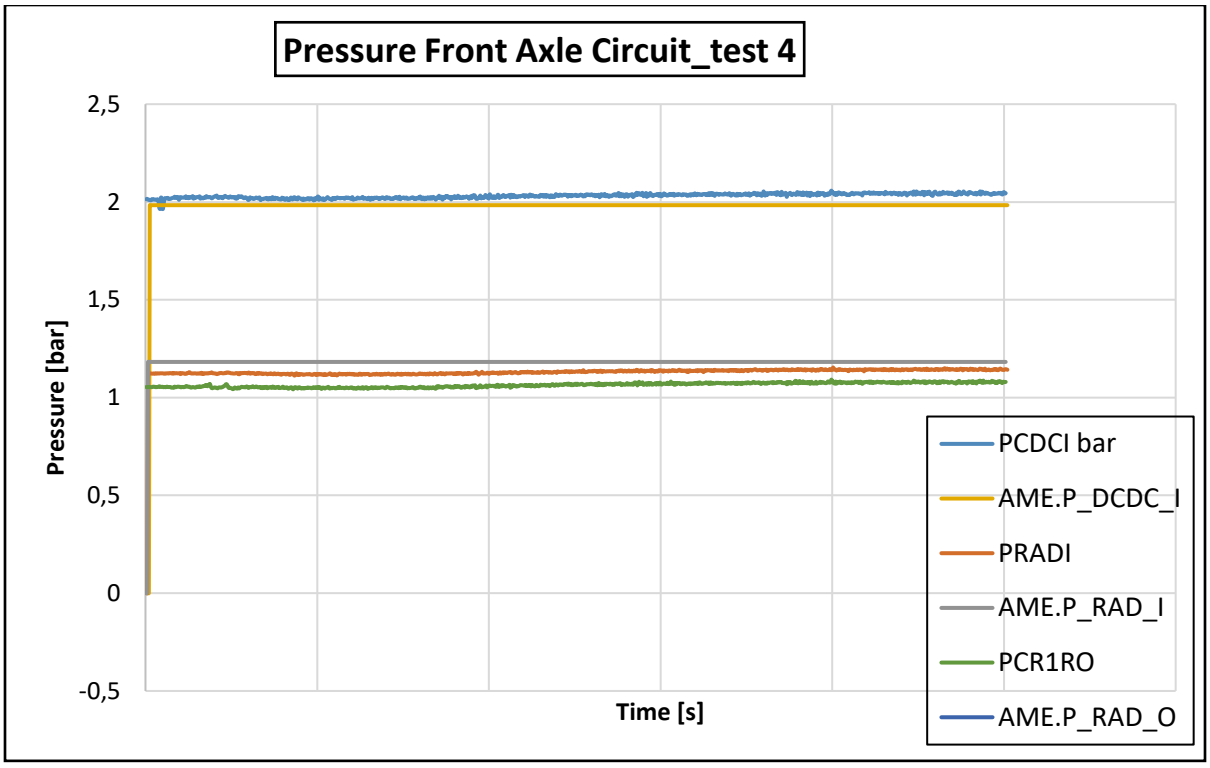

Figure 35b: pressure validation for medium temperature circuit

For the high temperature circuit, the model is different since the pump is not electric but is driven by engine belt. As a consequence, the flow rate and the pressure drops are not constant but always change following the engine rotational speed. The rotational speed of the pump has a fixed ratio with the engine and the flow rate is calculated as rotational speed times displacement. In some of the test cases the thermostat was not used and these are chosen for the hydraulic validation, since it is not possible to include this thermal component. As described in the previous chapter, a different pump block is used for the engine circuit because the pump characteristic was not available. In *figure 36a* and *36b*, flow rate and pressures obtained with the model are compared to experimental data. The test considered is the same of the previous charts. While the flow rate and pressure were constant using the e-pump, the engine pump follows engine rotational speed and its flow rate is more variable. The error between the two curves was calculated after that a stationary operating point was reached.

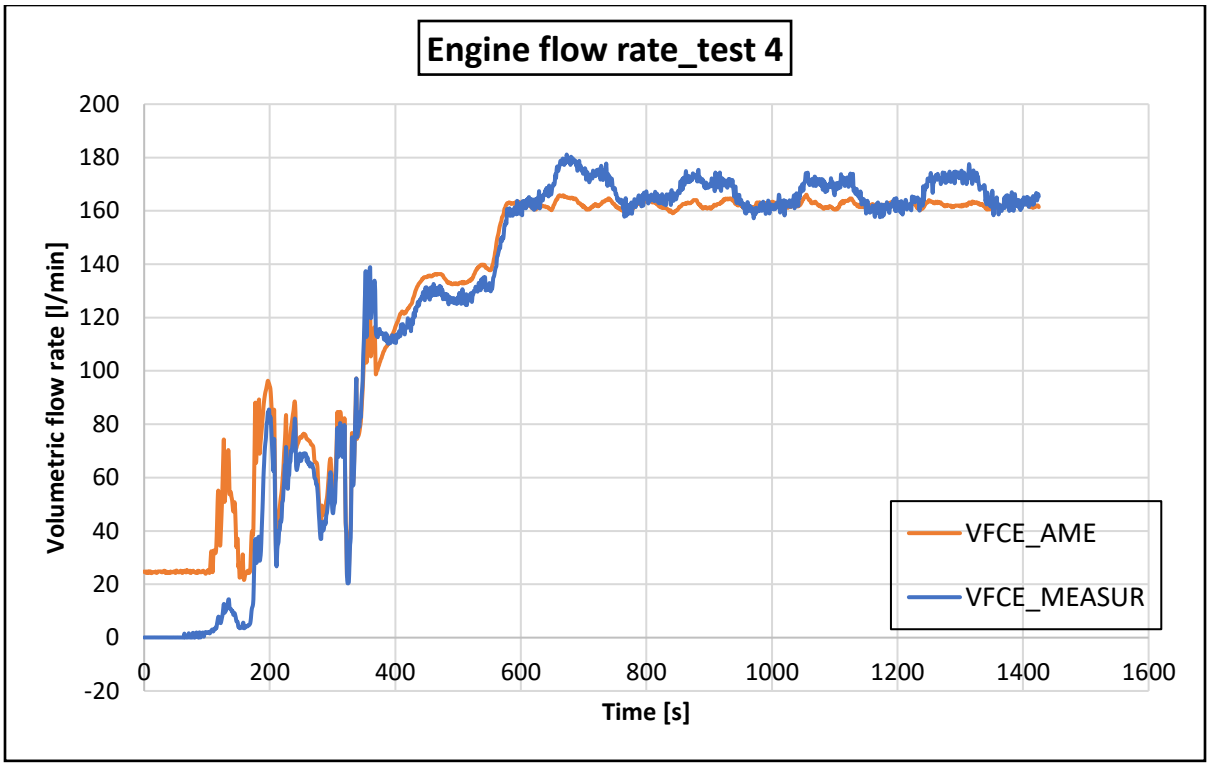

Figure 36a: engine flow rate validation for high temperature circuit

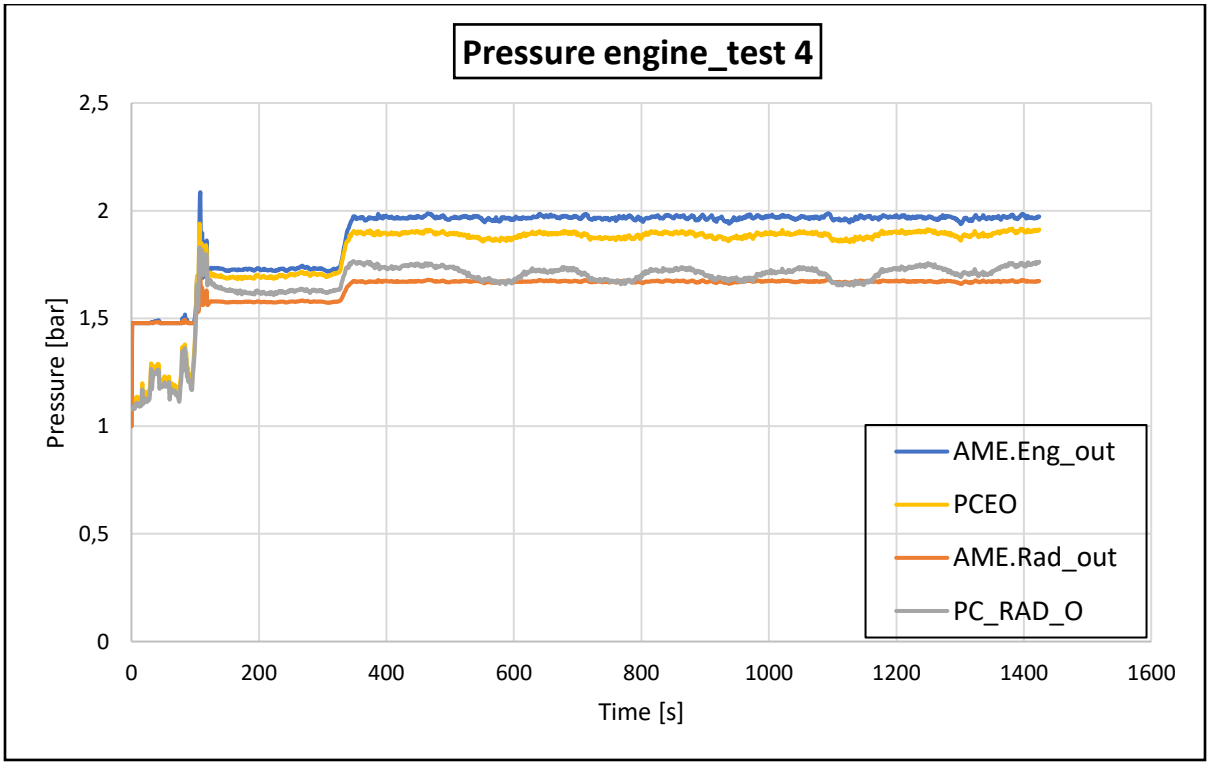

Figure 36b: engine pressure validation for high temperature circuit

The different curves are compared and the percentage error has been calculated. The results obtained are reported in *table 5*. The medium error does not overtake the 5%, which is considered acceptable for the aim of the project. Therefore, the hydraulic model is considered validated.

	Variable	Position	Medium error	Maximum error
			%	%
HT	Flow rate	(steady)	**3,69**	**8,88**
	Pressure	*Engine out*	**4,45**	**5,73**
		Radiator out	**1,75**	**4,15**
MT	Flow rate	*EM*	**5,11**	**5,95**
		ISG	**3,51**	**10,1**
	Pressure	*EM input*	**0,62**	**3,74**
		FA Rad outlet	**2,97**	**5,41**
		IPU (ISG) in	**3,33**	**5,29**
LT	Flow rate		**1,55**	**2,57**
	Pressure	*Battery inlet*	**4,63**	**8,7**

Table 5: summary hydraulic circuit errors

4.2 Thermal model map-based validation

Once the hydraulic part is validated, it has been converted into the thermal-hydraulic library and no other modifications are necessary. The volumetric flow rate and the coolant pressure of the model are still valid and no other results are presented. This is the main advantage of the step-by-step procedure.

The first step of the thermal model calculates the heat exchange between the coolant and the heat source/sink using maps. For the engine and for the radiators, the heat exchanged with the coolant is directly calculated from these thermal maps and no other operations are necessary. For the electric motor, inverter and battery, the total power losses are obtained from the maps and they have to be converted to heat exchange with the coolant. To do so, in this first step, a fixed ratio is calibrated, as described in the previous chapter. The results compare heat flows and coolant temperature in some of the test cases available. They are presented divided in the three circuits.

High temperature circuit

The developed model for the engine coolant circuit is reported in Appendix. The engine heat exchange with the coolant is calculated using a map of fuel consumption. The total energy

available is obtained and then the heat-transfer rate to the cooling medium is calculated considering a calibrated percentage. The values found are, generally, lower than the values in literature, around 25% for low rotational speed to 15% for high rotational speed. For the two radiators, heat exchange map as function of coolant flow rate and air velocity are used and the results have already been reported in the previous chapter. In addition, the thermostat is included. Putting together the heat source and the two heat sinks, providing the different external input necessary (engine rpm, engine load, etc..) and the initial conditions, the coolant temperature is calculated. In *figure 37*, the engine and one of the radiator outlet temperatures are compared to the measured values. The test is always the test 4, that is the same used for the previous comparison of the engine and radiator heat flows.

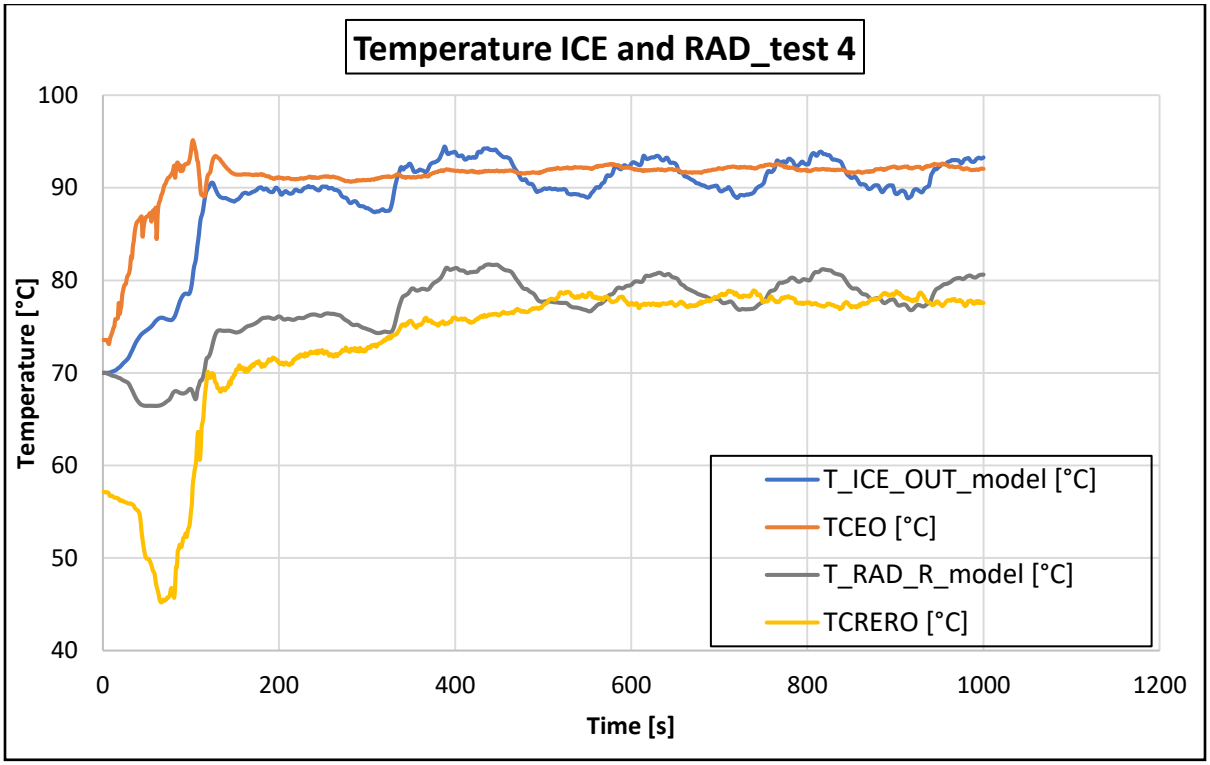

Figure 37: engine coolant temperature, model values and measurements

The heat flows were reported in *figure 23* and *29* and they were quite similar to the experimental values. Once the temperature is stable, the two temperature curves are quite similar as well and this proof the model is correctly built and calibrated. Once the stationary state is reached, in this case after 200s, the medium temperature error is ± 3°C and the maximum error is ± 5°C, values considered acceptable in the present work. Higher errors are

obtained in the first part, during the warm up of the engine. This is due to the thermostat model, which has to be better calibrated to obtain better results also in transient cycles. While for the other two circuits thermal masses will be included in the second step, for the engine circuit these are the final results.

Medium temperature circuit (first step)

The conversion of the power losses to a heat exchange with the coolant is based on a calibrated gain without any physical meaning. This is done considering a test case at constant speed/constant inverter current and finding the value between 0 and 1 that matches the experimental curve. For the electric motor is 0.7 and the curves obtained are reported in *figure 38.* The grey and the orange curves match each other only once heat flows are stable and it is evident that the approach is too simplified to obtain good results also in transient conditions. For this scope, a model which includes thermal masses and convective exchange is necessary. Thermal inertia is not modelled with this approach: when the current request increases, in the same time step also the heat absorbed by the coolant increases and this is not realistic.

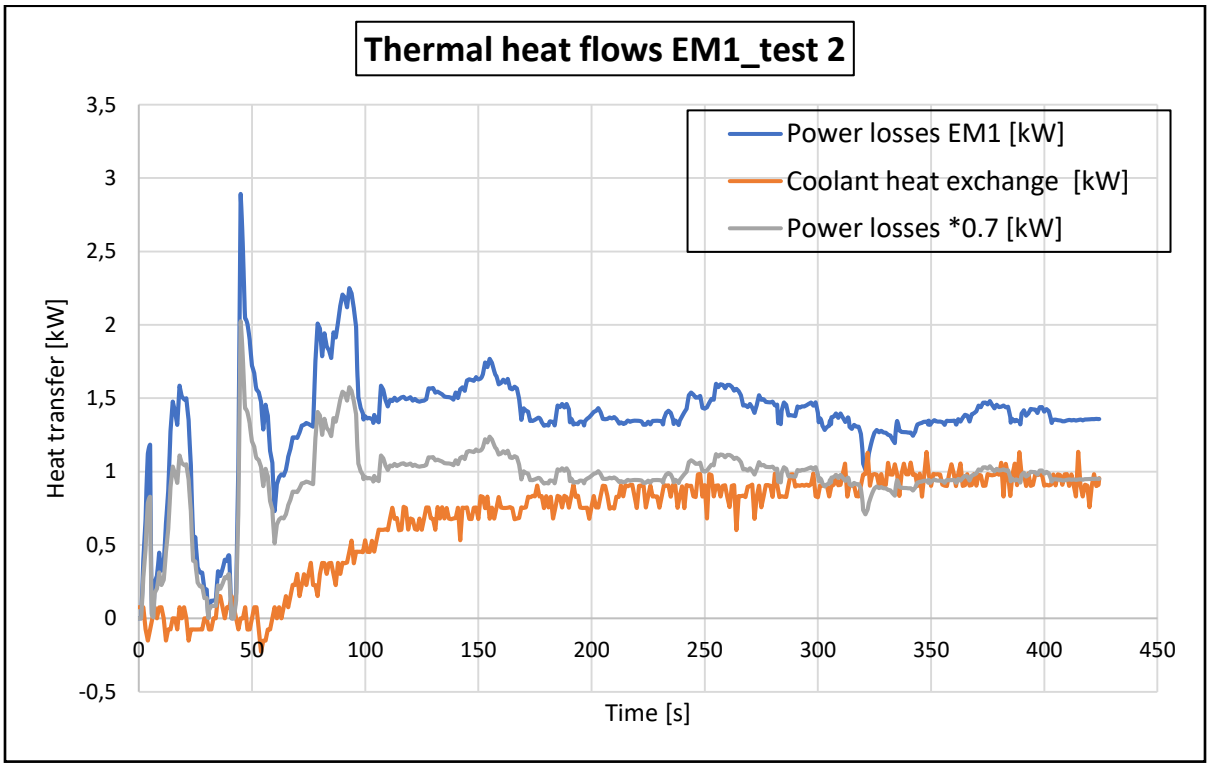

Figure 38: electric motor power losses and heat experimental coolant heat exchange

The absence of thermal inertia is also a problem when the car is stopping. In fact, in this situation the current is zero but the coolant is still cooling down the motor. Due to this, parts of test, when the car is at standstill, are not considered in this step, but they will be taken into account in the next one. Once a suitable value is found, another test available is simulated to compare the results and validate the model. The test chosen is a pure electric driving cycle: for the first 300s the torque load is low, then it increases until a stable velocity is reached (*figure 39a*). The electric motor and radiator outlet coolant temperature are compared with the acquisited values. In figure 39b, the four curves are reported.

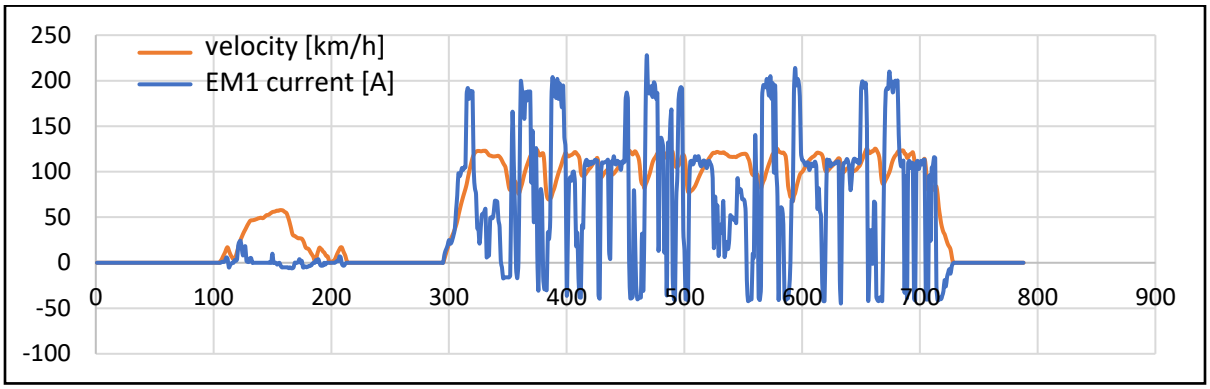

Figure 39a: velocity and IPU1 current for handling electric cycle

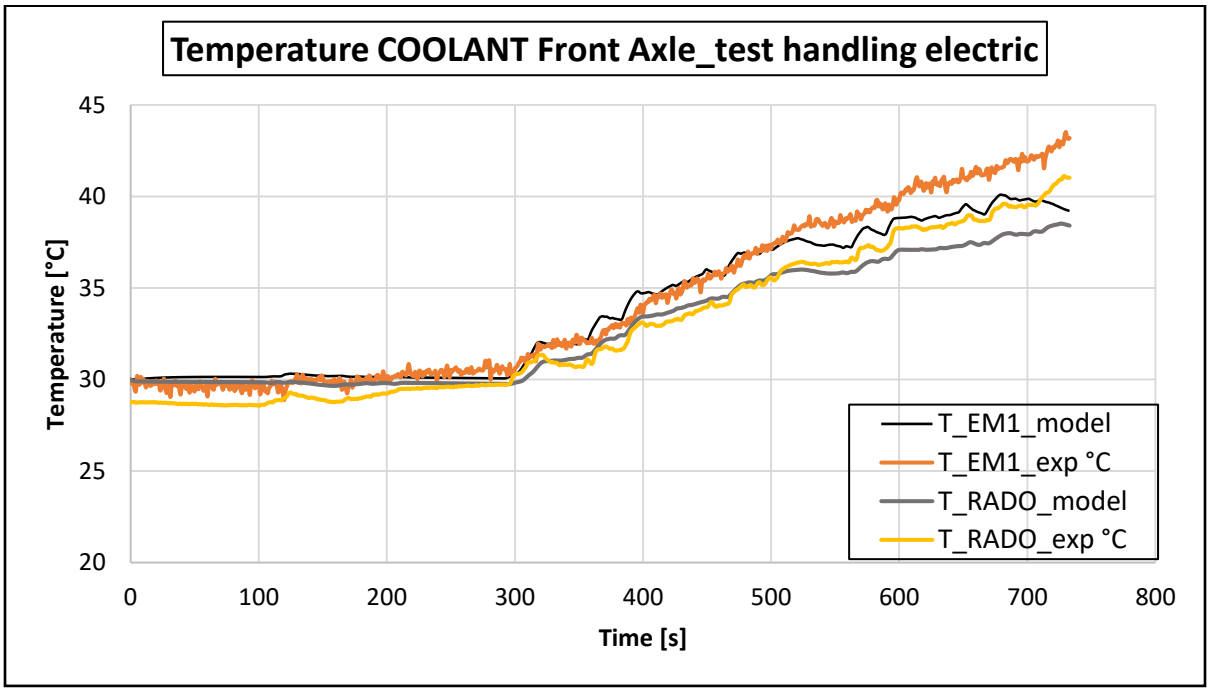

Figure 39b: e-motor and radiator coolant temperature

Although the model is simplified and based on map, the calibration was correct and the coolant temperature are well predicted. The medium error of temperature is ± 1°C and the maximum error is ± 5°C.

The same approach is used for the validation of the ISG circuit. The test chosen for the calibration of the gain is roughly at constant speed (it is the same used for the hydraulic calibration). In particular, in this situation (high torque load and low SoC value) the ICE is providing power to the wheels but part of its energy is used to recharge the battery moving the generator. The ISG power losses are calculated using the map of efficiency as well. Actually, its torque is negative since it works as generator but no data of this region was available. So, a symmetric behavior of the efficiency was estimated. In figure 40, the calibration of the gain is considered: multiplying the power losses by 0.8, the heat flow value matches the experimental coolant heat exchange.

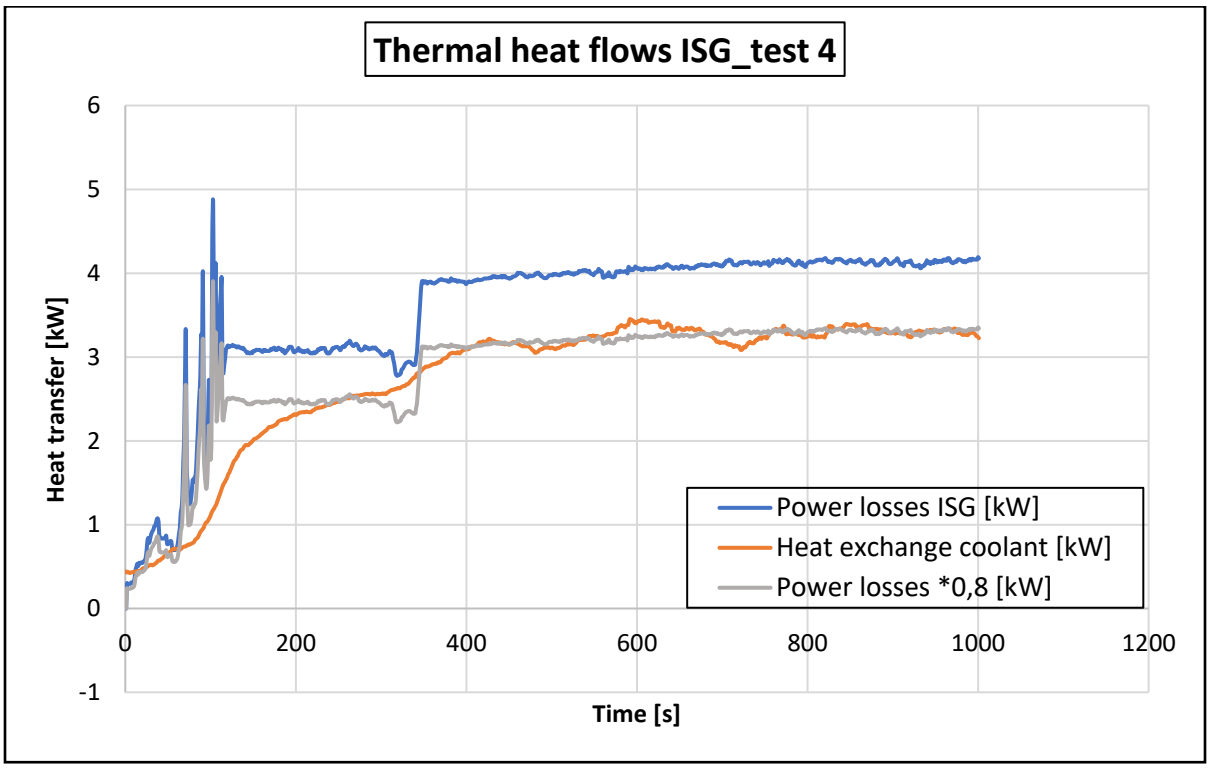

Figure 40: ISG losses and experimental coolant heat exchange

Like for the front axle circuit, thermal inertia cannot be considered and the gain guarantees a reduced error only after a steady state has been reached. The test used for the validation is a handling run in which, like in the previous one, the ICE powers the wheels and recharges the

battery. Velocity and current absorbed by the ISG are reported in *figure 41a*. The coolant temperature comparison is shown in *figure 41b*: like for the e-motor, the ISG and radiator outlet temperature are chosen for the validation.

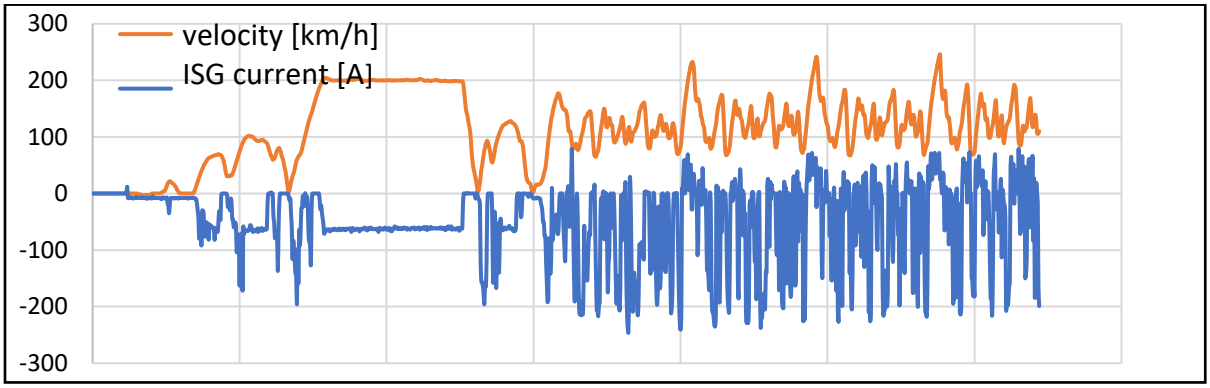

Figure 41a: velocity and ISG current for handling_corsa

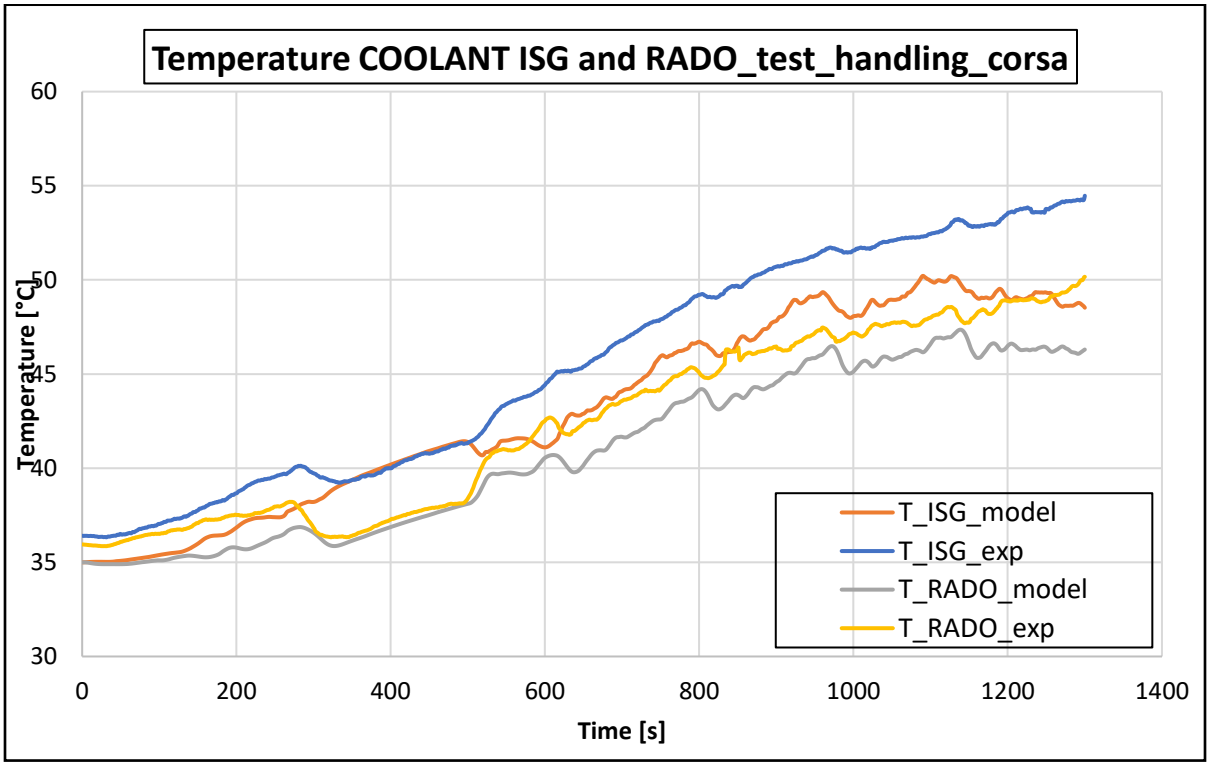

Figure 41b: ISG and radiator outlet coolant temperature

Also, these results are acceptable: the medium temperature error between the two curves is ± 2.5 °C and the maximum error is ± 5.5°C.

Low temperature circuit (first step)

While for the medium temperature circuit, experimental heat exchange data was available for both the heat sources and the heat sinks (radiators), for the low temperature circuit, only the battery coolant temperatures were measured but for the chiller no information was available. The only way to validate the heat exchange in the chiller was to build a model using the experimental coolant heat exchange of the battery and validate the model using the coolant temperature. In addition, the battery has a huge thermal inertia since its weight is very important. Due to this, the conversion of its power losses to coolant power is less accurate compared to an electric motor. So, in this first step, battery power losses are not calculated but the experimental value of heat exchange is provided directly. This curve, together with the chiller heat exchange, is reported in *figure 42a*, while battery coolant temperature obtained is shown in *figure 42b*.

The test considered is the same explained in the electric motor validation. The heat removed by the chiller is higher than the one absorbed to cool down the battery, as a consequence the coolant cools down too (thanks to the refrigerant). The temperature medium error is ± 2°C and the maximum error is 4°C and the chiller model is considered valid. As mentioned in chapter 3, the chiller heat exchange map is function of the outlet refrigerant pressure. In this step, the air conditioning is not modelled at all and the external signal (available from the control unit) is used. Both the external signals, battery heat exchange and refrigerant pressure, will be switched with internal variables of the model in the second step and in further developments.

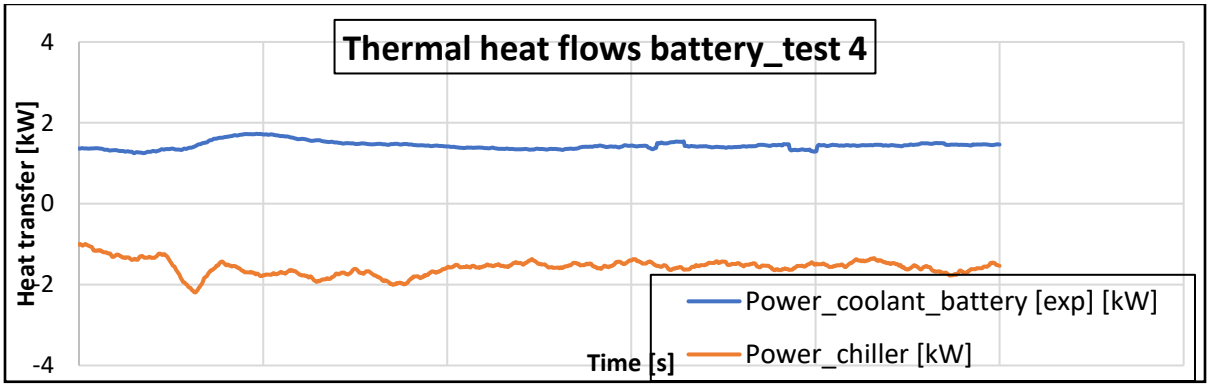

Figure 42a: battery and chiller heat flows

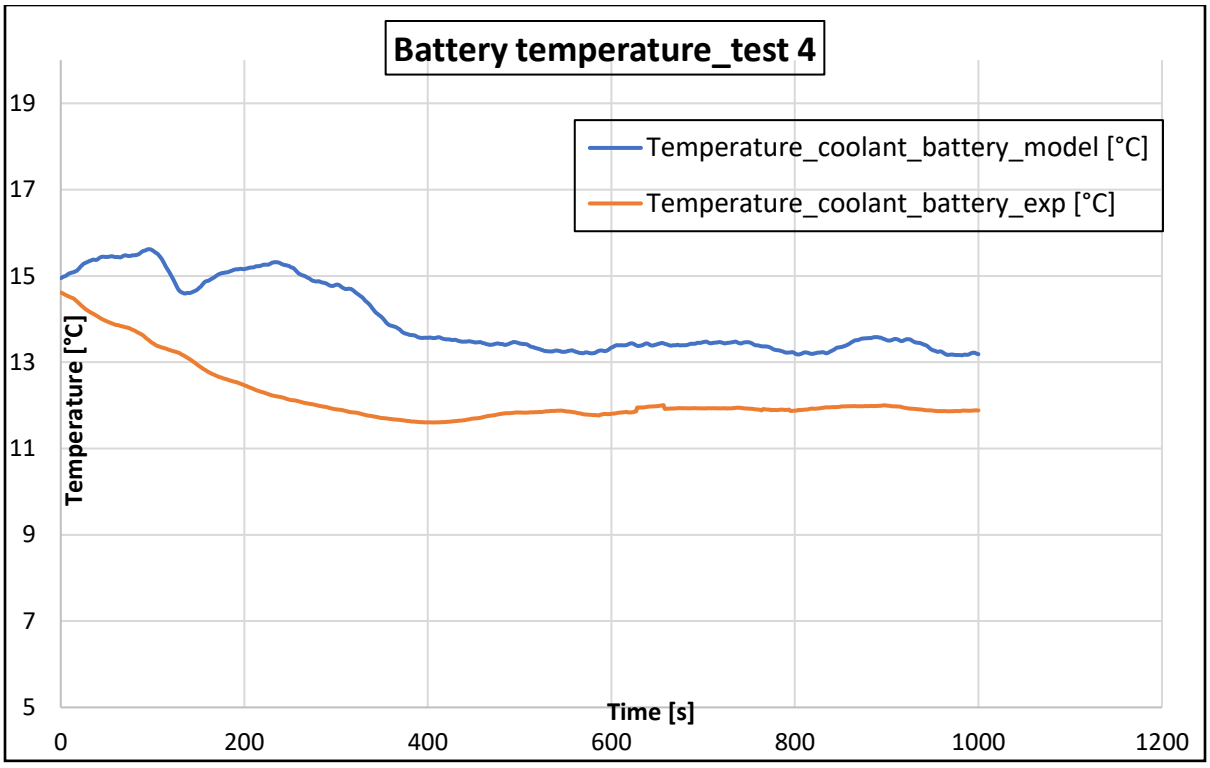

Figure 42b: battery coolant temperature for validation

4.3 Thermal model with thermal masses validation

In this last step, electric motors, inverter and battery power losses are modelled with one/two thermal masses in order to predict their temperature. This allows to calculate their temperature and evaluate if the coolant power is enough or not. The thermal mass is then linked to the coolant circuit with a block that describe the convective heat exchange. Additional parameters have to be set, some of them are known but others have to be calibrated.

Electric motor and ISG

Two thermal masses are used to model the electric motor. A summary of all the parameters necessary is reported in *table 6.*

The values of first attempts used for the calibration are the default values proposed by the software. More variables are present, compared to the previous step, and the real heat exchanged by the model depends on all of them. The calibration is more difficult and not perfect results are obtained.

Model	Parameter	Known	Calibrated	Value
Motor (thermal mass 1)	Weight	x		15 kg
	Material (for *cp*)	x		*copper*
Conduction	Contact surface		x	50000 mm^2
	Thermal conductance		x	550 $W/m^2/K$
Cooling plate (thermal mass 2)	Weight	x		5 kg
	Material (for *cp*)	X		*aluminum*
Convection exchange	Pipe diameter	x		20 mm
	Length heat exchange		x	2 m

Table 6: electric motor parameters for two thermal masses model

The test case used for the calibration is the handling pure electric drive, in which reasonable results are obtained with the parameter values shown in the table. In *figure 43a,* the calculated heat flows are shown: the motor power losses are the blue curve, the heat exchanged between motor and coolant calculated by the model is the orange, and the experimental heat exchanged is the grey. The medium difference between the last two curves is 0.1 kW and the maximum difference is 0.4 kW.

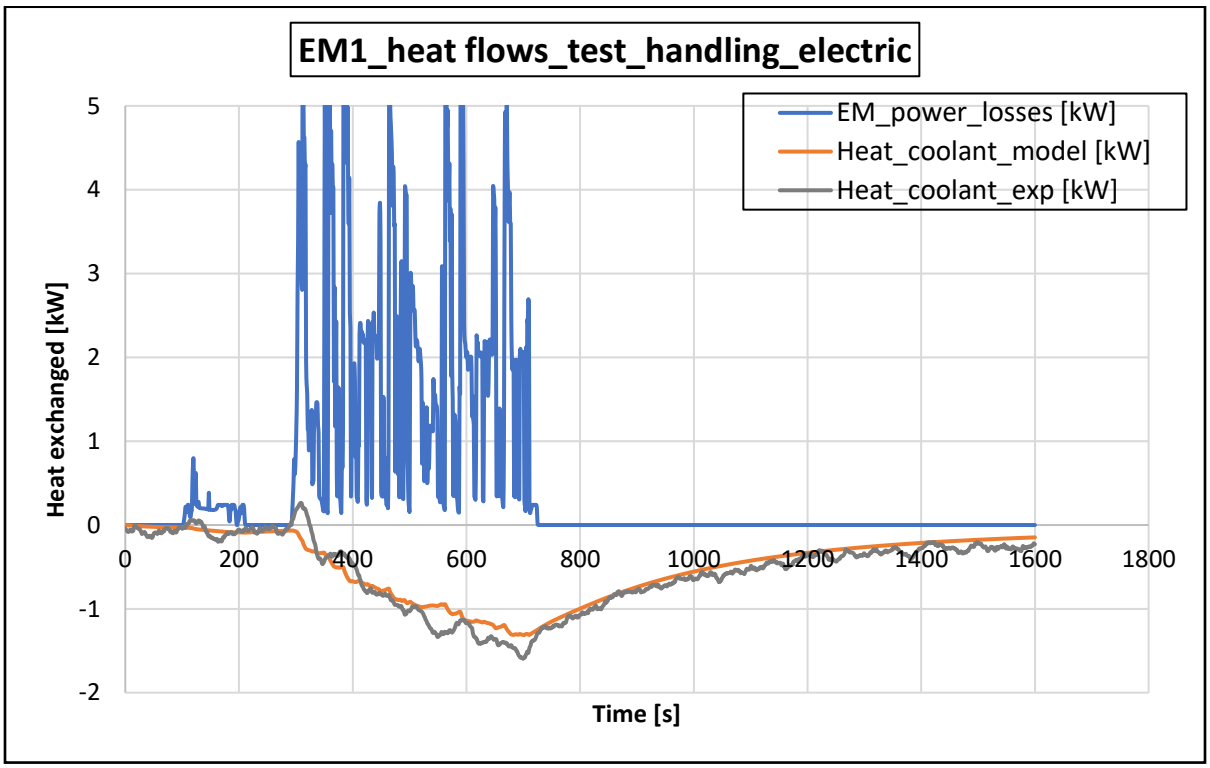

Figure 43a: EM power losses and coolant heat exchange calibration in hand_electric test

While in the previous model, when the power losses were zero, also the thermal power exchanged with the coolant was zero, in this one a thermal inertia is present. This can be seen in the previous chart: after 700s the car stops and the motor current is zero but the coolant carries on to cool down the motor. This is also a clear advantage of the electric pump, completely independent of the powertrain load.

The calibration is not completely since also the motor temperature has to be considered. The results are reported in *figure 43b*, the temperature of the thermal mass obtained by the model is compared with the motor temperature signal from the control unit. The medium error is ± 5°C and the maximum is ± 11.4 °C: they are quite high especially during the cooling phase, showing that some thermal contributions are not well considered.

In the same figure, the inverter temperature is reported as well. Only one thermal mass is used to model it, so only its weight and its thermal properties have to be set. A 5kg aluminum plate is modelled to obtain this result. As it can be seen, its temperature remains at low value: its power losses are small and the cooling system seems really efficient.

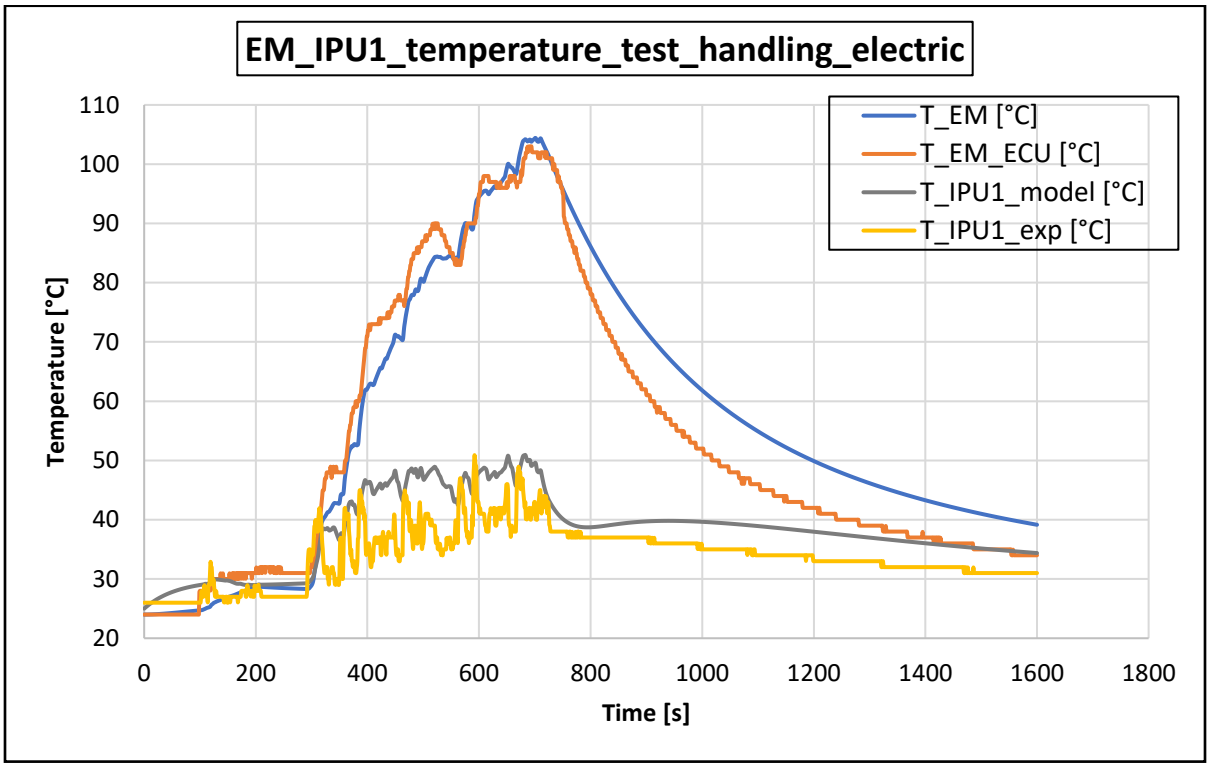

Figure 43b: electric motor and inverter temperature calibration, handling electric

It has been demonstrated that the heat flows of the heat sources and heat sinks match experimental data, so also the coolant temperature should be well predicted. In fact, the values obtained are really similar to the ones proposed in figure 39b (first step validation without thermal masses). In addition, also the standstill phase can be validated thanks to the thermal masses.

Once that all the parameter values are set, performing another simulation is necessary to validate the model. The other test available for the front axle is the test 2, already proposed in the previous pages. The results are reported in *figure 44a, 44b, 44c.*

The heat flow result is acceptable, the medium error is 0.13kW and the maximum error is 0.67kW. A first conclusion is that the convective heat exchange is correctly described and the use of predefined correlations could be acceptable for the scope of the work. Since the heat flows have acceptable error, so the coolant temperature. The medium coolant temperature error in this test case is ± 3.9°C and the maximum error is ± 5.9°C (*figure 44b*).

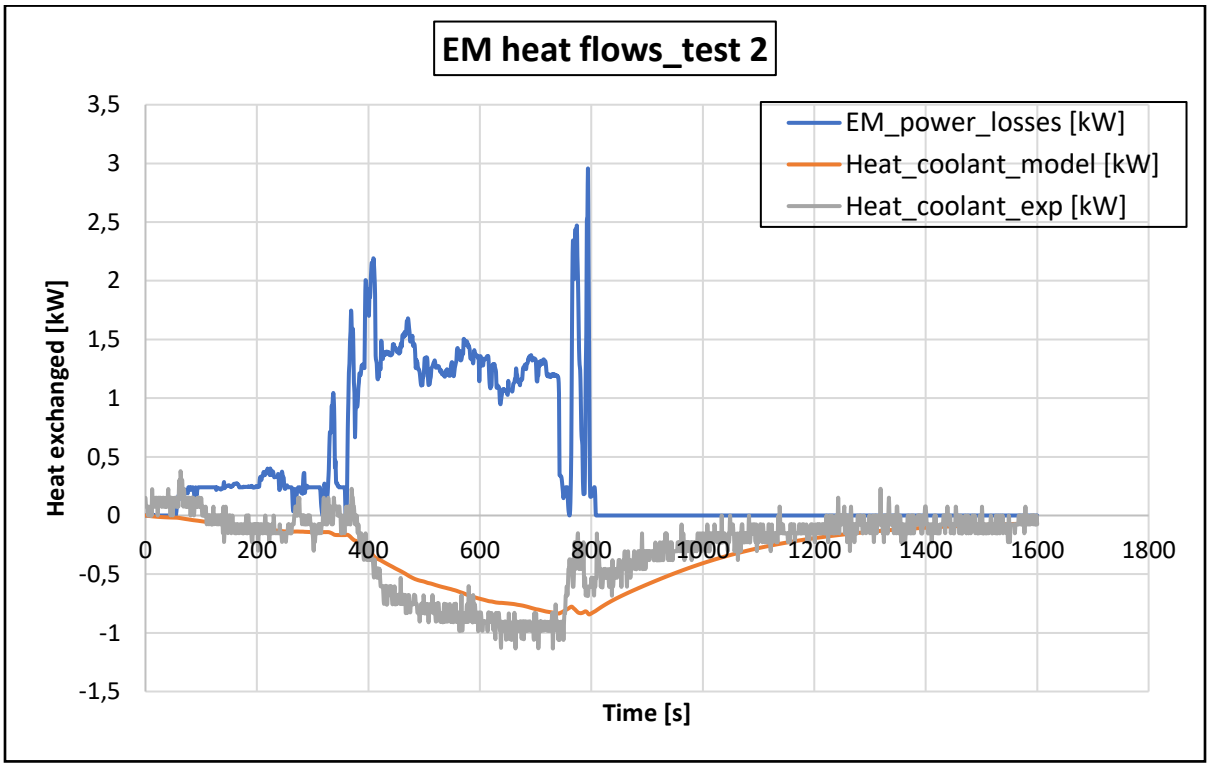

Figure 44a: electric motor power losses and coolant heat flow validation

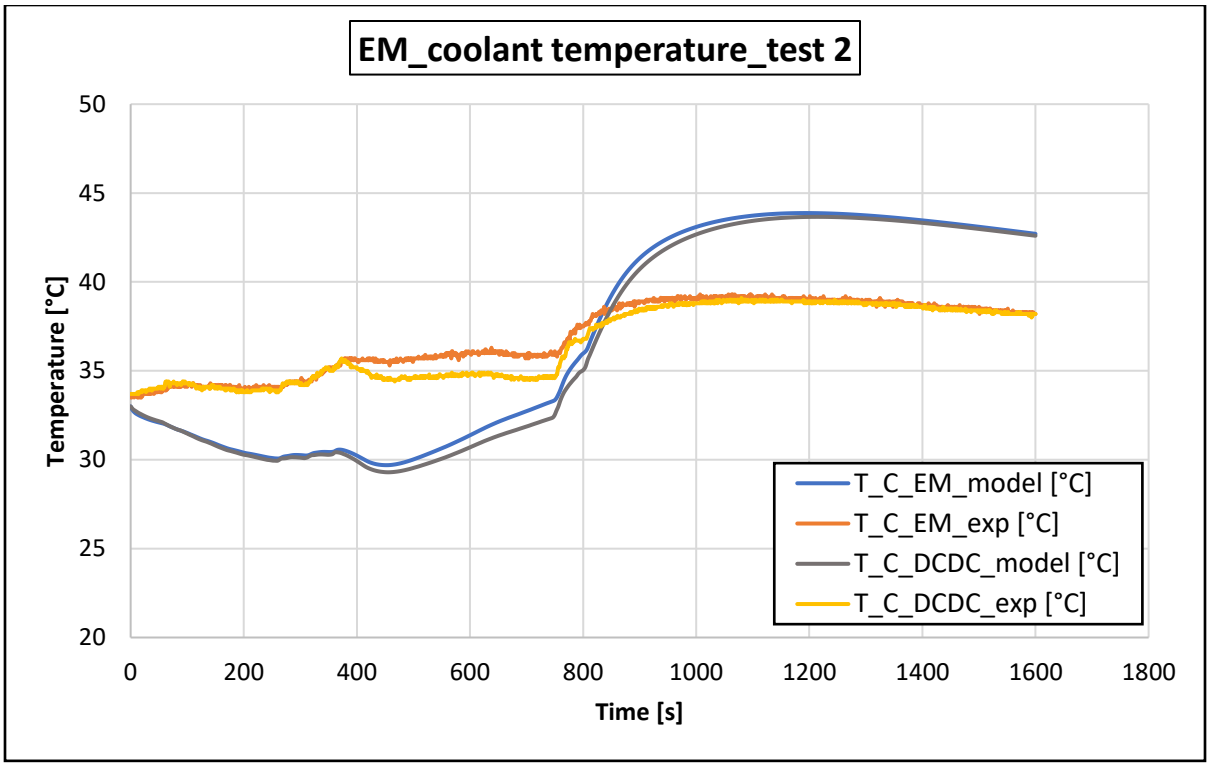

Figure 44b: e-motor and DCDC outlet coolant temperature validation

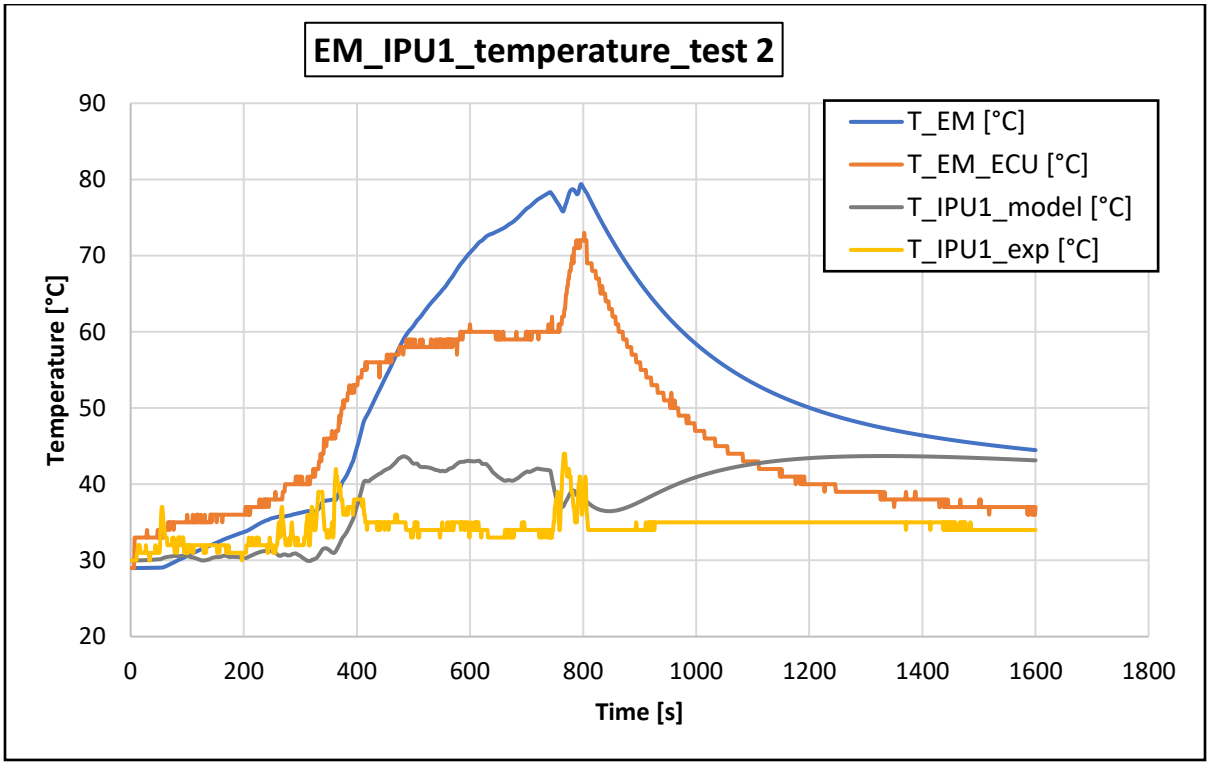

Figure 44c: e-motor and inverter temperature validation

For what concerns the motor temperature, the results are less accurate. The medium and maximum error are respectively ± 8°C and ± 16°C. The reasons of these incomplete results are due to:

- too simplified electric motor thermal model, more thermal masses and materials must be taken into consideration;
- incomplete calibration, some of the 'not known' parameters could be modified in order to obtain better results;
- the model considers a uniform temperature inside the thermal mass, while the motor has a complex temperature distribution that cannot be represented with this modelling approach.

The same parameters are used also for the ISG circuit model. The only difference is the pipe diameter for which the ISG circuit value is changed to the front axle value. The two motors are identical and also the cooling properties should be equivalents. The test used for the ISG circuit validation is the 'handling_corsa', already described in figure 41. The heat flows and component temperatures are compared and reported in *figure 45a*, *45b* and *45c*. The errors are calculated: for the coolant heat flow the medium error is 0.65kW and the maximum error is 1.4 kW. The percentage error is quite important, over 10%, Although this, the coolant temperature prediction is accurate anyway (error less than ± 5°C). For the motor temperature, as it is possible to see from the graph, the error is higher and model improvements are necessary in order to consider validate it. Generally, the coolant circuit models and the heat exchange description (with convection predefined correlations) can be considered acceptable while the motor thermal mass model need further developments.

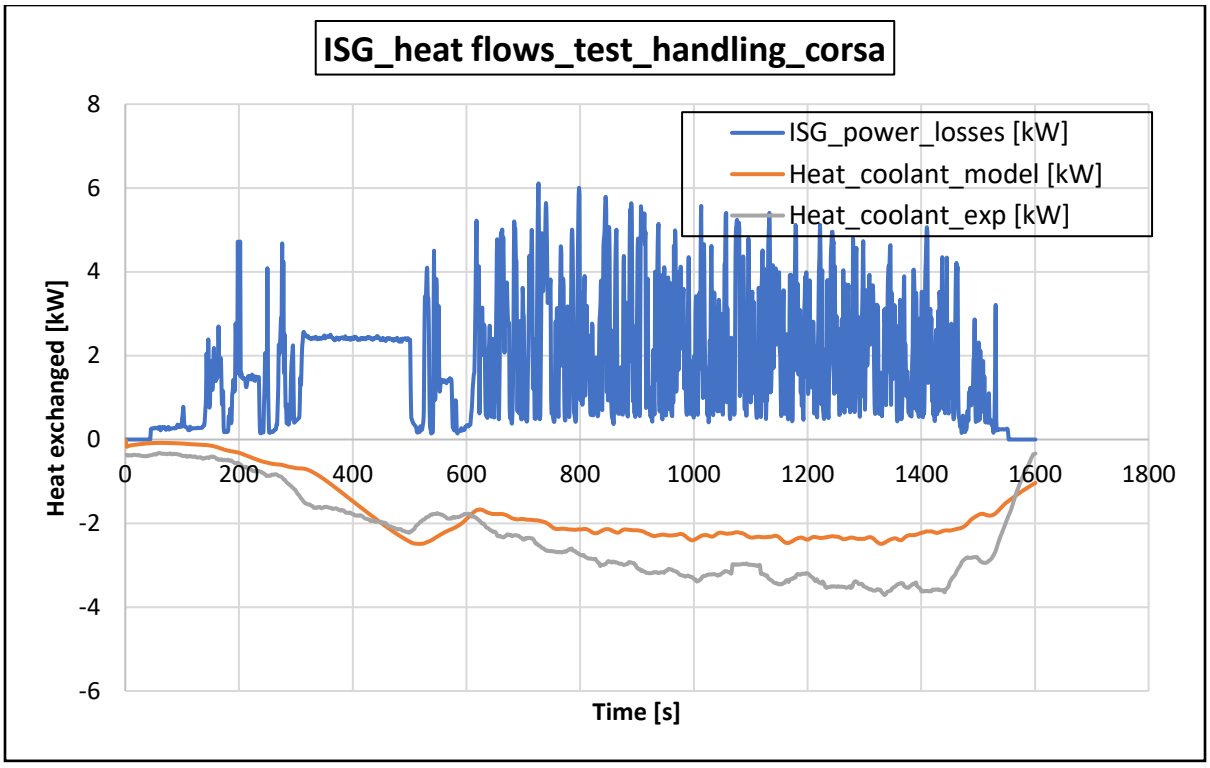

Figure 45a: ISG power losses and coolant heat flow validation

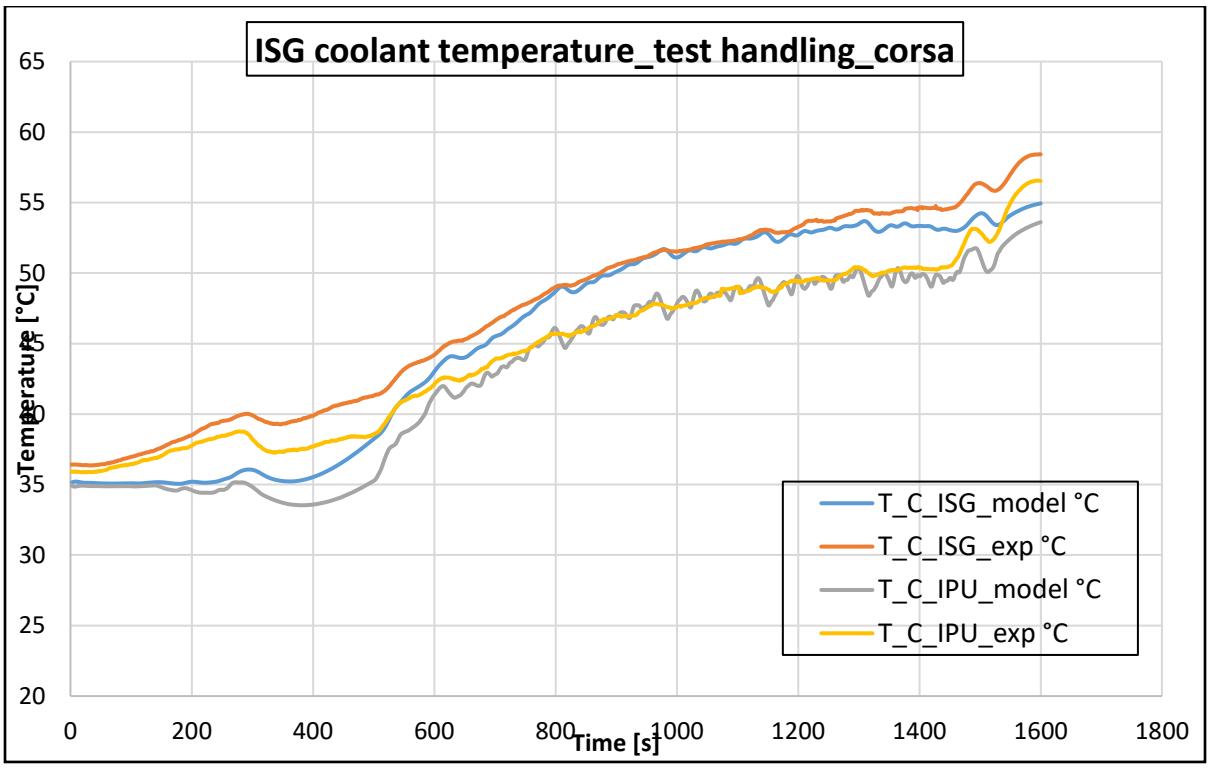

Figure 45b: ISG and IPU outlet coolant temperature validation

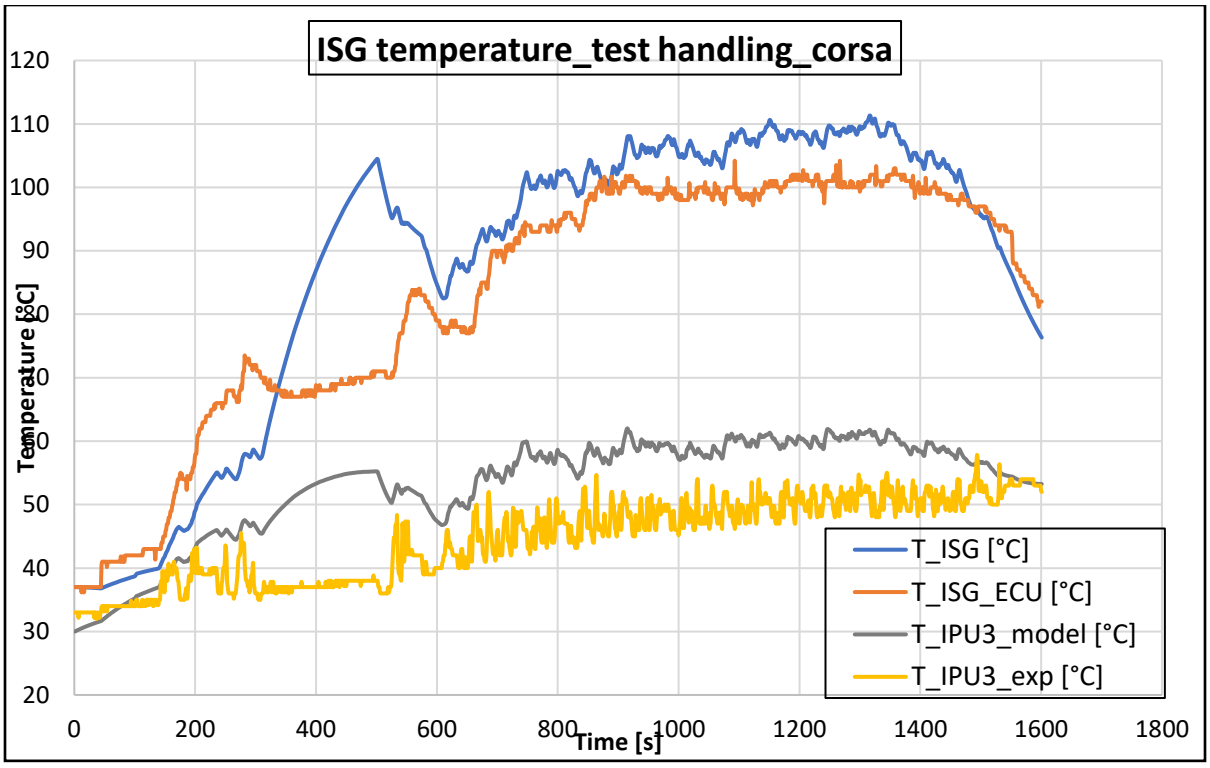

Figure 45c: ISG and inverter temperature validation

Battery

As described in chapter 3, the battery thermal model has only one thermal mass and the calculated temperature is used to obtain internal resistance. The setting of the parameters is reported in *table 7.* Its weight is the product of the single cell weight times the cell number multiplied by an additional contribution that consider all the other parts of the entire battery pack. An amount which goes from 60% to 80% is added. The specific thermal capacity is chosen from literature values, where many works have investigated Li-ion battery thermal properties. The only value to calibrate is the length of heat exchange for the convection description.

Model	Parameter	Value	notes
Battery (thermal mass 1)	Weight	*cell_w * number *gain*	*from company benchmark*
	Material (for *cp*)	*1100 kJ/kg/K*	*from literature [20,21]*
Convection exchange	Pipe diameter	*25 mm*	
	Length heat exchange	*2,5 m*	*calibrated*

Table 7: battery parameters setting for thermal mass model

Two tests have been simulated, one for the calibration and one for the validation. In *figure 46*, the battery and coolant temperature in the calibration test are reported.

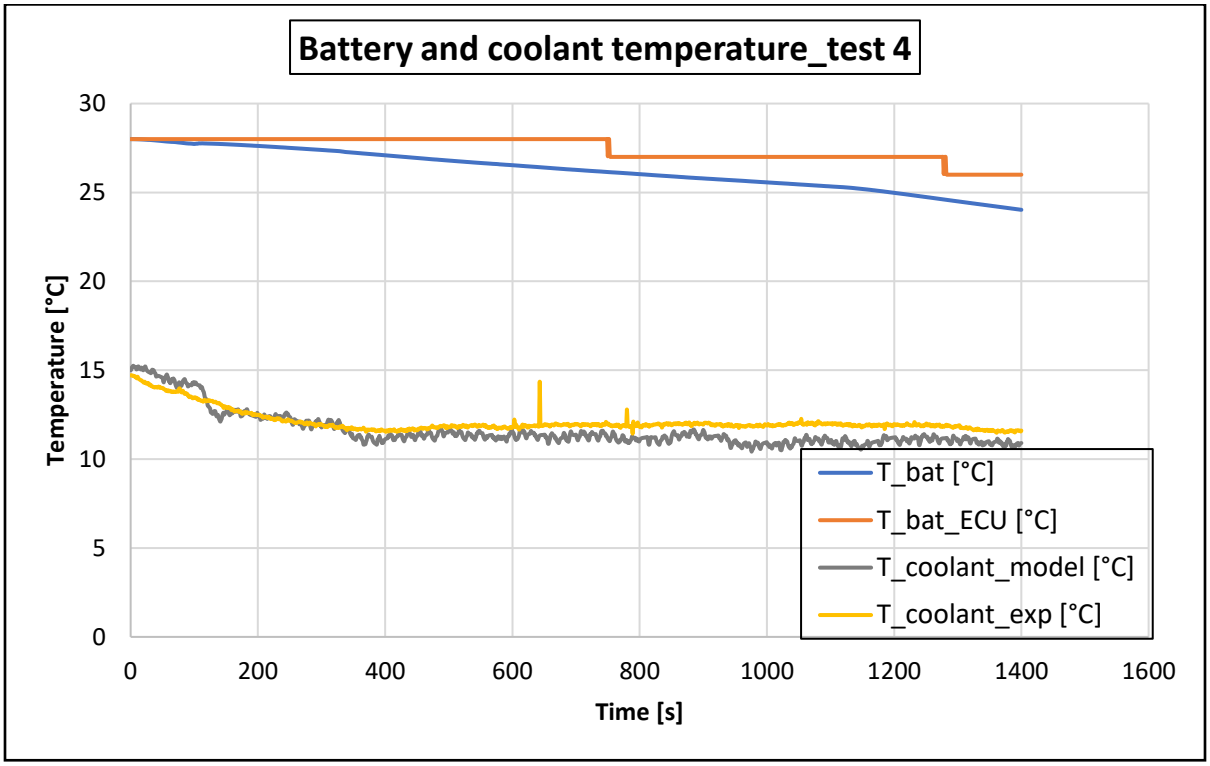

Figure 46: battery and coolant temperature calibration

The test used for the calibration is the test 4, already considered in the first step of the model. The battery is quite heavy, as a consequence its thermal capacity is really high and its temperature changes slowly. It is interesting to notice that from an initial temperature of 28°C, the BMS decides to cool down it, running the coolant pump. Both the two temperatures are well predicted and the length heat exchange value has been used in the other simulations.

The test used for the validation is the 'handling electric', in which the battery is completely discharged (after 800s) and then it is cooled down by the coolant. The four temperatures (two fo the model and two from measurements) are reported in *figure 47*. The medium errors are ±1 °C for the battery and ±2 °C for the coolant, and the maximum errors are respectively ±3.5 °C and ±6 °C.

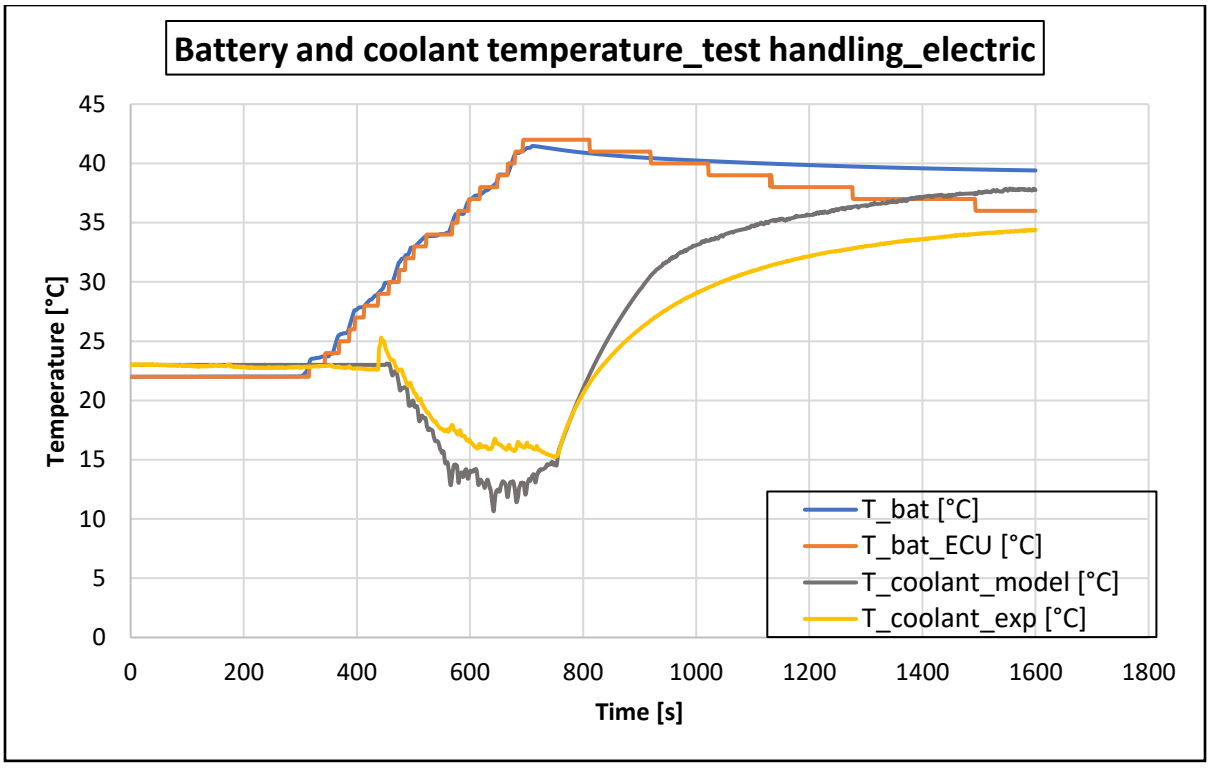

Figure 47: battery and coolant temperature for validation

Compared to the electric motor thermal mass, better results have been obtained for the battery circuit. As it has already been described, the chiller heat exchange map is function of the refrigerant pressure. Since the air conditioning model has not been included in the validation stage, this signal has provided from external data.

4.4 Validation summary

A summary of the results obtained is reported in *table 8.* The medium errors for the coolant temperature, thermal heat flows and thermal mass temperature are summed up.

	Validation test	Coolant temp	Heat flow	Thermal mass temperature	Notes
HT	*test 4*	**± 5 °C**		*not modelled*	Only in steady state condition
MT_F	*test 2*	**± 6 °C**	**0.2 kW**	**± 10 °C**	Improve thermal mass
MT_IS	*hand_cors*	**± 5 °C**	**0.5 kW**	**± 10 °C**	Improve thermal mass
LT	*hand_el*	**± 2 °C**		**± 4 °C**	

Table 8: validation final summary

5. Conclusions and future developments

In the last chapter, some conclusions and possible future works are described.

For what concerns the model, three different circuits of a PHEV have been modelled. Following a step-by-step procedure, the hydraulic and thermal model have been developed. In addition to the cooling circuits, the air conditioning has been considered as well. A first attempt of modelling has been done using the specific library. However, the A/C model is not calibrated and it has not been taken into account during the validation. To complete thermal management model, cabin climatization should be included as well. In fact, it is known that it has a strong impact on fuel consumption and, in order to develop innovative control strategies, its contribution cannot be neglected. The development of a cabin model is quite complex and it has not been considered at all in the present work, but it can represent a possible future development. The same is valid for the PTC heaters: it would be really interesting predict their impact on battery SoC and AER. In table 9, a complete list of the circuits just mentioned is reported. It is specified what it has been developed and validated in the present work and what else it could be interesting to include in future.

Circuit	*Modelled*	*Validated*	*Rating*	*Reliability*
HT	***YES***	***YES***	***Sufficient***	***Limited***
MT	***YES***	***YES***	***Good (except for e-motor temp)***	***Good (except for e-motor temp)***
LT	***YES***	***YES***	***Good***	***Good***
A/C	***YES***	***NO***		
Cabin	***NO***	***NO***		
PTC heaters	***NO***	***NO***		

Table 9: thermal management model circuits list

In addition, for the circuits for which a validation has been done, a rating and the reliability of the model are evaluated. A justification of these judgements is now described.

For the engine cooling circuit, two limits must be highlighted: the calibration of the thermostat and how the heat exchange between engine and coolant was calculated. For what concerns the thermostat, the results (figure 37) show the coolant temperature are correctly predicted only after a steady state is reached, and so the thermostat has reached a thermal balance. Instead, during the opening and the closure of the thermostatic valve, the temperatures and the flow rate are not correct. The calibration of the thermostat model, as wax characteristic and hysteresis effect, is incomplete. The other limit is due to the absence of the engine thermal map and the use, instead, of a fuel consumption map. This forces to estimate the amount of total heat exchanged with the coolant: a table of this value as function of the rotational speed has been built. A couple of points are calibrated considering experimental data, but from different rpm the value has been estimated from literature values. Due to this factor, its reliability is must be considered limited.

For the electric motor circuit and ISG circuit, the reported results show that the model has been correctly developed and calibrated. Coolant temperatures and heat flows of heat sources and heat sinks are well predicted. On the other hand, the e-motor temperature is not correct: as mentioned, the thermal model is too simplified and the calibration of some parameters is incomplete. A good level of accuracy can be reached only with higher effort in both the modelling phase and the parameters calibration. At the present status, the model cannot correctly predict the temperature of the electric motor, but only the coolant temperature. Improvements in this topic could be a further development as well.

For the battery coolant circuit both the coolant and the battery temperature are predicted in a quite accurate way. The results are satisfying and the model general validity can be tested in new cases. Once that the A/C model has been validated, the two circuits can be integrated and the chiller can be modelled as liquid-liquid heat exchanger, as already described at the end of chapter 3. In addition, the heat exchange map can be replaced by physical correlations, improving model accuracy.

The general approach to the model is quite simple, the heat produced/absorbed by heat source/sink is always map-based. The accuracy cannot be so high but, on the other hand, the simulations are fast (the MT circuit with thermal masses simulates 1000s in 25 real seconds).

In order to enter in these maps, external signals must be provided, as reported in *table 3* (chapter 3). This is an important limit that has to be considered. It would be really interesting integrate the thermal management model with a hybrid powertrain and vehicle model. This can allow to start only from the car velocity, calculate engine and e-motors rotational speed and torque and be able to enter in the desired maps. In the present work, the e-motor torque was not available and this has been calculated starting from inverter current and voltage. With an integration with a powertrain model, this can be directly calculated. The software used allows to integrate different libraries and different model. As an alternative, the model could be converted to Simulink and then integrated with an existing powertrain model. The conversion from AMESim® to Simulink should be very easy, the software is able to compile a S-function that can be directly used into a Simulink environment.

The main target of the model is to develop control strategies. As described in chapter 1, they can increase the cooling performance reducing the fuel consumption; their impact is very remarkable. All the control signals are summed up in *table 4*. Strategies can be developed in two ways:

- using the AMESim® control library
- convert the model into Simulink and use this environment

Appendix

Figures of the completed models are here reported.

High temperature circuit

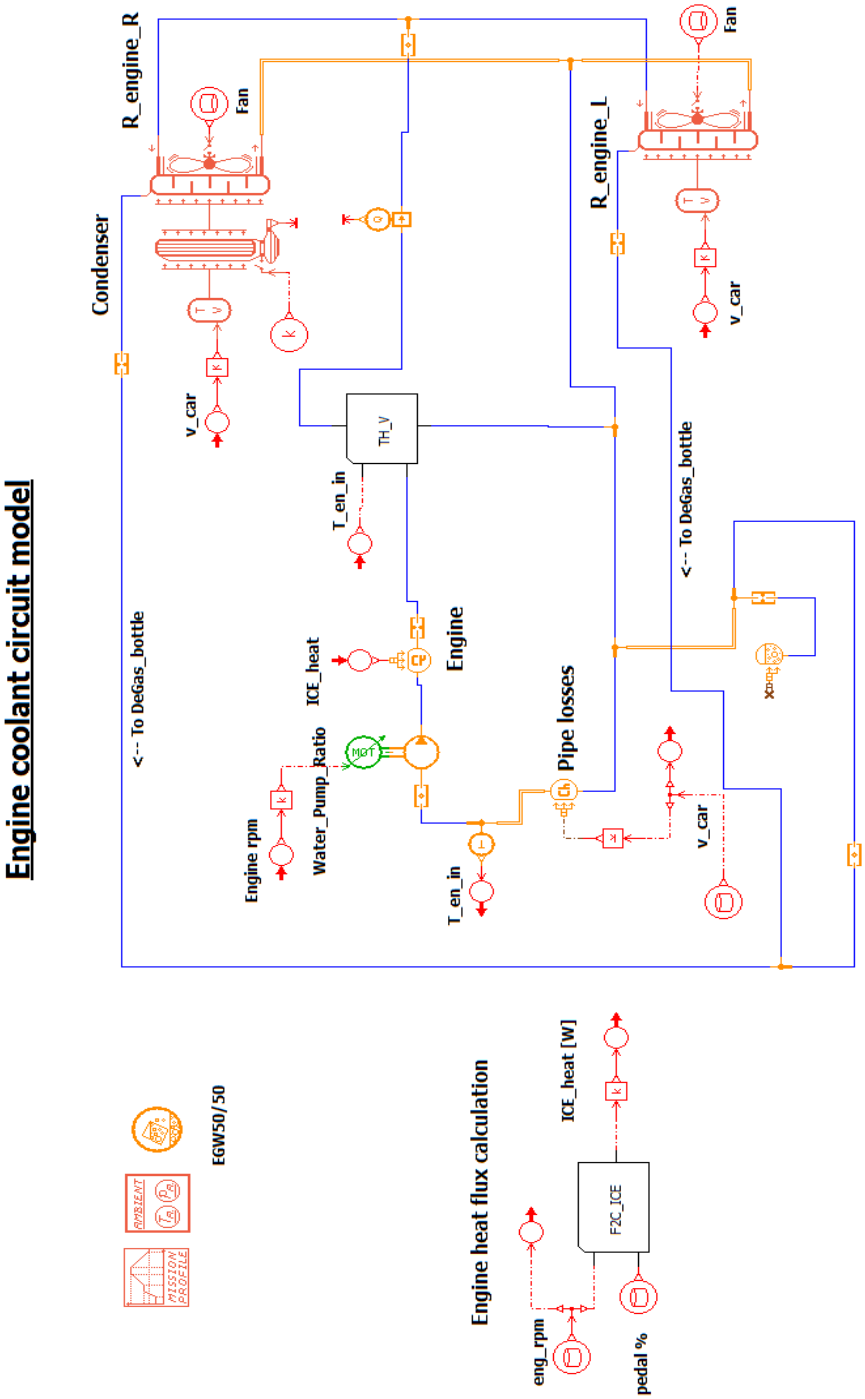

Medium Temperature Circuit

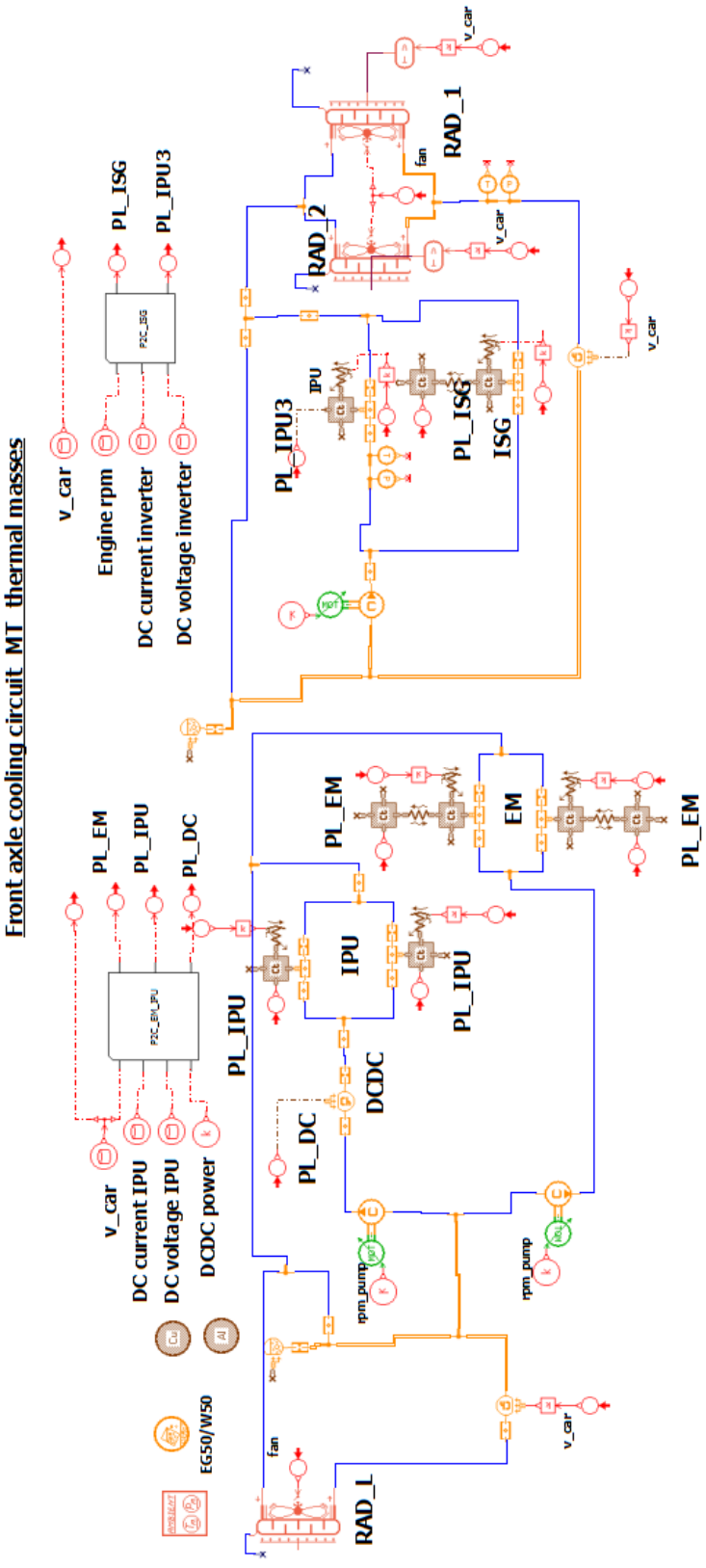

Low temperature circuit

Battery Circuit integrated with Air Conditioning

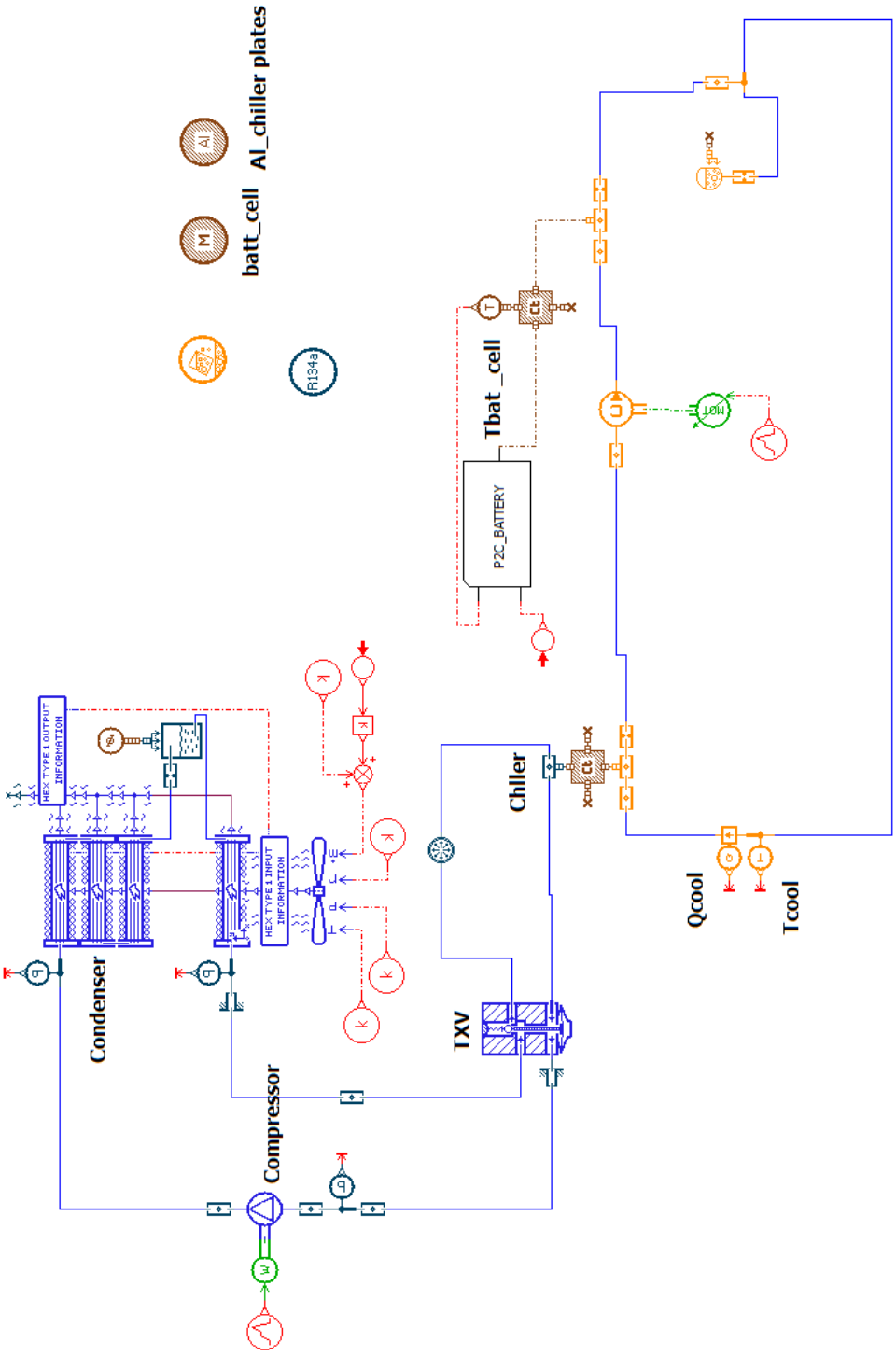

Bibliography

[1] www.EngineeringToolBox.com

[2] L. Lefebvre, Smart Battery Thermal Management for PHEV Efficiency,
Oil & Gas Science and Technology – Rev. IFP Energies nouvelles, Vol. 68 (2013)

[3] G.M. Corporation Data, Dec 2010. Available, http://gm-volt.com/

[4] K. Bennion and M. Thornton , Integrated Vehicle Thermal Management for Advanced Vehicle Propulsion Technologies, *National Renewable Energy Laboratory, SAE 2010 World Congress*

[5] www.optemus.eu

[6] M. Hopp, C. Ebert, K.-H. Hassel, H. Dismon, Thermal Conditioning and Efficiency Increase of Electric Vehicles Using a Heat Pump, KSPG AG, 25th Aachen Cooloquium 2016

[7] S.Gmeiner, P. Rajan, J. Gissing, D. Backes , VOSS Innovative Valve Technology for Thermal Management, 25th Aachen Colloquium 2016

[8] Nicholas R. Jankowski, F. Patrick McCluskey, A review of phase change materials for vehicle component thermal buffering, Applied Energy, 2012

[9] Rainer W. Jorach, Fritz Atschreiter, Axel Gößling,
Integrated Thermal Management: System Approach towards CO2 Reduction
Magna Powertrain GmbH - Fluid, Pressure & Controls Group, 25th Aachen Cooloquium 2016

[10] G.Caramia, Development of an innovative non rule-based energy management strategy for a hybrid electric vehicle, structured for predictive driving controls based on external information knowledge, Master thesis, University of Bologna, 2016

[11] Marcel Stöcker, Norbert Rohleder, Heiko Möckel, Ulf Säger, Matthias Hailer,
Thermal Management for Energy – Efficient Improvement of Automobile Cooling Systems Based on Navigation Data, Daimler AG, 25th Aachen Cooloquium 2016

[12] J.Lopez-Sanz, Carlos Ocampos-Martinez et al. Nonlinear Model Predictive Control for Thermal Management in Plug-in Hybrid Electric Vehicles, IEEE 2015

[13] H.Esen, T.Tashiro, D. Bernardini, A. Bemporad, Cabin Heat Thermal Management in Hybrid Vehicles using Model Predictive Control, 2014 22nd Mediterranean Conference on Control and Automation (MED), University of Palermo, June 16-19 2014

[14] G.Negri di Montenegro, M. Bianchi, A. Peretto, Sistemi energetici e macchine a fluido Volume 1, Ed. Pitagora, 2009

[15] The Centrifugal Pump, GRUNDFOS®, www.grundfos.com

[16] C.Cesario, M.Vrardi, S.Borges, J.Carlos da Silva, A.A Martins Oliveira, Transient thermal amalysis of an induction electric motor, 18th International Congress of Mechanical Engineering, 2005

[17] F.P.Incropera, D.P. DeWitt, Fundamentals of Heat and Mass Transfer, 1998

[18] AMESim® guide Help

[19] John B. Heywood, Internal Combustion Engine Fundamentals, Ed. McGraw-Hill, 1988, p. 674

[20] Hossein Maleki, Said Al Hallaj, J. Robert Selman, Ralph B. Dinwiddie,b and H. Wangb. Thermal Properties of Lithium-Ion Battery and Components, Journal of The Electrochemical Society, 146 (3) 947-954 (1999)

[21] O.S. Burheima,b, M.A. Onsrudc , J.G. Pharoahd,e, F. Vullum-Bruerc , P.J.S. Vie, Thermal Conductivity, Heat Sources and Temperature Profiles of Li-ion Secondary Batteries, The Electrochemical Society, 2013

[22] Thomas GILLET, Emmanuelle ANDRES, Amin EL-BAKKALI, Gérard OLIVIER, Vincent LEMORT , Romuald RULLIERE, Philippe HABERSCHILL, Modelling of an automotive multi-evaporator air-conditioning system, Purdue University, Purdue e-pubs, 2016

Acknowledgements

I would like to thank Ing. Michele Caggiano and Professor Nicolò Cavina for giving me the opportunity to develop this project in such a high-level company and for their support and their advice.

I would like to express my gratitude also to Dipl. Ing. David Hemkemeyer, Ing. Enrico Suzzani and Ing. Alberto Garaffoni for their precious help during the whole thesis period.

Finally, I would like to thank Laura, Simone and my parents for supporting and inspiring me during the course of my studies.